12-1-2011

THERMAL CONDUCTIVITY ENHANCEMENT IN NANOFLUIDS - MATHEMATICAL MODEL

Anand Natchimuthu Chinnaraj

Southern Illinois University Carbondale, anand.chinnaraj@gmail.com

Follow this and additional works at: http://opensiuc.lib.siu.edu/theses

THERMAL CONDUCTIVITY ENHANCEMENT IN NANOFLUIDS

-MATHEMATICAL MODEL

By

Anand Natchimuthu Chinnaraj

B.TECH, Bharathiyar University, Coimbatore 2004

A Thesis

Submitted in Partial Fulfillment of the Requirements for the

Masters of Science Degree

Department of Mechanical Engineering and Energy Process

In the Graduate School

Southern Illinois University Carbondale

December 2011

THESIS APPROVAL

THERMAL CONDUCTIVITY ENHANCEMENT IN NANOFLUIDS

-MATHEMATICAL MODEL

By

Anand Natchimuthu Chinnaraj

A Thesis Submitted in Partial

Fulfillments of the Requirements

For the Degree of

Master of Science

In the field of Mechanical Engineering

Approved by

Dr. Kanchan Mondal, Chair

Dr. Tsuchin P Chu

Dr. James A Mathias

Graduate School

Southern Illinois University

November 07, 2011

AN ABSTRACT OF THE THESIS OF

ANAND NATCHIMUTHU CHINNARAJ, for the Masters of Science degree in Mechanical

Engineering and Energy Processes presented on 07, November, 2011, at Southern Illinois

University, Carbondale.

TITLE: THERMAL CONDUCTIVITY ENHANCEMENT IN NANOFLUIDS

-MATHEMATICAL MODEL

MAJOR PROFESSOR: Dr. Kanchan Mondal

A mathematical model for thermal conductivity enhancement in nanofluids was developed

incorporating the following: formation of nanoparticles into nanoclusters, nanolayer fluid

thickness, Brownian motion and volume fraction of nanoclusters. The expression developed was

successfully validated against experimental data obtained from the literature. The model was

able to comprehensively explain the enhanced thermal conductivity of nanofluids. Following the

validation, parametric study resulted in drawing up some important conclusions. It was found

that in this study that the nanoparticles tend to form nanoclusters and the volume fraction of the

nanoclusters and the trapped fluid in the nanocluster contributed to the overall thermal

conductivity. Various types of cluster formation were analyzed and it was generally found that

employing spherical nanocluster models were more effective in predicting the thermal

conductivity of nanofluids. The contribution of Brownian motion of nanoparticles to the overall

thermal conductivity of nanofluids was found to be very important albeit small in comparison to

the cluster effect. The study investigated the impact of the nanoparticle size which has been

suggested to be an important factor the results were found to be in concord with the

experimental observations. The values of the thermal conductivity for different nanofluid

combinations were calculated using the expression developed in this study and they agreed with

published experimental data. The present model was tested against several nanofluid combinations. The variables scrutinized under the parametric study to understand thermal conductivity enhancement were nanoparticle diameter, nanolayer thickness, nanocluster stacking and Brownian motion. From the study, it was observed that Brownian motion is significant only when the particle diameter is less than 10 nm. The major factor for the thermal conductivity enhancement in nanofluids is the formations of nanoclusters and the thickness of the nanolayer. The combination of the base fluid and nanoparticles to from nanoclusters is expected provide better cooling solution than the conventional cooling fluids.

ACKNOWLEDGEMENTS

TABLE OF CONTENTS

LIST OF TABLES

LIST OF FIGURES

NOMENCLATURE

a = characteristic length (nm)

A = surface area (nm^2)

A$'$=constant=40000

C = empirical constant

c_p= Specific Heat (J/kg k)

d_f = diameter of the base fluid molecule (nm)

D_f = fractal dimension

h = heat transfer coefficient (W/m^{2}k)

k = thermal conductivity (W/m-k)

k_B = Boltzmann constant = 1.382×10^{-23} J/K

m = mass (kg)

n = number

Nu = Nusselt number

Pr = Prandtl number

q = heat transferred (W)

q$'$ = electric power (W)

Q = heat flux (W/m^2)

r = radius (nm)

R_b=interfacial thermal resistance=0.77×10^{-8} K m^2/W

Re = Reynolds number

t = time of collision of nanoparticles (Sec)

t' = time at which the temperature is T (Sec)

t_1 = time at temperature T_1 (Sec)

t_2 = time at temperature T_2 (Sec)

t_p = thickness of the nanolayer (nm)

T = temperature of the nanofluid (K)

T_{ref} = temperature of the cell (K)

V = velocity of the nanoparticle (nm/sec)

x = distance by which nanoparticles moves in X-direction

$\overline{X}$ = root mean square displacement of nanoparticle (nm)

V_s = Total volume of nanoparticles

V_f = Volume of the fluid

V_p = Volume of the nanoparticles

N_c = Number of particles in a cluster

V_{cb} = Total bulk volume of the cluster

V_{cf} = Total bulk volume of the fluid inside the cluster

t_p = Nanolayer thickness in nm

M_s = Molar mass of the fluid

N_A = Avagadro's Number $\left(= \dfrac{6.023 \times 10^{23}}{Mol} \right)$

Greek Letters

α = thermal diffusivity (m^2/s)

γ_p = diameter of the nanoparticle (nm)

δ = hydrodynamic boundary layer (nm)

δ_T = thermal boundary layer (nm)

λ = ratio of thickness of nanolayer to that of radius of the nanoparticle

μ = dynamic viscosity of the base fluid (kg/ms)

v = kinematic viscosity of the base fluid (m^2/s)

ρ = density of nanoparticles (kg /m^3)

φ = volume fraction of the nanoparticles

φ' = volume fraction of nanocluster

φ_c = volumetric ratio

Δ = differential

λ_{nano} = nanolayer to radius ratio

Subscripts

b = Brownian

bc = Brownian convection

conv = convection

e = equivalent

eff = effective

f = base fluid

m = matrix

nf = nanofluid

min = minimum diameter of the particle

sc= simple cubic

bc=body centered

fc= face centered

sp= spherical cluster

CHAPTER 1

INTRODUCTION

In the past 25 years, research progress in the micro-scale thermo-physics not only advanced a deep understanding in matter science, such as surface physics, agglomerative state, and phase transport phenomena, but also promoted technology innovation for equipment miniaturization, and thus providing new opportunities for researching new types of working liquids and their thermal properties [1]. Research in the area of heat transfer have been carried out over the previous several decades, leading to the development of data for heat transfer performance of currently used base fluids. The use of additives is a technique applied to enhance the heat transfer performance of these base fluids [2].

Passive enhancement methods such as enhanced surfaces are often employed in thermofluid systems. This is because the thermal conductivities of the working fluids such as ethylene glycol, water, and engine oil, are comparatively lower than that of the solid phases. In general, most of the solids have better heat transfer properties compared to traditional heat transfer fluids. Therefore, the development of advanced heat transfer fluids with higher thermal conductivity and improved heat transfer is in strong demand [3].

The use of additives is another technique applied to enhance the heat transfer performance of base fluids. The suspended metallic or nonmetallic particles change the transport properties and heat transfer characteristics of the base fluid [4]. An effective way of improving the thermal conductivity of fluids is to suspend small solid particles in the fluids. In the past, solid particles of micrometer or millimeter magnitudes were mixed in the base liquid.

Although the solid additives may improve heat transfer co-efficient, practical use of such aggregates are limited since the micrometer or millimeter-sized particles tend to settle rapidly, clog flow channels, erode pipelines and cause severe pressure drops [5]. Most of all, fluid with micron-sized particles was found not to be efficient enough to outweigh the disadvantages associated with their application and as a result research into the use of suspended nanoparticles in heat transfer liquids (nanofluids) have increased in the latter half of the last decade [2].

Nanofluids are heat transfer liquids with dispersed nanoparticles. Recent research has shown that they are capable of improving the thermal conductivities and heat transport properties of the base fluid and enhancing energy efficiency and may have potential applications in the field of heat transfer enhancement [6]. The effectiveness of heat transfer enhancement has been found to be dependent on the amount of dispersed particle, material type, particle shape and so on. It is expected that nanofluids can be utilized in airplanes, cars, micro machines in MEMS, micro reactors among others.

Nanofluids can be considered to be the next-generation heat transfer fluids as they offer exciting new possibilities to enhance heat transfer performance compared to pure liquids. They are expected to have superior properties compared to conventional heat transfer fluids, as well as fluids containing micro-sized metallic particles. The much larger surface area to volume ratio of nanoparticles, compared to those of conventional particles, should not only significantly improve heat transfer capabilities, but also increase the stability of suspensions. In addition, nanofluids can suppress abrasion-related issues often encountered in conventional solid/fluid mixtures. Successful employment of nanofluids will support the current trend towards component miniaturization by enabling the design of smaller and lighter heat exchanger systems [7].

Since the concept of nanofluids has been introduced, there have been many efforts to understand the mechanism of heat transfer enhancement together with experimental measurements of the thermal conductivity of nanofluids and the methods of utilization of nanofluids. Early attempts to explain this behavior have made use of the classical model of Maxwell [32] for statistically homogeneous, isotropic composite materials with randomly dispersed spherical particles. This model is generally applicable to dilute suspensions with micro particles but when applied to nanofluids the models predicted lower thermal conductivity enhancement as compared to the experimental observations. In order to improve the predictability of thermal conductivities of nanofluids, Hamilton and Crosser modified Maxwell's theory for non-spherical particles [32] and is the most commonly used model today. The development of nanofluids is still hindered by several factors such as lack of agreement between results, poor characterization of suspensions, and the lack of theoretical understanding of the mechanisms [7]. The reason may arise from the difficulty caused by the fact that the heat-transfer between the base fluid and particles occurs while the particles are in Brownian motion. This can be further complicated by the dependence of the dispersion state upon the flow condition and chemical nature of the particles [4].

So far no general mechanisms to have been formulated to explain the strange behavior of the nanofluids including the highly improved effective thermal conductivity, although many possible factors have been considered, including Brownian motion, liquid-solid interface layer and surface charge state. Currently there is no reliable theory to predict the anomalous thermal conductivity of nanofluids satisfactorily. From the experimental results of many researchers, it is known that thermal conductivity of nanofluids depends on parameters including the thermal conductivities of the base fluid and the nanoparticles, the volume fraction of the nanoparticles,

3

the surface area, and the shape of the nanoparticle and the temperature. [7]. Recent research of nanofluids has offered particle clustering as a possible mechanism for the abnormal enhancement of thermal conductivity when nanoparticles are dispersed in the liquids [8].

The research conducted under this thesis was aimed at developing a more comprehensive model incorporating e critical factors responsible for the abnormal thermal conductivity of nanofluids. The nanolayer formation around a nanoparticle, Brownian motion of the nanoparticles, the size distribution of nanoparticles and the clustering effect are considered to be the most important parameters that thermal conductivity in nanofluids. Considering the above mentioned factors a model was developed. To understand the accuracy of the predicted results and relative improvement in the predictability, the results from developed model were compared to experimental observation and prediction obtained from other models in existence. After that, a parametric study was carried out to develop an insight of the dependence of effective thermal conductivity of nanofluids on the properties of nanoparticles and base fluid. The parameters that were considered are nanoparticle diameter, Brownian motion, the cluster shapes and their effect on thermal conductivity behavior in nanofluids.

CHAPTER 2

REVIEW OF LITERATURE

A.Overview

Cooling is one of the most important technical challenges facing many diverse industries, including microelectronics, transportation, solid state lighting and manufacturing. Technological developments such as microelectronic devices with smaller features and faster operating speeds, high power engines, and brighter optical devices are driving increased thermal loads, and thus requiring advances in cooling. The conventional method for increasing heat dissipation is to increase the area available for exchanging heat with a heat transfer fluid [8].

With increasing heat transfer rate of the heat exchange equipment, the conventional utility fluid with low thermal conductivity can no longer meet the requirements of high-intensity heat transfer. The concept of nanofluids refers to a new kind of heat transport fluids by suspending nano-scaled metallic and nonmetallic particles in base fluids. Some experimental investigations have revealed that the nanofluids have remarkably higher thermal conductivities than those of conventional pure fluids and shown that nanofluids have great potential for heat transfer enhancement [5].

B. Mathematical Models for thermal conductivity of nanofluids

Nanofluids connote a colloidal suspension with dispersed nano-size particles. Experiments over the past decade have revealed that the thermal conductivity of such a suspension can be significantly higher than that of the base medium. Early attempts to explain

this behavior have made use of the classical model of Maxwell for statically homogenous, isotropic composite materials with randomly dispersed spherical particles of uniform size [10].

Keblinski et al. [11] explored the four possible explanations for anomalous increase of thermal conductivity: Brownian motion of particles, molecular level layering of the fluid at the liquid-fluid/particle interface, the nature of heat transport in nanoparticles and the effects of nanoparticle clustering. Jacob Eapen [12] found that most of the models are phenomenological in nature and believed that effectiveness of nanofluids depends not only on the thermal conductivity but also on other properties such as viscosity and specific heat.

Xuan et al. [13] applied the theory of Brownian motion and diffusion-limited aggregation model to simulate random motion and the aggregation process of the nanoparticles. According to the paper, distribution structure (morphology) of the suspended nanoparticles is one of the main factors affecting the thermodynamic properties of nanofluid besides nanoparticle diameter and volume fraction.

Shukla and Dhir [14] developed a model for thermal conductivity of nanofluids based on the theory of Brownian motion of particles in a homogeneous liquid combined with the macroscopic Hamilton- Crosser model and predicted that the thermal conductivity will depend on the temperature and particle size. The model predicts a linear dependence of the increase in thermal conductivity of nanofluid with the volume fraction of solid nanoparticles.

Prasher et al. [15] showed that enhancement in the thermal conductivity of nanofluids is mainly due to the localized convection caused by the Brownian movement of particles. The model captured the effects of particle size, choice of base liquid, thermal interfacial resistance between the particles and liquid, temperature. The model is in good agreement with

experimental data and showed that lighter the nanoparticles the greater is the convection effect in the liquid regardless of thermal conductivity of the nanoparticles.

Prasher et al. [16] used aggregation kinetics of nanoscale colloidal solutions combined with physics of thermal transport to capture the effects of aggregation on the thermal conductivity of nanofluids. The study developed a unified model which combines the micro convective effects due to Brownian motion with the change in conduction due to aggregation. The results showed that colloidal chemistry plays a significant role in deciding the conductivity of colloidal suspensions.

Feng et al. [17] proposed a new model for effective thermal conductivity of nanofluids based on nanolayer and nanoparticles aggregation. The study derived a model based on the fact that a nanolayer exists between nanoparticles and fluid and some particles in nanofluids may contact each other to form clusters. An effective thermal conductivity equation governed by both the agglomerated clusters and nanoparticles suspended in the fluids was developed.

Jie et al. [18] proposed a new model for thermal conductivity of nanofluids, which is derived from the fact that nanoparticles and clusters coexist in the fluids. The effects of compactness and perfectness of contact between the particles in clusters on the effective thermal conductivity are analyzed. The study used the model of Hsc *et al*. [14] to describe the thermal conductivity of the clusters formed by the nanoparticles. The model indicated that the effective thermal conductivity of nanofluids decreases with the increasing concentration of clusters.

Patel et al. [19] proposed that specific surface area and Brownian motion are supposed to be the most significant reasons for the anomalous enhancement in thermal conductivity of nanofluids and they presented a semi-empirical approach for the same by emphasizing the above two effects through micro-convection. The model is in agreement with the experimental

data. Prasher et al. [20] demonstrated that using effective medium theory, the thermal conductivity of nanofluids can be significantly enhanced by the aggregation of nanoparticles into clusters. The model is in agreement with experimental data and showed the importance of cluster morphology on the thermal conductivity enhancements.

Patel and Sundararajan [21] presented a cell model for predicting the thermal conductivity of nanofluids. Effects due to the high specific surface area of the mono-dispersed nanoparticles and the micro-convection heat transfer enhancement associated with the Brownian motion of particles are addressed in detail. The model showed the nonlinear dependence of thermal conductivity of nanofluids on particle concentration at low volume fractions.

Murugesan and Sivan [22] developed upper and lower limit for thermal conductivity of nanofluids. The upper limit was estimated by coupling heat transfer mechanisms like particle shape, Brownian motion and nanolayer while the lower limit was the Maxwell equation. In this paper experimental data from a range of independent publisher's source was used for validation of the developed limits. The comparison indicated that the experimental data considered lie between the new developed limits. The paper also revealed that the present limits are more rigorous in placing a narrow lower and upper limit. The study indicated that most of the experimental data lies within the newly developed limits, thereby concluding that particle shape, Brownian motion, and nanolayer thickness are significant in enhancing the thermal conductivity of nanofluids.

Trisaksri and Wongwises [23] reviewed the recent developments in research on the heat transfer characteristics of nanofluids for the purpose of suggesting some possible reasons why the suspended nanoparticles can enhance the heat transfer of convectional fluids. The review concluded that the nanofluids containing small amounts of nanoparticles have substantially

higher thermal conductivity than those of base fluids and the thermal conductivity enhancement

of nanofluids depends on the particle volume fraction, shape and size of nanoparticles, types of

the base fluids and nanoparticles, pH value of nanofluids and the particle coating.

C. Experimental and Modeling work on thermal conductivity of nanofluids

Zhou et al [24] reviewed the definition of heat capacity and clarifies the defined specific

heat capacity and volumetric heat capacity. In the study, the specific heat capacity, volumetric

heat capacity and their measured experimental data for CuO nanofluids were considered. Their

results indicated that the specific heat capacity of CuO nanofluids decreases gradually with

increasing volume concentration of nanoparticles. They also indicate that the effect of

adsorption on suspended nanoparticles surface will also increase the specific heat capacity of

nanofluid to some extent with increasing nanoparticles volume concentration.

Evans et al. [25] used kinetic theory based analysis of heat flow in fluid suspensions of

solid nanoparticles to demonstrate that the contribution of hydrodynamics effects associated

with the Brownian motion to the thermal conductivity of the nanofluid are very small and

cannot be responsible for the extra ordinary thermal properties of nanofluids. The argument was

supported with the results of the molecular dynamic simulations of a model nanofluid. The

results were compared with EM (Effective Medium) theory and found that the EM theory is

well described about the thermal conductivity of a nanofluid with dispersed nanoparticles.

Shima et al [26] investigated the role of micro convection induced by Brownian motion

of nanoparticles on thermal conductivity enhancement in stable nanofluids containing

nanoparticles. The study mentioned that increasing the aspect ratio of the linear chains in

nanofluids, lead to a very large enhancement of thermal conductivity. The findings also confirm

9

that micro convention is not the key mechanism responsible for thermal conductivity enhancements in nanofluids whereas aggregation has a more prominent role.

Karthikeyan et al [27] synthesized CuO nanoparticles of average diameter 8 nm by a simple precipitation technique and study the thermal properties of the suspensions. The experimental results showed that the nanoparticle size, polydispersity, cluster size, and the volume fraction of the particles have a significant influence on thermal conductivity. The paper also mentioned that nanofluids containing ceramic or metallic nanoparticles showed large enhancement in thermal conductivity that cannot be explained by conventional theories. The paper indicated that the enhancement in thermal conductivity in a colloidal dispersion is mainly due to microconvention caused by the Brownian motion of the nanoparticles and aggregation of nanoparticles causing a local percolation and clustering to the nanoparticle occurs more actively in fluid with higher concentration.

Hong et al [28] found that the reduction of the thermal conductivity of nanofluids is directly related to the agglomeration of nanoparticles. The studies have mentioned that the thermal conductivity of Fe nanofluids increases nonlinearly as the volume fraction of nanoparticles increases. The nonlinearity is attributed to the rapid clustering of nanoparticles in condensed nanofluids. The Fe nanofluids showed a more rapid increase of the thermal conductivity than Cu nanofluids as the volume fraction of the nanoparticles increased. Their paper claims that from those variations of the cluster size and thermal conductivity as a function of time, it was found that the thermal conductivity of nanofluids was related closely to the clustering of nanoparticles.

Wu et al [29] verified experimentally and theoretically the significance of the effect by altering the cluster structure, size distribution, and thermal conductivity of solid particles in

10

water. The aggregation kinetics of SiO_2 sols in water was done by adjusting the pH. Their present experiment showed that clustering did not show any discernible enhancement in the thermal conductivity even at high volume loading. A series of fractal model calculated by them not only suggested that the conductive benefit due to clustering might be completely compensated by the reduced convective distribution due to particle growth, but also recommended the need for higher thermal conductivity and optimized fractal dimensions of particles maximizing the clustering effect.

Wang et al [1] proposed a statistical structural model to determine the macroscopic characteristics of clusters, and then the thermal conductivity of nanofluids can be estimated according to the existing effective media approximation theory. This paper mentioned that particles suspended in a fluid will aggregate naturally into clusters under the control of the Brownian motive force and the Van der Walls force against gravity. The calculations of thermal conductivities corresponding to different particle concentrations as a numerical example for nanofluids with CuO particles (50 nm in diameter) suspended in de-ionized water were carried out. The proposed statistical model was sound in physical concepts and potentially useful as an effective tool for screening and optimizing nanofluids as advanced working fluids.

Lee et al [30] applied a surface complexation model for the measurement data of hydrodynamic size, zeta potential, and thermal conductivity and showed that the surface charge states are mainly responsible for the increase in the present condition and may be the factor incorporating all mechanisms as well. The paper has also mentioned that the pH of the colloidal liquid strongly affects the performance of thermal fluid. As the pH of the solution goes far from the isoelectric point of particles, the colloidal particles get more stable and eventually alter the thermal conductivity of the fluid. The paper has demonstrated that surface charge state is a basic

parameter that is primarily responsible for the enhancement of thermal conductivity of nanofluids.

D. Conclusion

The factors such as nanolayer thickness, convection of liquid due to Brownian motion of nanoparticles, nature of heat transport, inter-particle potential, size distribution of nanoparticles, clustering of nanoparticles have been discussed in section 2.2 and 2.3. Among the discussed models, there are a few of them which able to significantly explain the thermal conductivity enhancement in nanofluids. The review of literature indicated that a single factor is not responsible for high thermal conductivity of the nanofluids. Instead a combination of factors will provide the answer for the overall thermal conductivity of nanofluids. This study estimated that the clustering of nanoparticles, nanolayer thickness and Brownian motion of nanoparticles are important factors in energy transport in nanofluids. The next section will discuss the development of the model.

CHAPTER 3

DEVELOPMENT OF MATHEMATICAL MODEL

Xuan et al. [31] investigated the random motion process and distribution structure of the suspended nanoparticles by taking in to the account the additive assumption of thermal conductivities. Koo and Kleinstreuer [33] postulated that the thermal conductivity of the stationary particles and the thermal conductivity due to Brownian motion are additive. Xuan et al. [31] proposed a model based on the fact that the thermal conductivity of entire nanofluids is the sum of the thermal conductivity of static suspension (k_s) and the thermal conductivity of the stochastic motion (k_{bc}) of the nanoparticles. Based on the above findings, it was decided that the additive function of the k_s and k_{bc} will be used in determining the final form of the effective thermal conductivity, $k_{eff,}$ of the nanofluids. The effective thermal conductivity can be written as

$$k_{eff} = k_s + k_{bc} \tag{3.1}$$

In most of the reported literature, the thermal conductivity of stationary nanoparticles, k_s, in the liquid is obtained by the Hamilton-Crosser (H-C) model [32]. In this model, the particle shape is assumed to be spherical. The spherical approximation may cause some slight deviation from real situation; however, no study of different particle shapes has been reported. The suspended particles alter the fluid composition and make the original base fluid in to suspension, thus affecting the energy transport process. he H-C model for the spherical nanoparticles suspended in base fluids is expressed as 32the following

$$\frac{k_s}{K_f} = \frac{K_p + 2K_f - 2\varphi(K_f - K_p)}{K_p + 2K_f + \varphi(K_f - K_p)} \tag{3.2}$$

where, K_p and K_f are the thermal conductivities of particle and fluid, respectively, and φ is the volume fraction of the nanoparticles in the nanofluid.

The thermal conductivity by heat convection, k_{bc}, caused by Brownian motion of nanoparticles and the model development for this term is discussed in the following. In the viewpoint of the mechanism of heat transfer in nanofluids, the observed enhancements are also partially due to the effects of stationary liquid layer formation on the particles and the effect of Brownian motion of the particles. The liquid on the interface has a strong interaction with the particles and this interaction makes the interfacial liquid layer a more ordered structure. The interface between solid and liquid is regarded as a very thin nanolayer and has semi-solid material properties [34]. To introduce the effect of nanolayer, an equivalent volume fraction is considered.

The value for the thickness of the nanolayer was calculated by the equation [42],

$$t_p = \frac{1}{\sqrt{3}} \left(\frac{4M_f}{\rho_f N_A} \right)^{\frac{1}{3}}$$

Where,

t_p = Nanolayer thickness in nm

M_f = Molar mass of the fluid

N_A = Avagadro's Number $\left(\frac{6.023 \text{ x } 10^{23}}{\text{Mol}} \right)$

This study also considered the effect of the Brownian motion of the particles resulting in relative motion of the liquid near the particles which would contribute to convective heat transfer between the liquid and the nanoparticles. Jang and Choi [35] were the first group to take into account the convection induced by Brownian motion.

The Nusselt number for a flow over spherical particles with a diameter, d, is given by

$$Nu = \frac{hd}{K_f}$$

where, h is the convective heat transfer coefficient. Rearranging the above equation and

defining γ_p as the average nanoparticle size, the heat transfer coefficient can be defined

by

$$h = \frac{Nu\, K_f}{\gamma_p} \qquad (3.3)$$

It must be noted that the characteristic length is taken as diameter of the particle since

the shape is assumed to be spherical. The heat transferred by convection for a nanoparticles

moving in liquids is then given by

$$q_{conv} = -h\,(T_p - T_f)\; n_p A_p \qquad (3.4)$$

Where, T_p and T_f are the temperatures of particle and liquid, respectively, np is the

number of nanoparticles and Ap ($=4\Box\Box p2/4$) is the surface area of the nanoparticle. The

equivalent thermal conductivity contributed by heat convection can be approximated by the

following equation [35]

$$k_{bc} = \frac{q_{conv}}{-\dfrac{T_p - T_f}{\delta_T}\, A} \qquad (3.5)$$

where, δ_T the thermal boundary layer of heat convection is caused by nanoparticles

Brownian's motion, where A is the total surface area of all the nanoparticles (npAp). In flow

over spheres, the ratio of the hydrodynamic boundary layer ($\Box$) and the thermal boundary layer

($\Box$T) is proportional to from the Prandtl number (the ratio of the thermal disffusivity to the

momentum diffusivity). Thus the thermal boundary layer can be estimated by the following:

$$\delta_T \propto \frac{\delta}{Pr} \qquad (3.6)$$

15

$$\delta_T = C \frac{\delta}{Pr} \tag{3.7}$$

where, 'C' is a proportional constant.

Little information is known about the hydrodynamic boundary layer for flow over spheres but the previous researchers, Jang and Choi et al. [35], and Prasher et al. [16], made an assumption that it is proportional to the diameter of the liquid molecule (d_f) and it is given by

$$\delta \; \alpha \; d_f$$
$$\delta = 3 \; d_f \tag{3.8}$$

Equation 7, shows that the hydrodynamic boundary layer is a function of only the characteristic length and not the Reynolds number which is inconsistent with estimating boundary layer for flow over flat plate. From equations 3.7 and 3.8 we get,

$$\delta_T = C \; \frac{3 \; d_f}{P_r} \tag{3.9}$$

The value of the constant was found to be 4 for water based nanofluids and 107 for ethylene glycol based nanofluids. The constant C for both water based nanofluids and ethylene glycol based nanofluids was found to 0.7*Pr and this has been used in this thesis. Since the thermal boundary layer is also inversely proportional to the Prandtl number, incorporating $C = 0.7$ Pr results in conclusion that the thermal boundary layer thickness is no longer a function of the Pr.

From equations 3.4, 3.5 and 3.7 we obtain a simplified relationship for k_{bc} .

$$k_{bc} = h \; \delta_T \tag{3.10}$$

In order to obtain an estimated value for h, we considered the use of Brownian motion kinetics. The Brownian Motion velocity based on Kinetic Theory of Gases is given by [24]

$$V_b = \frac{2\,k_B T}{\pi \mu_f \gamma_p^2} \qquad (3.11)$$

Where k_B is the Boltzmann's constant, T is the temperature in K, and m is the viscosity.

Brownian-Reynolds number based on Brownian velocity is given by,

$$R_e = \frac{V_b\,\rho\gamma_p}{\mu} \qquad (3.12)$$

where, ρ is the density. From equations 3.11 and 3.12 we get,

$$R_e = \frac{2\,k_B T \rho}{\pi {\mu_f}^2 \gamma_p} \qquad (3.13)$$

The Re values have been calculated for different nanofluids and it was found that Re << 1 so for

convection, the flow falls in Stokes regime [37]. In Stokes' regime, the heat transfer coefficient

is given by [35].

$$h = \frac{K_f}{a}\,[2 + 0.5 R_e P_r] \qquad (3.14)$$

Where, 'a' is the characteristic length for a sphere which is taken as the diameter (γ_p).

The above equation is valid for a single sphere. However, in case of nanofluids, multiple

spheres

exist and they interact with each other even for small volume fractions. Therefore, the value of

'h' estimated from the above equation needs to be modified. In order to obtain a better

predictive model for 'h' for nanofluids, the energy transport is based on the particle-to-fluid

heat

transfer in fluidized beds. Based the concept of Nu correlations for a particle to fluid heat

transfer in fluidized beds, Prasher et al. [16] proposed a general correlation for heat transfer

coefficient for Brownian motion for the flow of a multiple spheres as

$$h = \frac{K_f}{a}\,[1 + A' R_e{}^m P_r{}^{0.333} \varphi] \qquad (3.15)$$

17

Where A' and m are constants derived from experimental data. According to Prasher et al. [16] A is independent of fluid type and its value is 40,000; whereas the value of m value depends on the fluid type. The value of m = 2.5 ± 15% for water based fluids and m=1.6±15% for EG based fluids.

By definition, Prandtl number is given as

$$P_r = \frac{v}{\alpha} = \frac{\mu_f c_p}{k_f}$$ (3.16)

Where, μ_f is the viscosity.

The added nanoparticles will increase the viscosity of the fluid. The viscosity of nanofluids not only increases with increase in the volume fraction of the nanoparticles but also by nanolayer formation. Due to the formation of nanolayer around a particle the surface area of the particle increases which causes more resistance to flow increasing the viscosity. Jang and Choi [38], Patel et al. [21], Jang and Choi [35], Prasher et al. [15], Prasher et al. [37], Patel et al.[19], Kumar et al. [39] and Feng et al. [40] have used viscosity in their respective models but none of them have considered the effect of suspension of nanoparticles on the viscosity of the nanoparticles.

The first major contribution to the theory of the viscosity of suspensions of spheres was made by Einstein. The Einstein equation [41] for effective viscosity is given by

$$\mu_{eff} = \mu_f (1 + \frac{5}{2} \varphi)$$ (3.17)

where, μ_f is the dynamic viscosity of the fluid and φ is the volume fraction of the nanoparticles.

Feng et al. [40] proposed that the distribution of particles in nanofluids is analogous to the porous media whose sizes vary from γ_p to $\gamma_p + d\gamma_p$ and the number of particles is given as [42]

18

$$-dN = D_r \gamma_{max}{}^{D_f} \gamma_p{}^{-(D_f+1)} d\gamma_p \tag{3.18}$$

Where D_f is the fractal dimensions for particles which is given by [43] as

$$D_f = d - \frac{\ln \varphi}{\ln(\frac{\gamma_{min}}{\gamma_{max}})} \tag{3.19}$$

Where d = 2 in two dimensions, φ is the concentration of the nanoparticles, γ_{min} and γ_{max} are the minimum and maximum diameters of nanoparticles, respectively.

As mentioned earlier, the heat transfer by convection for a single nanoparticle moving in liquids is given by

$$q_{\gamma_p} = hA_{\gamma_p}(T_p - T_f) \tag{3.20}$$

where T_p and T_f are the temperatures of particle and fluid, respectively, $A_\gamma = \pi \gamma_p{}^2$ is the surface area of the nanoparticle with diameter γ_p.

The above equation explains the heat transfer around single nanoparticle. Since we have assumed the differential diameter of nanoparticles, the heat transferred by convection of all the nanoparticles is given as,

$$q_{bc} = - \int_{\gamma_{min}}^{\gamma_{max}} q_\gamma dN \tag{3.21}$$

From equations 3.20 and 3.21 we get

$$q_{bc} = - \int_{\gamma_{min}}^{\gamma_{max}} hA_{\gamma_p}(T_p - T_f) dN \tag{3.22}$$

Substituting equation 3.22 in 3.5 we get

$$k_{bc} = \frac{\int_{\gamma_{min}}^{\gamma_{max}} h\pi\gamma_p{}^2 (T_p - T_f) dN}{\frac{(T_p - T_f)}{\delta_T} \int_{\gamma_{min}}^{\gamma_{max}} \pi\gamma_p^2 dN} \tag{3.23}$$

Assuming that $(T_p - T_f)$ is constant,

$$k_{bc} = \frac{\delta_T \int_{\gamma_{min}}^{\gamma_{max}} h \gamma_p^2 dN}{\int_{\gamma_{min}}^{\gamma_{max}} \gamma_p^2 dN} \tag{3.24}$$

Substituting the thermal boundary layer estimation from equation 3.10 and the Nusselt number

correlation from equation 3.15 in 3.25 we get

$$k_{bc} = \frac{2.1 d_f \int_{\gamma_{min}}^{\gamma_{max}} \frac{K_f}{\gamma_p}[2 + 0.5 R_e P_r] \gamma_p^2 dN}{\int_{\gamma_{min}}^{\gamma_{max}} \gamma_p^2 dN} \tag{3.25}$$

$$k_{bc} = \frac{2.1 d_f \int_{\gamma_{min}}^{\gamma_{max}} K_f [2 + 0.5 R_e P_r] \gamma_p dN}{\int_{\gamma_{min}}^{\gamma_{max}} \gamma_p^2 dN} \tag{3.26}$$

$$k_{bc} = \frac{2.1 d_f \left(\int_{\gamma_{min}}^{\gamma_{max}} 2 \gamma_p dN + \int_{\gamma_{min}}^{\gamma_{max}} 0.5 R_e P_r \gamma_p dN \right)}{\int_{\gamma_{min}}^{\gamma_{max}} \gamma_p^2 dN} K_f \tag{3.27}$$

In order to simplify the equation for analysis, some parameters are introduced to individual

terms. Let

$$R = 2.1 \, d_f K_f \tag{3.28}$$

$$A = \int_{\gamma_{min}}^{\gamma_{max}} 2 \gamma_p dN \tag{3.29}$$

$$B = \int_{\gamma_{min}}^{\gamma_{max}} 0.5 R_e P_r \gamma_p dN \tag{3.30}$$

$$C = \int_{\gamma_{min}}^{\gamma_{max}} \gamma_p^2 dN \tag{3.31}$$

Since we consider the nanoparticles as particle with a single diameter the $\int_{\gamma_{min}}^{\gamma_{max}} dN = N$.

Therefore the integral equations reduce to

$$A = 2 \gamma_p N \tag{3.32}$$

$$B = 0.5 R_e P_r \gamma_p N \tag{3.33}$$

20

$$C = \gamma_p^2 N \tag{3.34}$$

For a case where the particle size distribution is known, a more complicated form for the three terms would be found. So now the reduced form of equation 3.27 can be written as

$$k_{bc} = \frac{R(A+B)}{C} \tag{3.35}$$

$$\frac{R(A+B)}{C} = 2.1d_f \frac{\left[2\gamma_p N + 0.5 R_e P_r \gamma_p N\right]}{\gamma_p^2 N} K_f \tag{3.36}$$

$$\frac{R(A+B)}{C} = 2.1d_f \frac{\left[2 + 0.5 R_e P_r\right]}{\gamma_p} K_f \tag{3.37}$$

Combining equations 3.13 and 3.14 in 3.37 we get,

$$k_{(bc)} = 2.1d_f \frac{\left[2 + \left(\frac{k_b T \rho C_p}{\pi \mu_{eff} K_f \gamma_p}\right)\right]}{\gamma_p} K_f \tag{3.38}$$

Where μ_{eff} is given by Equation 3.17. In order to modify the Hamilton Crosser model to incorporate the clustering effect, several cluster shapes were assumed. Foe each cluster, only unit cells were considered for clusters. If a distribution of cluster sizes were considered then, the derivation for k_{bc} needs to be modified by incorporating Equations 3.18 and 3.19 or any suitable distribution into Equations 3.29 – 3.31 to obtain a corresponding relation for Equation 3.38. The equation for Thermal Conductivity of Stationary nano-clusters is developed as shown below. It has been assumed in this derivation that the liquid between the pores and the nanolayer are stationary and behave as a part of the cluster. Applying the Hamilton-Crosser derivation along with the above assumption the effective thermal conductivity of the cluster is

found to be the following.

$$\frac{K_c}{K_f} = \frac{\left[K_p + 2K_f - 2\varphi_c(K_f - K_p)\right]}{\left[K_p + 2K_f + \varphi_c(K_f - K_p)\right]} \tag{3.39}$$

Where φ_c is the volume fraction of the particles in a cluster, K_p is the particle thermal conductivity.

The volume fraction of nanoparticles is

$$\varphi = \frac{V_s}{V_f} \tag{3.40}$$

Where,

V_s = **Total volume of the nanoparticles**, V_f = **Volume of the fluid**

Re arranging 3.40 we obtain

$$V_s = \varphi V_f \tag{3.41}$$

The volume of a spherical nanoparticle with a diameter γ_p is given by:

$$V_p = \frac{4\pi}{3}\left(\frac{\gamma_p}{2}\right)^2 \tag{3.42}$$

$$\frac{V_s}{V_p} = N_p \tag{3.43}$$

Where, V_p= Volume of the nanoparticles for a given number of particles in a cluster (n_c), the total number of clusters (N_c) is given by

$$\frac{N_p}{n_c} = \frac{V_s}{n_c V_p} = N_c$$

n_c = Number of particles in a cluster

N_c = Number of clusters

For a given number of clusters (N_c), and volume of a cluster (V_c), the total volume of clusters is given by

$$N_c V_c = V_{cb} \tag{3.44}$$

Given

V_{cb} = Total bulk volume of the cluster

V_{cf} = Total bulk volume of the fluid inside the cluster

The effective cluster volume fraction is given by:

$$\varphi' = \frac{V_{cb}}{V_f - V_{cf}} \tag{3.45}$$

Replacing V_{cb} in equation 3.45 using equation 3.44 we get

$$\varphi' = \frac{V_c N_c}{V_f - (1 - \varphi_c)V_c N_c} \tag{3.46}$$

Further rearranging can be conducted on the above equation rendering the following

$$\varphi' = \frac{(V_f \varphi / n_c V_p)V_c}{V_f - (1 - \varphi_c)V_c(V_f \varphi / n_c V_p)} \tag{3.47}$$

$$\varphi' = \frac{(V_f \varphi / n_c V_p)V_c}{\left[V_f - V_c\left(\frac{V_f \varphi}{n_c V_p}\right)\right] + \left[\frac{V_c V_f \varphi_c \varphi}{n_c V_p}\right]} \tag{3.48}$$

Where

$$\varphi_c = \frac{V_{s,c}}{V_c} \tag{3.49}$$

And

$$n_c V_p = V_{s,c} \tag{3.50}$$

Thus,

$$\varphi' = \varphi\left(\frac{V_c}{V_{s,c}}\right)/[1 - (V_c \varphi / V_{s,c}) + \varphi_c \varphi\,(\frac{V_c}{V_{s,c}})] \tag{3.51}$$

Combining equations 3.49 in equation 3.51 we get,

$$\tag{3.52}$$

$$\varphi' = \frac{[\varphi / \varphi_c]}{\left[1 - \varphi / \varphi_c + \varphi\right]}$$

23

Using equation 3.52 in the Hamilton-Crosser equation [29] the K_{eff} of the nanoclusters is as

shown below

$$\frac{K_s}{K_f} = \frac{\left[K_c + 2K_f - 2\varphi'(K_f - K_c)\right]}{\left[K_c + 2K_f + \varphi'(K_f - K_c)\right]} \tag{3.53}$$

 Incorporating 4.39 in 4.53

$$\frac{K_s}{K_f} = \frac{\left[K_p + 2K_f - 2\varphi'\varphi_c(K_f - K_p)\right]}{\left[K_p + 2K_f + \varphi'\varphi_c(K_f - K_p)\right]} \tag{3.54}$$

Substituting 3.3 and 3.54 in equation 3.1

The total K_{eff} of the system is

$$k_{eff} = \frac{\left[K_p + 2K_f - 2\varphi'\varphi_c(K_f - K_p)\right]}{\left[K_p + 2K_f + \varphi'\varphi_c(K_f - K_p)\right]} K_f + 2.1d_f \frac{\left[2 + \left(\frac{K_b T \rho C_p}{\pi \mu_{eff} K_f \gamma_p}\right)\right]}{\gamma_p} K_f \tag{3.55}$$

CHAPTER 4

DISCUSSION OF RESULTS & COMPARISION WITH OTHER MODELS

This chapter describes the comparison of results obtained from the developed mathematical model with the results published from the experimental data. The experimental data was obtained from various relevant researches so as to validate the model for various nanofluids combinations. The mathematical model was then compared with other models developed to understand and compare the proximity of the results. The mathematical models that are used to compare are described as follows:

1. Hamilton & Crosser [32]:

$$\frac{k_{eff}}{K_f} = \frac{K_p + (n-1) K_f - (n-1)\phi (K_f - K_p)}{K + (n-1) K_f + \varphi (K_f - K_p)} \tag{4.1}$$

2. Hemanth Kumar [39]

$$\frac{k_{eff}}{K_f} = 1 + \frac{K k_p \varphi \, r_f}{K_f (1 - \varphi) \, r_p} \tag{4.2}$$

3. Prasher [16]

$$\frac{k_{eff}}{K_f} = \left(1 + \frac{Re \times Pe}{4}\right) \left[\frac{(1 + 2\alpha) + 2\phi(1 - \alpha)}{(1 + 2\alpha) - \phi(1 - \alpha)}\right] \tag{4.3}$$

where $\alpha = \frac{2 R_b K_m}{d_p}$

4. Timofeeva [44]

$$\frac{k_{eff}}{k_f} = 1 + \frac{3(K_p - K_f)\varphi}{K_p + 2 K_f} \tag{4.4}$$

5. Leong [45]

$$k_{eff} = \frac{(K_p - \gamma_{nano})\,\phi_1\,\gamma_{nano}\left[2\beta_1^3 - \beta^3 + 1\right] + (K_p + 2\gamma_{nano})\,\beta_1^3\left[\phi_1\,\beta^3\,(\gamma_{nano} - K_f) + K_f\right]}{\beta_1^3\,(K_p + 2\gamma_{nano}) - (K_p - \gamma_{nano})\phi_1\left[\beta_1^3 - \beta^3 + 1\right]} \quad (4.5)$$

Where $\beta = 1 + \dfrac{\lambda_{nano}}{d_p}$, $\beta_1 = 1 + \lambda_{nano}\,2\,d_p$

6. Jeffrey [46]

$$\frac{k_{eff}}{K_f} = 1 + 3\beta\phi + \left(3\beta^2 + \frac{3\beta^3}{4} + \frac{9\beta^3}{16}\frac{\alpha+2}{2\alpha+3} + \frac{3\beta^4}{26} + \ldots\right)\phi^2 \quad (4.6)$$

Where $\beta = \dfrac{\alpha-1}{\alpha+1}$ and α = thermal conductivity of particle/thermal conductivity of the base fluid.

The following nanofluids combinations were used to compare the mathematical model with the experimental data and various other mathematical models developed as mentioned above

(1)   CuO – Water [47]

(2)   CuO - Ethylene Glycol [48]

(3)   Cu – Water [31]

(4) Al_2O_3 – Water [40]

(5) TiO_2 - Water [49]

(6) $Ti\,O_2$ - Ethylene Glycol [49]

(7)   ZnO – Water [10]

(8)   ZnO – Ethylene Glycol [49]

(9)   Al – Water [31]

(10) Fe – Ethylene Glycol [50]

(11) Al_2O_3 – Ethylene Glycol [40]

Nanolayer Thickness-Sample Calculations

The value for the thickness of the nanolayer was calculated by the equation [38],

$$t_p = \frac{1}{\sqrt{3}} \left(\frac{4M_f}{\rho_f N_A} \right)^{\frac{1}{3}}$$
(4.9)

Where,

t_p = Nanolayer thickness in nm

M_f = Molar mass of the fluid

N_A = Avagadro's Number $\left(\dfrac{6.023 \times 10^{23}}{\text{Mol}} \right)$

The value of t_p was found to be 2.8441 x 10^{-10} nm for water.

Cluster Parameters - Sample Calculations

Using the diameter of nanoparticle of CuO of d_p= 60.4 nm the volumetric ratio for the clusters and their mean diameter in four different lattices were calculated.

Simple Cubic Cluster:

$\varphi_c = 0.524$

$\gamma_p = 1.513 \times 10^{-7}$ nm
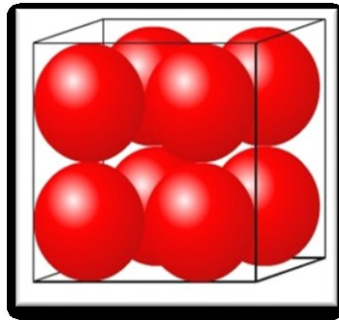
Figure 4. 1 Simple cubic cluster

Body Centered Cubic Cluster:

$\varphi_c = 0.650$

$\gamma_p = 1.513 \times 10^{-7}$ nm
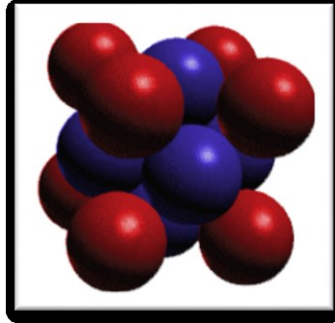
Figure 4. 2 Body centered cubic cluster

Face-Centered Cubic Cluster

$\varphi_c = 0.740$

$\gamma_p = 1.464 \times 10^{-7}$ nm
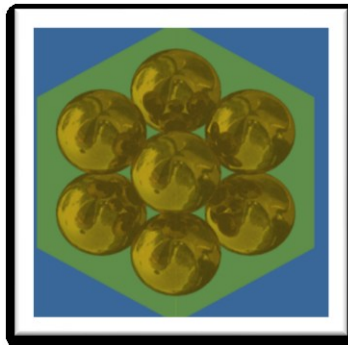
Figure 4. 3 Face centered cubic cluster

For Spherical Cluster:

$\varphi_c = 0.740$

$\gamma_p = 1.829 \times 10^{-7}$ nm
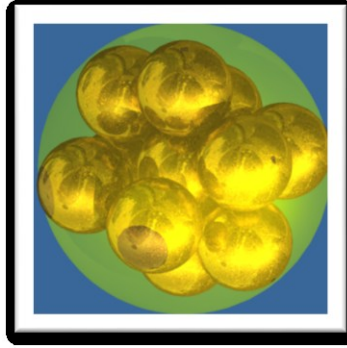
Figure 4. 4 Spherical cluster

CuO – Water: 18 nm

The experimental data for CuO – Water was obtained from Lee et al. [47].

Experimental Procedure:

For the experiments, Lee et al. [47] used a hot-wire system involving a wire suspended symmetrically in a liquid in a vertical cylinder container to measure the thermal conductivity. The wire serves as a heating element and as thermometer. This method is called transient because the power is applied abruptly and briefly. The temperature of the wire is calculated by a specific solution of Fourier's law which is given by [47]

$$T(t') - T_{ref} = \frac{q'}{4 \pi k} \ln\left(\frac{4 \alpha t}{a^2 C}\right) \qquad (4.7)$$

Once the temperatures are calculated, thermal conductivity can be calculated from

$$k = \frac{q'}{4 \pi (T_2 - T_1)} \ln\left(\frac{t_2}{t_1}\right) \qquad (4.8)$$

Platinum is used for hot-wire. A Wheatstone bridge is used to measure the resistance of hot-wire.

Switching the power from stabilizer resistance to the Wheatstone bridge initiates the voltage change in hot-wire and this varying voltage was recorded with resolution of 1.5 mV at

a sampling rate of ten times per second. From these measures of voltage and Ohm's law, the resistance change of the wire and the heating current through the wire can be calculated. Finally temperature variation of the wire can be calculated. Using these temperatures in equation 4.8 gives the thermal conductivity of the nanofluids.

Using the above mentioned values and solving using the proposed mathematical model the K_{eff} was found for different cluster formations. The parametric values for this analysis are as follows:

k_p = 20 W/m-k, k_f=0.613 W/m-k, C_p = 4170 J/kg k, μ_f = 8.55× 10^{-4} N s/m^2 ,

v_f = 8.55× 10^{-7} N s/m^2, T = 300K, ρ_f = 997 kg/m^3, t_p=2.844 x 10^{-10} m [9]. The above values were incorporated into the model described by Equation 3.55 and the predicted and experimental values by the various cluster models and models currently used in literature (equations (4.1-4.6)) are given in Table 4.2. K_exp, K_exp_sc, K_exp_fc,K_exp_bs and K_exp_sp denote the effective thermal conductivities obtained through experiments and prediction using simple cubic, face centered cubic, body centered cubic and spherical clusters, respectively. The columns with the model names contain the data of the thermal conductivites predicted by the use of the respective models. It is clearly seen from the Figure 4.5 that the results are in excellent agreement with the published experimental data.

Here Table 4.2 includes the effective thermal conductivities of CuO – water (18 nm) nanofluids for different volume fractions. These values were used to plot the effective thermal conductivity v/s volume fraction. The plot is shown in Figure 4.5 and it clearly indicates that the thermal conductivity increases with an increase in the volume fraction of nanoparticles. As seen from both Table 4.2 and Figure 4.5, the developed model is in good agreement with the experimental data. The value of C = 0.7*Pr is used for all the nanofluids. The results obtained

from Jeffrey [46], Timofeeva et al. [44], Hamilton & Crosser [32], Kumar et al.[39] under-predicted the experimental data whereas Prasher et al. [16] and Leong et al. [45] models over-estimated it. In figure 4.5, the experimental values which are shown by blue color lies at par with the results obtained for the developed mathematical model with spherical cluster structure, followed by the face centered cubic cluster formation. The body centered cubic cluster and face centered cubic cluster lie marginally above the spherical cluster model results. Overall, the mathematical model developed lies close to the experimental values.

Table 4. 1.Volume fraction and mean diameter of cluster for CuO (18 nm) –
Water nanofluids

Nanocluster	Simple Cubic	Body centered	Face Centered	Spherical
ϕ_c	0.4769	0.5925	0.6742	0.3711
γ_p (nm)	46.0767	46.0767	44.5890	55.7065

Table 4. 2. Comparison of k_{eff} values for CuO (18 nm) – Water nanofluids.

Volume Fraction	K_exp (W/m-)	K_exp_sc (W/m-K)	K_exp_bc (W/m-K)	K_exp_fc (W/m-K)	K_exp_sp (W/m-K)	Hamilton &Crosser (W/m-K)
0.01	0.6355	0.6516	0.65221	0.65153	0.64800	0.6297
0.02	0.6562	0.6695	0.66973	0.66916	0.66619	0.6468
0.03	0.6772	0.6881	0.68777	0.68739	0.68542	0.6643
0.04	0.6985	0.7075	0.70634	0.70624	0.70576	0.682
Volume Fraction	Prasher (W/m-)	Timofeeva (W/m-K)	Murshed (W/m-K)	Jeffrey (W/m-K)	Kumar (W/m-K)	
0.01	0.655	0.6296	0.6453	0.6299	0.6169	
0.02	0.6591	0.6463	0.6783	0.6472	0.6208	
0.03	0.6632	0.6629	0.7121	0.665	0.6249	
0.04	0.6674	0.6795	0.7466	0.6832	0.629	

Effective Thermal Conductivity vs Volume fraction for CuO-water 18 nm
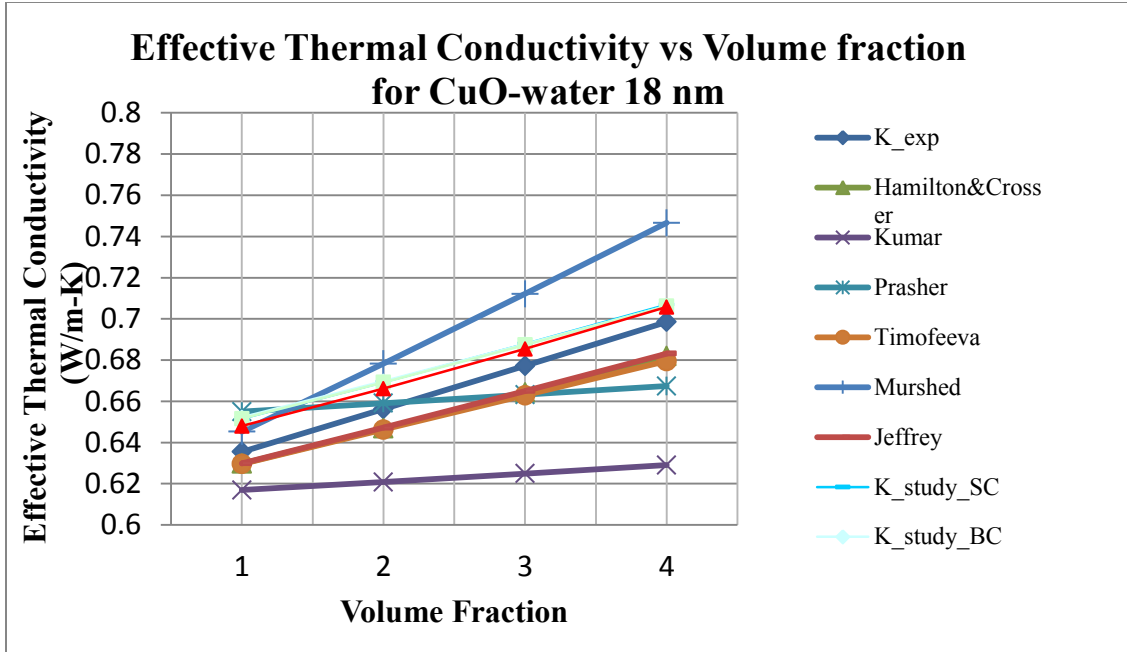
Figure 4. 5 Plot for the comparison of "K_eff" values for different CuO (18 nm) – Water

nanofluids.

CuO – Water: 23.6 nm

The experimental data for this analysis was obtained from Feng et al. [40].
For the experiment, Feng et al. [40] used a temperature oscillation technique. This technique

requires a specially fabricated test cell which is a flat cylinder. The cell was mounted with its

axis in a horizontal position. The measurements were made at three different locations – at the

interface of the Peltier element and the reference layer (polyoxymethylene), at the interface of a

reference layer and test fluid and the central axial plane of the test fluid. The thermocouples at

the interfaces were put in a small groove and welded at the tip. The temperature of the reference

material was given a periodic oscillation by the two Peltier elements from two ends. The

thermal diffusivity of the fluid was measured accurately by considering amplitude attenuation of

the thermal oscillation from the boundary to the center of the fluid. The thermal conductivity

was not measured directly from the experiment because of the material defects of the reference

material. So the density was first measured and specific heat was calculated from [40].

$$C_{p,nf} = \frac{m_p\, C_{p,p} + m_f\, C_{p,f}}{m_p + m_f}$$ (4.10)

Finally the thermal conductivity was calculated from [40]

$$k_{nf} = \alpha_{nf}\, \rho_{nf}\, C_{p,nf}$$ (4.11)

The parametric data used for calculating the effective thermal conductivity are as follows:

$k_p = 20$ W/m-k, $k_f = 0.613$ W/m-k, $C_p = 4170$ J/kg k, $\mu_f = 8.55 \times 10^{-4}$ N s/m^2 ,

$v_f = 8.55 \times 10^{-7}$ N s/m^2, T = 300 K, $\rho_f = 997$ kg/m^3, $t_p = 2.844 \times 10^{-10}$ m [9].

Table 4. 3.Volume fraction and mean diameter of cluster for CuO (23.6 nm) – water nanofluids

Nanocluster	Simple Cubic	Body centered	Face Centered	Spherical
ϕ_c	0.4875	0.6056	0.6891	0.3793
γ_p (nm)	59.9726	59.9726	58.0361	72.5065

Table 4. 4.Comparison of k$_{eff}$ values for CuO (23.6 nm) – Water nanofluids

Volume Fraction	K_exp (W/m-K)	K_exp_sc (W/m-K)	K_exp_bc (W/m-K)	K_exp_fc (W/m-K)	K_exp_sp (W/m-K)	Hamilton
0.01	0.6359	0.6516	0.6522	0.6515	0.6480	0.6297
0.02	0.6562	0.6695	0.6697	0.6691	0.6661	0.6468
0.03	0.6772	0.6881	0.6877	0.6873	0.6854	0.6643
0.04	0.6985	0.7075	0.7063	0.7062	0.7057	0.682
Volume Fraction	Prasher (W/m-K)	Timofeeva (W/m-K)	Murshed (W/m-K)	Jeffrey (W/m-K)	Kumar (W/m-K)	
0.01	0.6522	0.6296	0.6451	0.6299	0.6522	
0.02	0.6583	0.6463	0.6778	0.6472	0.6583	
0.03	0.6645	0.6629	0.7112	0.665	0.6645	
0.04	0.6707	0.6795	0.7453	0.6832	0.6707	
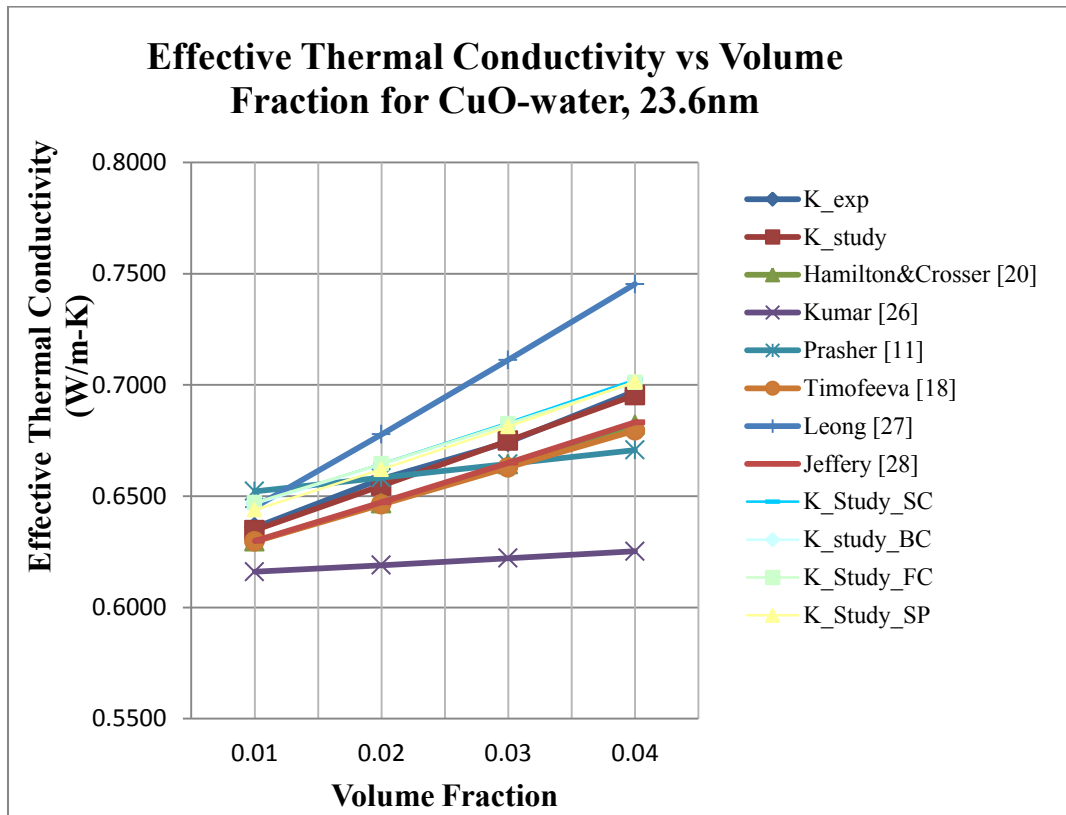
Figure 4. 6 Plot for the comparison of "K_eff" values for different models

CuO (23.6 nm) – Water nanofluids

The predicted values by the various models and the experimental values of the effective thermal conductivity are shown in table 4.4. Figure 4.6 contains the plots of the thermal conductivity as a function of solids volume fraction using the data in Table 4.4. It clearly shows that the thermal conductivity of nanofluids increases with the increase in the particle volume fraction. In addition, it is observed that the predicted thermal conductivity by the developed model is in good agreement with the experimental data. The results from the other models also followed the same trend as observed in the case of nanofluids with CuO particles of 18 nm.

CuO-EG 30.8 nm

The experimental data was collected from Eastman et al. [48]. For the experiment, Eastman et al. [48] used transient – hot wire (THW) method to measure the thermal conductivity of the nanofluid. It involves a wire suspended symmetrically in a liquid in a vertical cylinder container. THW technique works by measuring the temperature/time response of the wire to an abrupt electric pulse. The wire was used as both heater and thermometer and the thermal conductivity was measured by equation 4.8.

The parametric values used for model predictions are: k_p = 33 W/m-k, k_f=0.252 W/m-k, C_p = 2145 J/kg k, μ_f = 0.0157 N s/m^2 , v_f = 1.57× 10^{-5} N s/m^2, T = 300 K, ρ_f = 1113.2 kg/m^3, t_p=4.146 x 10^{-10} m [9].

The values for the effective thermal conductivities were calculated and are shown in Table 4.6. It should be noted that the nanofluids in this case was comprised of Ethylene Glycol as the base fluid. And thus there is a clear difference in the t_p as compared to the previous two cases. The data in Table 4.6 is plotted as a function of the volume fraction in Figure 4.7. It is

observed in Figure 4.7 that the experimental values are a nonlinear function of the volume

fraction. On the other hand, all the models evaluated showed a linear relationship. A close

observation of the models shows that at low concentrations, a linear relationship is expected.

This deviation may be a result of three causes. The first could simply be an experimental error.

The second reason may be due to the assumptions. For example, the Hamilton crosser assumes

a single particle with no nanolayer and no Brownian motion and such an assumption may be

valid at these volume fractions for the current nanofluids systems. However with an increase in

the volume fraction, clustering may become more evident and as a result, the model developed

in this thesis shows better correlation. The final cause may be that the mean particle diameter

shown is not sufficient to accurately predict the nanofluids behavior since the particles/cluster

may have a size distribution which is not very narrow. Thus care needs to be taken in

understanding the size distribution and the aggregation phenomena for accurate predictions.

Table 4. 5. Volume fraction and mean diameter of cluster for CuO (30.8 nm) – EG nanofluids.

Nanocluster	Simple Cubic	Body centered	Face Centered	Spherical
ϕ_c	0.4875	0.6056	0.6891	0.3793
γ_p (nm)	78.4848	78.4848	75.9507	94.8877

Table 4. 6.Comparison of k_eff values for CuO (30.8 nm) – EG nanofluids.

Volume Fraction	K_exp (W/m-K)	K_exp_sc (W/m-K)	K_exp_bc (W/m-K)	K_exp_fc (W/m-K)	K_exp_sp (W/m-K)	Hamilton
0.01	0.2621	0.26711	0.26732	0.26708	0.26585	0.2594
0.02	0.2797	0.27497	0.27504	0.27485	0.27386	0.267
0.03	0.2873	0.28318	0.28299	0.28288	0.28233	0.2748
0.04	0.2974	0.29176	0.29118	0.29120	0.29130	0.2827
Volume Fraction	Prasher (W/m-K)	Timofeeva (W/m-K)	Murshed (W/m-K)	Jeffrey (W/m-K)	Kumar (W/m-K)	
0.01	0.2724	0.2594	0.2668	0.2595	0.2581	
0.02	0.2778	0.2668	0.2819	0.2672	0.2643	
0.03	0.2816	0.2742	0.2974	0.2752	0.2706	
0.04	0.2862	0.2816	0.3133	0.2834	0.277	
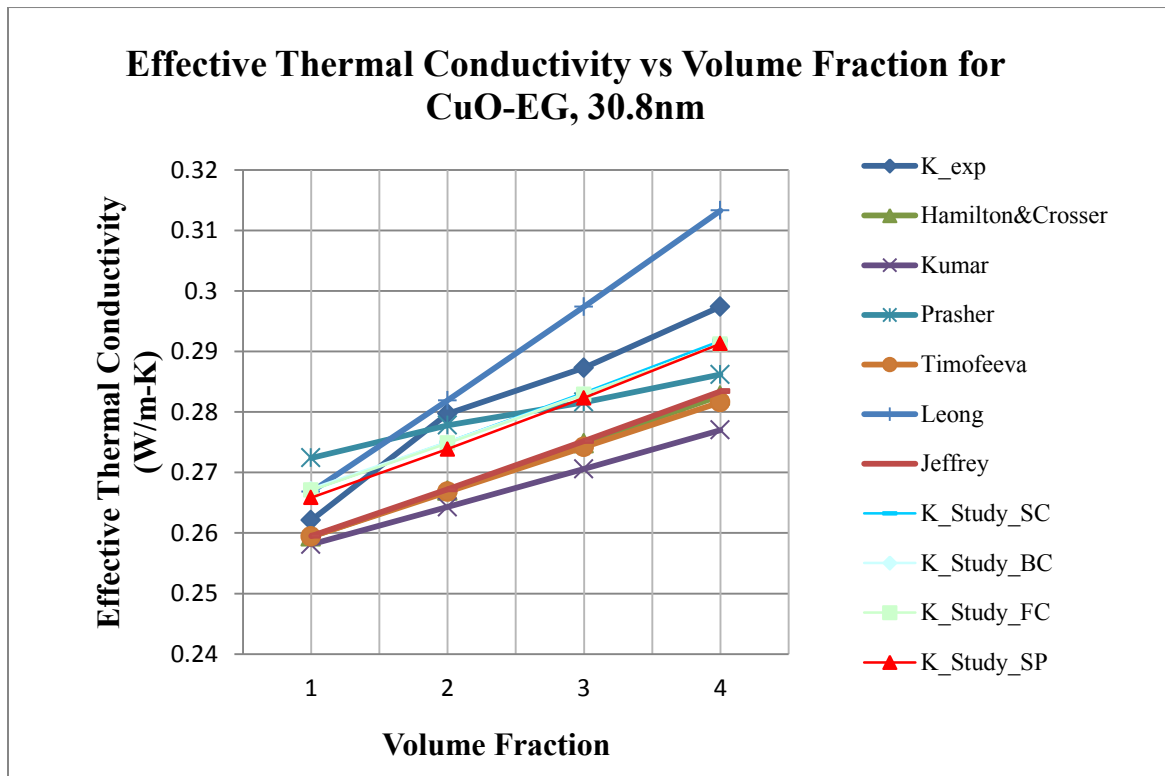
Figure 4. 7.Plot for the comparison of "K_eff " values for different models

CuO (30.8 nm) – EG nanofluids

Al_2O_3 – Water 60.4 nm

The experimental data was collected from Feng et al. [40]. The experimental procedure used is identical to that described in Section 4.2. The parametric values for this nanofluids are follows: $k_p = 42.34$ W/m-k, $k_f = 0.613$ W/m-k, $C_p = 4170$ J/kg k, $\mu_f = 8.55 \times 10^{-4}$ N s/m^2 , $v_f = 8.55 \times 10^{-7}$ N s/m^2, T = 300 K, $\rho_f = 997$ kg/m^3, $t_p = 2.844 \times 10^{-10}$ m the above data was used to calculate the effective thermal conductivity of the nanofluids using the various models developed and discussed.

The predicted values of the effective thermal conductivity are given in Table 4.8 and plotted as a function of volume fraction in Figure 4.8. It can be seen from the Figure 4.8 that the results are in excellent agreement with the published experimental data. From the Figure 4.8, the experimental values are not clearly seen as these values are jacketed by predicted values obtained from the developed model in thesis. Thus, it shows that the present model is the more accurate model.

Table 4. 7. Volume fraction and mean diameter of cluster for Al_2O_3 (60.4 nm) – Water nanofluids.

Nanocluster	Simple Cubic	Body centered	Face Centered	Spherical
ϕ_c	0.4875	0.6056	0.6891	0.3793
γ_p (nm)	151.2882	151.2882	146.4033	182.9065

Table 4. 8 Comparison of Effective Thermal Conductivity values for Al_2O_3 (60.4 nm) Water

nanofluids.

Volume fraction	K_exp (W/m-k)	K_exp_sc (W/m-K)	K_exp_bc (W/m-K)	K_exp_fc (W/m-K)	K_exp_sp (W/m-K)	Hamilton &Crosser (W/m-k)
0.01	0.6375	0.63688	0.63697	0.63681	0.63596	0.6307
0.02	0.6589	0.65556	0.65532	0.65527	0.65497	0.6489
0.03	0.6804	0.67500	0.67419	0.67432	0.67499	0.6669
0.04	0.6988	0.69525	0.69359	0.69400	0.69612	0.6862
Volume fraction	Prasher (W/m-k)	Timofeeva (W/m-k)	Murshed (W/m-k)	Jeffrey (W/m-k)	Kumar (W/m-k)	
0.01	0.6458	0.6306	0.6526	0.6309	0.6157	
0.02	0.6581	0.6482	0.6936	0.6493	0.6185	
0.03	0.6705	0.6658	0.7361	0.6682	0.6213	
0.04	0.6831	0.6835	0.7801	0.6877	0.6242	
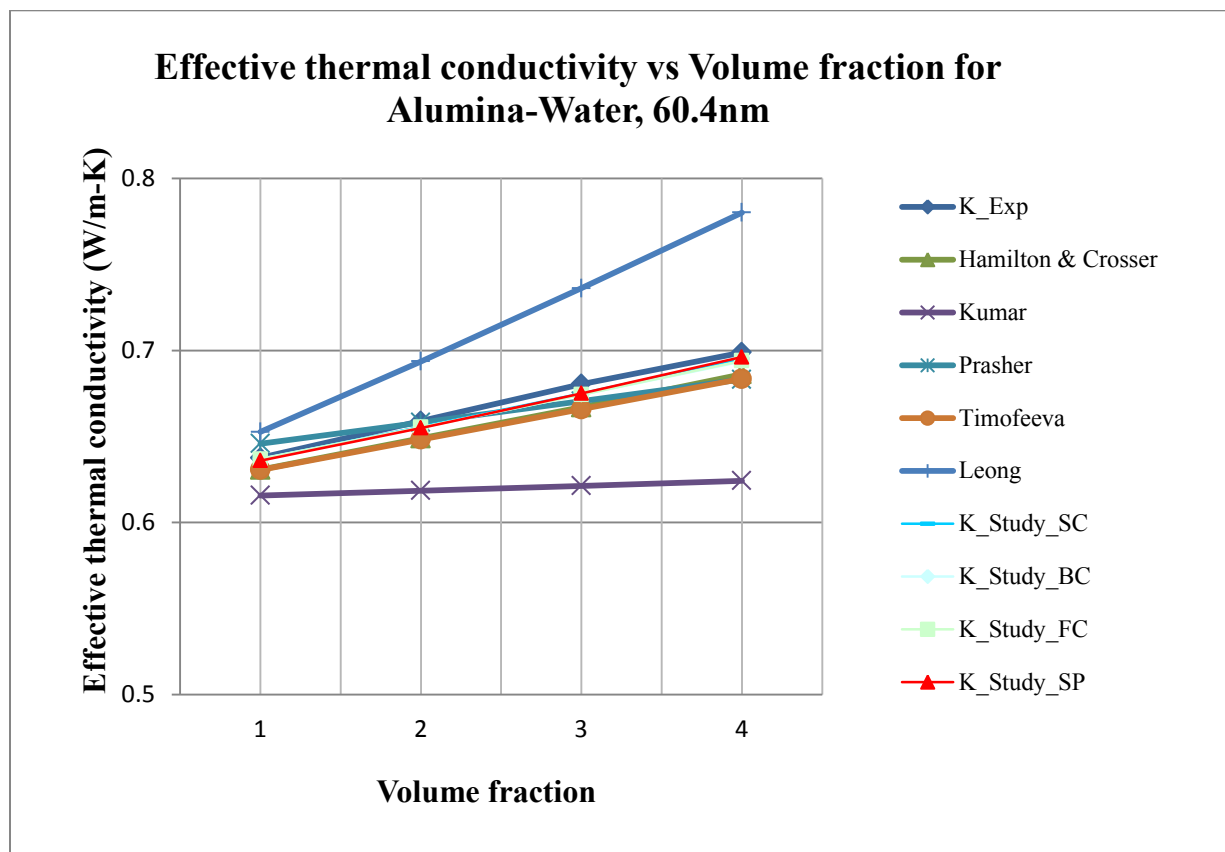
Figure 4. 8.Plot for the comparison of "K_eff' values for different models Alumia

(60.4 nm)– Water nanofluids.

Al$_2$O$_3$ – EG 26 nm

The experimental data was collected from Feng et al. [40]. The experimental conditions

are identical to that described in Section 4.2. The parametric values used for prediction are:

k_p = 42.34 W/m-k, k_f = 0.252 W/m-k, C_p = 2145 J/kg k, μ_f = 0.0157 N s/m^2 ,

ν_f = 1.57× 10^{-5} N s/m^2, T = 300K, ρ_f = 1113.2 kg/m^3, t_p=4.146 x 10^{-10} m.

To further validate the developed model,, it was used for the prediction of another

alumina-ethylene nanofluids wherein the diameter of nanoparticle is 26 nm. The effective

thermal conductivity values were estimated and the results are tabulated in Table 4.10 and

plotted as a function of volume fraction in Figure 4.9. Once again, the experimental values

coincide with the mathematical model values and slightly deviate at lower volume fractions

(Figure 4.9).

Table 4. 9. Volume fraction and mean diameter of cluster for Al$_2$O$_3$ (26 nm) – EG nanofluids.

Nanocluster	Simple Cubic	Body centered	Face Centered	Spherical
ϕ_c	0.4875	0.6056	0.6891	0.3793
γ_p (nm)	32.2582	32.2582	71.4892	80.4877

Table 4. 10.Comparison of Effective Thermal Conductivity values for Al_2O_3 (26 nm)– EG

nanofluids.

Volume fraction	K_exp (W/m-k)	K_exp_sc W/m-K)	K_exp_bc (W/m-K)	K_exp_fc (W/m-K)	K_exp_sp (W/m-K)	Hamilton &Crosser (W/m-k)
0.01	0.2625	0.27799	0.26784	0.27796	0.26701	0.2595
0.02	0.272	0.28590	0.27561	0.28577	0.27507	0.2682
0.03	0.2834	0.29417	0.28361	0.29386	0.28360	0.276
0.04	0.2909	0.30281	0.29186	0.30224	0.29265	0.284
Volume fraction	Prasher (W/m-k)	Timofeeva (W/m-k)	Murshed (W/m-k)	Jeffrey (W/m-k)	Kumar (W/m-k)	
0.01	0.2745	0.2594	0.2676	0.2595	0.2612	
0.02	0.2797	0.2669	0.2836	0.2673	0.2707	
0.03	0.285	0.2743	0.3002	0.2753	0.2803	
0.04	0.2904	0.2817	0.3173	0.2836	0.2898	
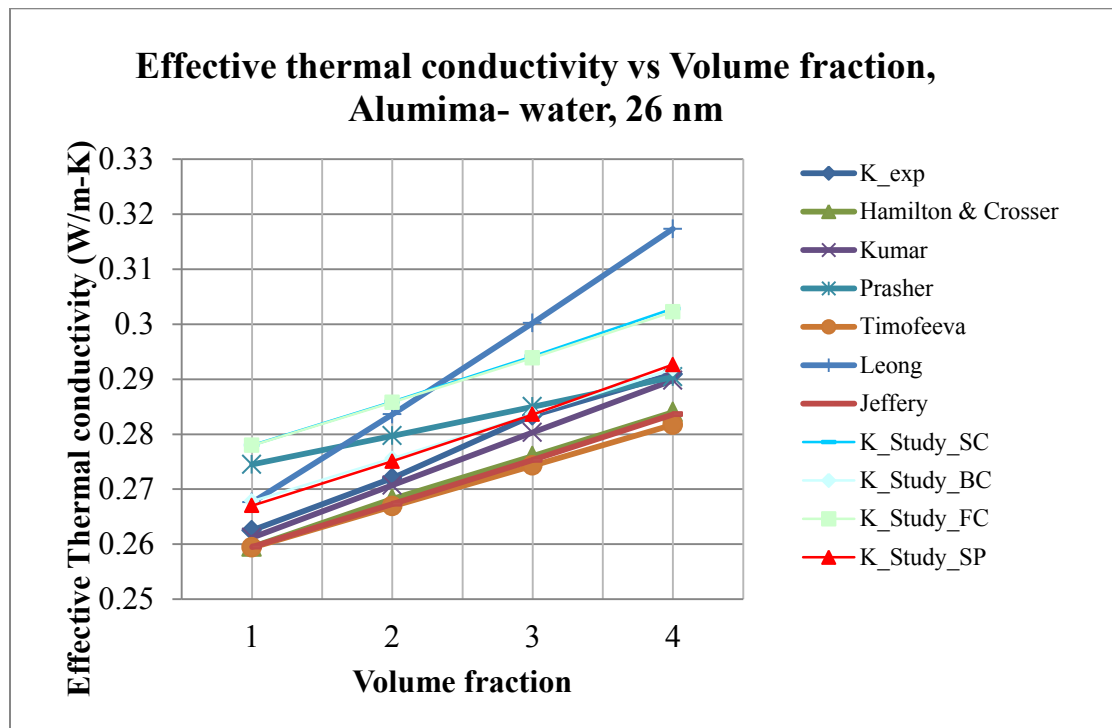
Figure 4. 9. Plot for the comparison of "K_eff " values for different model

Al_2O_3 (26 nm)– EG 26 nanofluids.

TiO$_2$ - Water 10 nm

The experimental data was collected from Kim et al. [49]. For the experiment, Kim et al. [49] used transient hot - wire method with an anodized tantalum wire to measure the thermal conductivity. A bare tantalum wire was electrically heated at an electrical potential of 50 v in citric-acid solution to form an oxide layer on the surface. The hot wire was calibrated in a constant temperature bath and the measured resistance was expressed in temperatures. Using this temperature Kim et al. [49] calculated the thermal conductivity. The electric current was adjusted to cause about 2 K temperature rise for 1 s. The voltage signal from the Wheatstone bridge was amplified by approximately 1000 times and a digital Oscilloscope reads the signal at a 2.5 kHz.

The parametric values used for model prediction in this case are as follows: $k_p = 8.37$ W/m-k, $k_f = 0.607$ W/m-k, $C_p = 4170$ J/kg k, $\mu_f = 8.55 \times 10^{-4}$ N s/m^2 , $v_f = 8.55 \times 10^{-7}$ N s/m^2, T = 300K, $\rho_f = 997$ kg/m^3, t_p=2.844 x 10^{-10} m.

Table 4.12 summarizes the effective thermal conductivity of titanium-dioxide nanofluids –both experimental and model predicted. The data is plotted as a function of volume fraction in Figure 4.10. From the Figure 4.10 it is clear that the present model is better than the competing models and is in concord with the experimental data. In addition, it is also observed that (Figure 4.10) the thermal conductivity values obtained by Prasher et al. [16] decreases with the increase in the volume fraction of the nanoparticles which is in the contrast to the results that Prasher et al. [37] got for other nanofluids. The results obtained from other models disagreed with the experimental data. Up to now the effective thermal conductivity results were presented for nanoparticle volume fractions 0.01, 0.02, 0.03 and 0.04. But in the case of Titanium oxide– Water/EG and Zinc oxide– Water/EG nanofluids the results are presented only for 0.01, 0.02

and 0.03 nanoparticle volume fraction due to the non-availability of data at volume fraction

0.04. The data shown in Figure 4.10 shows some degree of over-prediction by the current

models, while the Hamilton Crosser Model under-predicts the thermal conductivity values. The

over prediction by the current model may be a result of the clustering effect incorporated in the

model, but which may not be occurring in this manofluid. The Hamilton Crosser model may be

under predicting since it does not incorporate the Brownian motion and the resulting heat

transfer by convection. At such low particle sizes, Brownian motion should not be neglected.

Table 4. 11 Volume fraction and mean diameter of cluster for TiO_2 (10 nm) – Water nanofluids

Nanocluster	Simple Cubic	Body centered	Face Centered	Spherical
ϕ_c	0.4875	0.6056	0.6891	0.3793
γ_p (nm)	26.2255	26.2255	28.1617	31.7065

Table 4. 12.Comparison of k_{eff} values for TiO_2 (10 nm) – Water nanofluids

Volume fraction	K_exp (W/m-k)	K_exp_sc (W/m-K)	K_exp_bc (W/m-K)	K_exp_fc (W/m-K)	K_exp_sp (W/m-K)	Hamilton &Crosser (W/m-k)
0.01	0.627	0.65590	0.65347	0.65583	0.65015	0.6218
0.02	0.6537	0.67161	0.66886	0.67133	0.66617	0.6369
0.03	0.6761	0.68801	0.68471	0.68735	0.68315	0.6523
Volume fraction	Prasher (W/m-k)	Timofeeva (W/m-k)	Murshed (W/m-K)	Jeffrey (W/m-k)	Kumar (W/m-k)	
0.01	0.6577	0.6218	0.6357	0.6219	0.6102	
0.02	0.6576	0.6365	0.665	0.6372	0.6136	
0.03	0.6576	0.6513	0.6949	0.6528	0.6169	
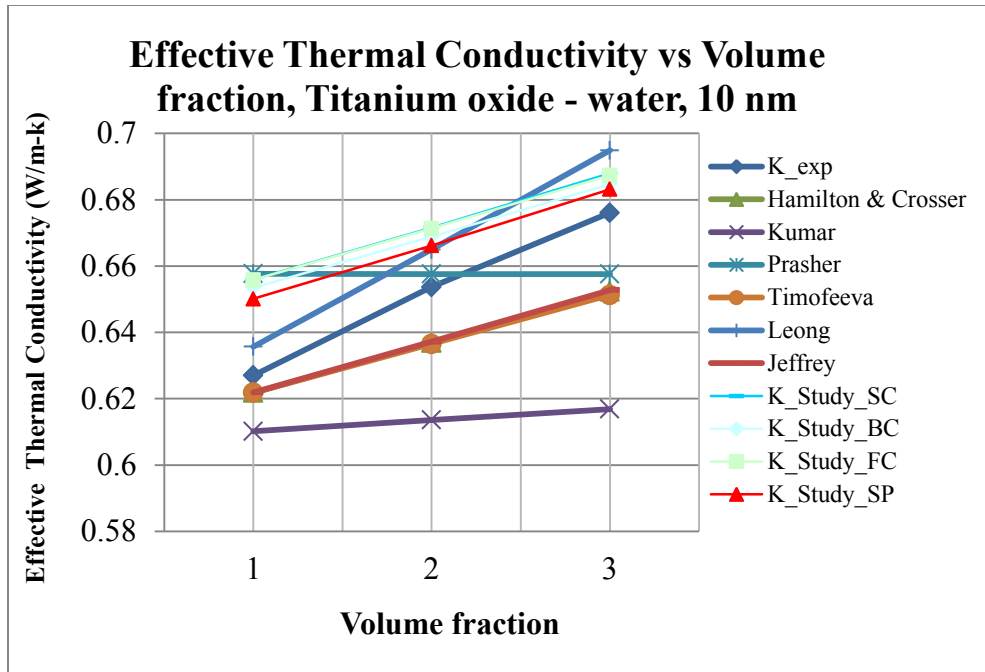
Figure 4. 10. Plot for the comparison of "K_eff " values for different TiO_2 (10 nm)–Water nanofluids.

TiO_2 - Water 34 nm

The experimental data was collected from Kim et al. [49]. The experimental conditions are identical as in the previous case. The parametric values used for the models are as follows:

k_p = 8.37 W/m-k, k_f = 0.607 W/m-k, C_p = 4170 J/kg k, μ_f = 8.55× 10^{-4} N s/m^2 ,

v_f = 8.55× 10^{-7} N s/m^2, T = 300K, ρ_f = 997 kg/m^3, t_p=2.844 x 10^{-10} m.

The thermal conductivity values were calculated for Titanium-oxide nanofluids and provided in table 4.14. From the figure 4.11 it is seen distinctly that thermal conductivity values are closer to the experimental data. The results from Jeffrey [46], Timofeeva et al. [44], Prasher et al. [16] and

Hamilton & Crosser [32] lie closer to the experimental data at different cases, but the

44

mathematical model displays better results in the entire range.

Table 4. 13 Volume fraction and mean diameter of cluster for TiO_2 (34 nm)– Water nanofluids

Nanocluster	Simple Cubic	Body centered	Face Centered	Spherical
ϕ_c	0.4875	0.6056	0.6891	0.3793
γ_p (nm)	85.7791	85.7791	92.1121	103.7065

Table 4. 14 Comparison of Effective Thermal Conductivity values TiO_2 (34 nm) – Water

nanofluids

Volume fraction	K_exp (W/m-k)	K_exp_sc (W/m-K)	K_exp_bc (W/m-K)	K_exp_fc (W/m-K)	K_exp_sp (W/m-K)	Hamilton &Crosser (W/m-k)
0.01	0.6239	0.6323	0.6315	0.6323	0.6306	0.6218
0.02	0.6452	0.6479	0.6468	0.6477	0.6465	0.6369
0.03	0.6598	0.6641	0.6625	0.6635	0.6632	0.6523
Volume fraction	Prasher (W/m-k)	Timofeeva (W/m-k)	Murshed (W/m-k)	Jeffrey (W/m-k)	Kumar (W/m-k)	
0.01	0.6432	0.6218	0.6338	0.6219	0.608	
0.02	0.6519	0.6365	0.6611	0.6372	0.6089	
0.03	0.6607	0.6513	0.6888	0.6528	0.6099	

Effective Thermal Conductivity vs Volume Fraction for Titanium Oxide-water, 34 nm
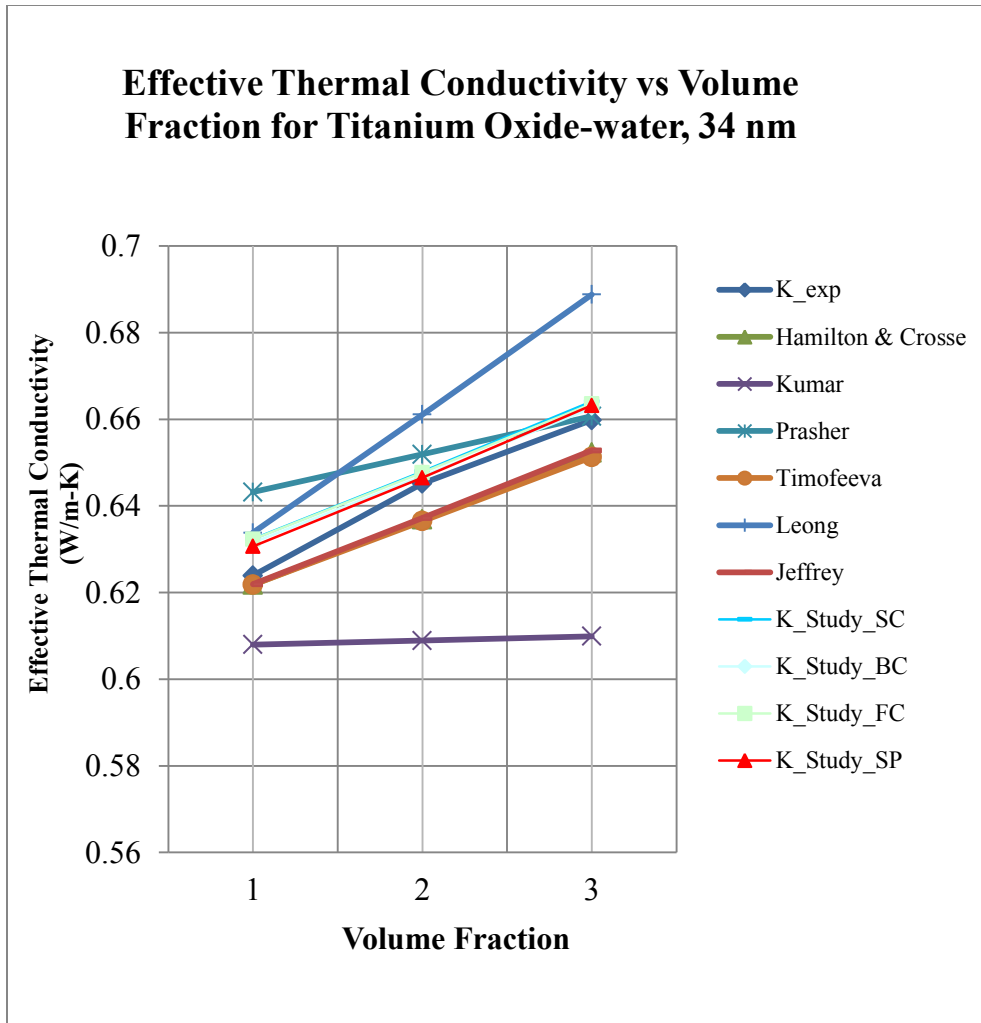
Figure 4. 11 Plot for the comparison of K _eff values for different models TiO_2 (33 nm) – Water

nanofluids

TiO_2 - Water 27 nm

The experimental data was collected from Xuan et al. [31]. The parametric values used for

model predictions are: k_p = 8.37 W/m-k, k_f = 0.613 W/m-k, C_p = 4170 J/kg k, μ_f =

8.55×10^{-4} N s/m^2 , $\nu_f = 8.55 \times 10^{-7}$ N s/m^2, T = 300K, ρ_f = 997 kg/m^3,

t_p=2.844 x 10^{-10} m.

The third set of validations was conducted to verify the consistency of the present model with the Titanium-oxide nanofluids. The results are tabulated in Table 4.16 and the data was plotted as function of volume fraction in Figure 4.12. It is seen in Figure 4.12 that thermal conductivity values are in excellent agreement with the experimental data. For this type of nanofluids combination the Kumar et al. [44] model did not show any significant enhancement which indicates the dominance of present model. The results from Hamilton & Crosser [32], Prasher et al. [16] and Timofeeva et al. [25] were able to explain significant portion of the enhancement but were not thorough enough to explain the unusual thermal conductivity of the nanofluids observed during experimentation.

Table 4. 15 Volume fraction and mean diameter of cluster for TiO$_2$ (27 nm) – water

      nanofluids

Nanocluster	Simple Cubic	Body centered	Face Centered	Spherical
ϕ_c	0.4875	0.6056	0.6891	0.3793
γ_p (nm)	68.4093	68.4093	73.4599	82.7065

Table 4. 16 Comparison of Effective Thermal Conductivity values for TiO$_2$ (27 nm) – water

nanofluids

Volume fraction	K_exp (W/m-k)	K_exp_sc (W/m-K)	K_exp_bc (W/m-K)	K_exp_fc (W/m-K)	K_exp_sp (W/m-K)	Hamilton &Crosser (W/m-k)
0.01	0.6314	0.64124	0.64025	0.64118	0.63907	0.628
0.02	0.6498	0.65697	0.65569	0.65671	0.65508	0.6432
0.03	0.6651	0.67330	0.67153	0.67272	0.67192	0.6587
Volume fraction	Prasher (W/m-k)	Timofeeva (W/m-k)	Murshed (W/m-k)	Jeffrey (W/m-k)	Kumar (W/m-k)	
0.01	0.651	0.6279	0.6402	0.628	0.6142	
0.02	0.6581	0.6427	0.6678	0.6434	0.6154	
0.03	0.6653	0.6576	0.6959	0.6592	0.6167	
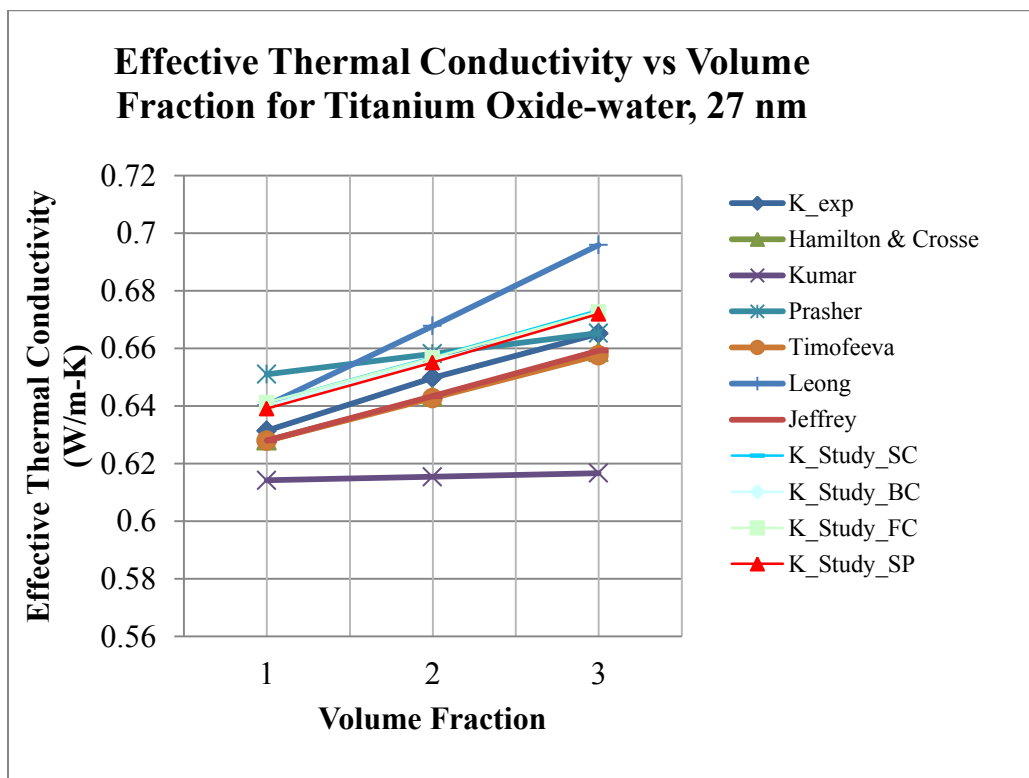
Figure 4. 12 Plot for the comparison of "K_eff " values for different models TiO$_2$ (27 nm) –

Water nanofluids

TiO$_2$ - EG 34 nm

The experimental data was collected from Kim et al. [49]. The experimental procedures are identical to that described in Section 4.6. The parametric values used for predicting thermal conductivities are as follows: k_p = 8.37 W/m-k, k_f = 0.252 W/m-k, C_p = 2145 J/kg k, μ_f = 0.0157 N s/m^2 , v_f = 1.57× 10^{-5} N s/m^2, T = 300K, ρ_f = 1113.2 kg/m^3, t_p=4.146 x 10^{-10} m. The developed model (for all cluster structures) was tested for Titanium oxide – Ethylene Glycol. The results are shown in Table 4.18 and plotted in Figure 4.13. As seen from the figure 4.13, it is once again shown that the model developed in this thesis explains the conductivity enhancement in nanofluids more comprehensively than competing models. As observed earlier, the results predicted by Prasher et al. [16] and Leong et al. [45] models overestimated the experimental data whereas the other models underestimated the data.

Table 4. 17 Volume fraction and mean diameter of cluster for TiO$_2$ (34 nm) - EG 34 nanofluids

Nanocluster	Simple Cu bic	Body cente red	Face Cent ered	Spherical
ϕ_c	0.4875	0.6056	0.6891	0.3793
γ_p (nm)	86.4253	86.4253	92.8060	104.4877

Table 4. 18 Comparison of Effective Thermal Conductivity values for TiO2 (34 nm) - EG 34

nanofluids

Volume fraction	K_exp (W/m-k)	K_exp_sc (W/m-K)	K_exp_bc (W/m-K)	K_exp_fc (W/m-K)	K_exp_sp (W/m-K)	Hamilton &Crosser (W/m-K)
0.01	0.261	0.26593	0.26541	0.26590	0.26478	0.2589
0.02	0.2719	0.27327	0.27262	0.27315	0.27226	0.267
0.03	0.2829	0.28092	0.28003	0.28064	0.28015	0.2733
Volume fraction	Prasher (W/m-k)	Timofeeva (W/m-K)	Murshed (W/m-K)	Jeffrey (W/m-K)	Kumar (W/m-K)	
0.01	0.2734	0.2599	0.2664	0.26	0.2544	
0.02	0.2782	0.2669	0.28	0.2673	0.2558	
0.03	0.2831	0.2738	0.2939	0.2747	0.2573	
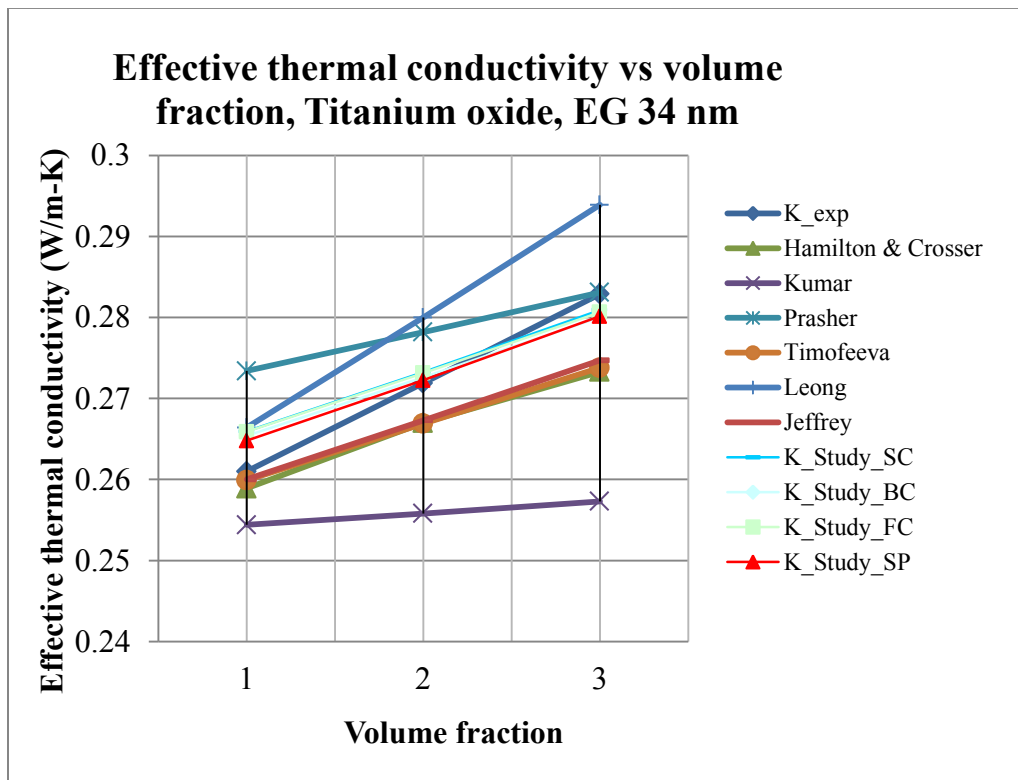
Figure 4. 13 Plot for the comparison of "K_eff" values for different models

TiO2 (34 nm) - EG 34 nanofluids

ZnO – Water 10 nm

The experimental data was collected from Kim et al. [49]. The experimental procedure is identical to that described in Section 4.6. The modeling parameters used are: $k_p = 29$ W/m-k, $k_f = 0.607$ W/m-k, $C_p = 4170$ J/kg k, $\mu_f = 8.55 \times 10^{-4}$ N s/m^2, $\nu_f = 8.55 \times 10^{-7}$ N s/m^2, T = 300K, $\rho_f = 997$ kg/m^3, $t_p = 2.884 \times 10^{-10}$ m.

Here the study investigated the validity of the model for ZnO – Water nanofluids. So far no previous models have shown their validation against ZnO - Water or Ethylene Glycol nanofluids. The present study has shown some good results for ZnO in Water or Ethylene Glycol. The values are calculated and tabulated in Table 4.20. Figure 4.14 shows that the thermal conductivity agreement with the experimental data at higher volume fraction and at lower fraction the mathematical model predicted values are slightly higher than the experimental data. The deviation may be a result of the fact that the clustering is either too low or thus single particle cases need to be considered. The trend seems to be similar to the previous case of 10 nm nanoparticle based nanofluids.

Table 4. 19 Volume fraction and mean diameter of cluster for ZnO (10 nm) -Water nanofluids

Nanocluster	Simple Cubic	Body centered	Face Centered	Spherical
ϕ_c	0.4875	0.6056	0.6891	0.3793
γ_p (nm)	26.2255	26.2255	28.1617	31.7065

Table 4. 20 Comparison of Effective Thermal Conductivity values for ZnO (10 nm) -Water

nanofluids

Volume fraction	K_exp (W/m-k)	K_exp_sc (W/m-K)	K_exp_bc (W/m-K)	K_exp_fc (W/m-K)	K_exp_sp (W/m-K)	Hamilton & Crosser (W/m-k)
0.01	0.6367	0.65833	0.65589	0.65825	0.65260	0.6242
0.02	0.6652	0.67663	0.67382	0.67631	0.67127	0.6419
0.03	0.6931	0.69579	0.69232	0.69503	0.69110	0.6579
Volume fraction	Prasher (W/m-k)	Timofeeva (W/m-k)	Murshed (W/m-k)	Jeffrey (W/m-k)	Kumar (W/m-k)	
0.01	0.6637	0.6303	0.6482	0.6305	0.6242	
0.02	0.6635	0.6475	0.6843	0.6486	0.6357	
0.03	0.6634	0.6648	0.7215	0.6671	0.6474	
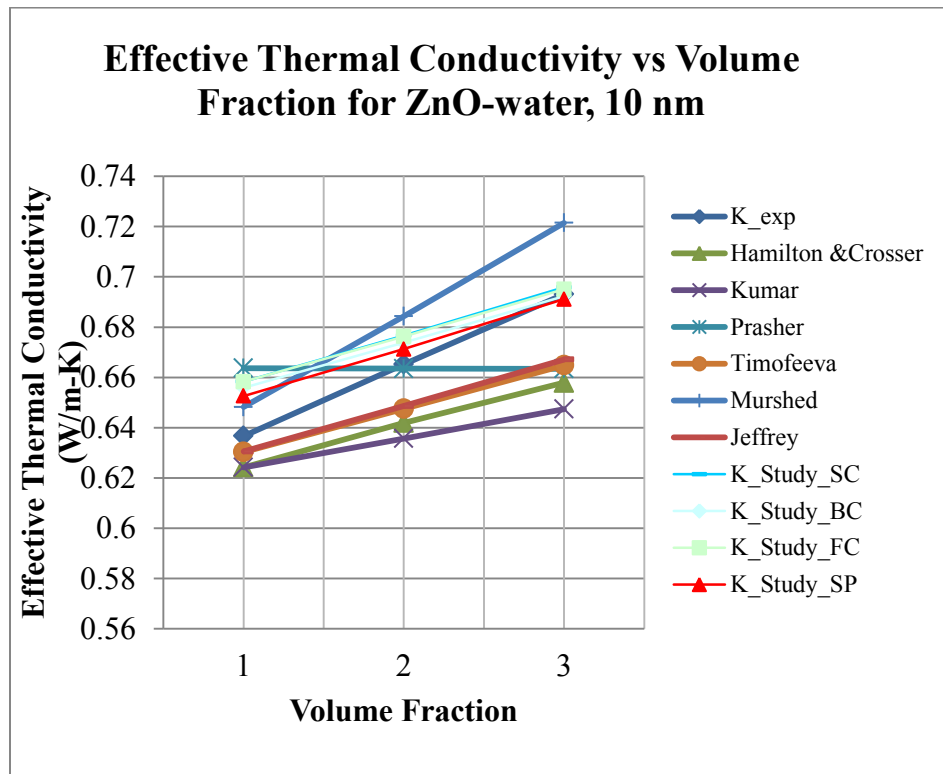
Figure 4. 14 Plot for the comparison of "K_eff " values for different models ZnO-water 10 nm

ZnO – Water 30 nm

The experimental data was collected from Kim et al. [49]. The experimental procedure is

identical to that described in Section 4.6. The values used for thermal conductivity predictions

are as follows:k_p = 29 W/m-k, k_f = 0.607 W/m-k, C_p = 4170 J/kg k, μ_f = 8.55× 10^{-4} N s/m^2 ,

v_f = 8.55× 10^{-7} N s/m^2, T = 300K, ρ_f = 997 kg/m^3, t_p=2.884 x 10^{-10} m.

Here the data obtained for 30 nm ZnO-water system has been used for comparison with

model prediction which are tabulated in Table 4.22 and plotted as a function of volume fraction

in Figure 4.15. It is clearly seen from the Figure 4.15 that the thermal conductivity increases

with an increase in the volume fraction of the nanoparticles. In addition, the predicted values

are seen to be a good match to the experimentally observed data. In this scenario, the results

obtained from Timofeeva et al. [44] and Prasher et al. [16] are somewhat closer to the

experimental data but enough to completely agree. This is slightly unusal since the models that

were previously under predicting the experimental data are also observed to over predict. This

may be a result of experimental error or (more likely) a result of other phenomenon such as

surface interactions with the fluid which result in these deviations.

Table 4. 21 Volume fraction and mean diameter of cluster for ZnO (30 nm) – Water nanofluids

Nanocluster	Simple Cubic	Body centered	Face Centered	Spherical
ϕ_c	0.4875	0.6056	0.6891	0.3793
γ_p (nm)	75.8535	75.8535	81.4537	91.7065

Table 4. 22 Comparison of Effective Thermal Conductivity values for ZnO (30 nm) – Water

nanofluids

| Volume fraction	K_exp (W/m-k)	K_exp_sc (W/m-K)	K_exp_bc (W/m-K)	K_exp_fc (W/m-K)	K_exp_sp (W/m-K)	Hamilton & Crosser (W/m-k)
0.01	0.627	0.63615	0.63524	0.63608	0.63423	0.6242
0.02	0.65	0.65432	0.65308	0.65403	0.65273	0.6419
0.03	0.6768	0.67324	0.67143	0.67257	0.67224	0.6598
Volume fraction	Prasher (W/m-k)	Timofeeva (W/m-k)	Murshed (W/m-k)	Jeffrey (W/m-k)	Kumar (W/m-k)	
0.01	0.6501	0.6303	0.6468	0.6305	0.6167	
0.02	0.658	0.6475	0.6814	0.6486	0.6206	
0.03	0.666	0.6648	0.7166	0.6671	0.6245	
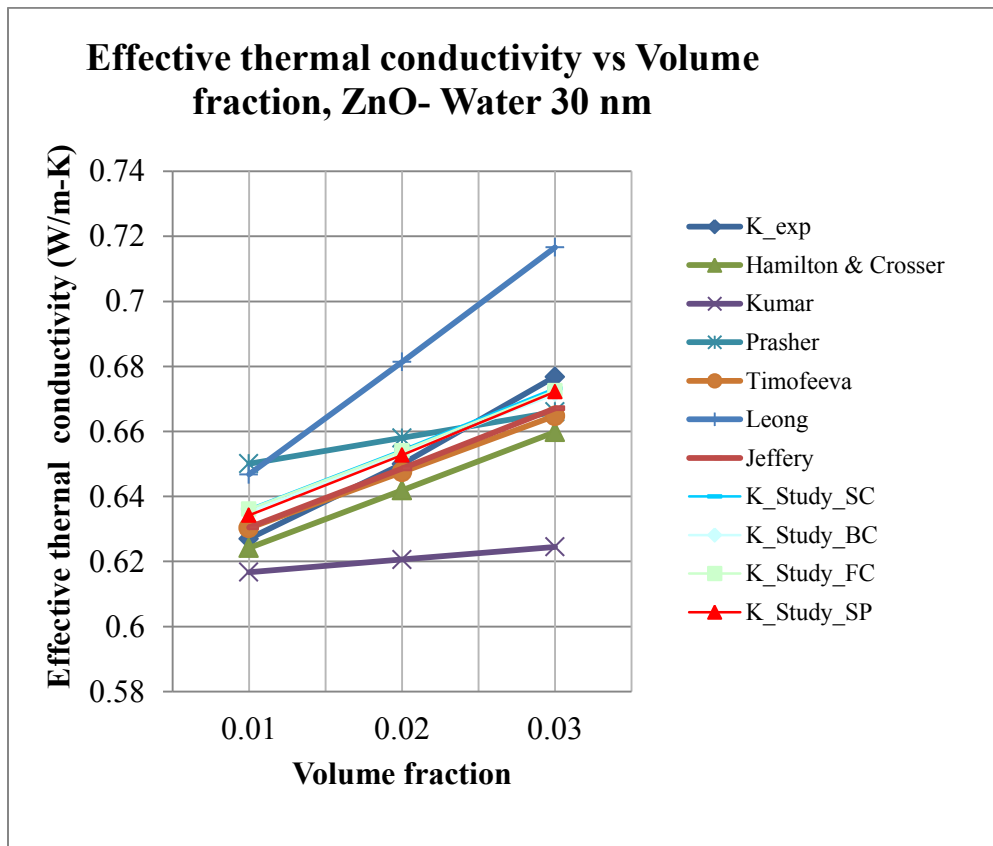
Figure 4. 15 Plot for the comparison of "K_eff " values for different models

ZnO (30 nm) – Water nanofluids

ZnO – EG 60 nm

The experimental data was collected from Kim et al. [49]. The experimental conditions are identical to that described in Section 4.6. The nanofluids characteristic values used for the model predictions are:k_p = 29 W/m-k, k_f = 0.252 W/m-k C_p = 2145 J/kg k, μ_f = 0.0157 N s/m^2 , ν_f = 1.57× 10^{-5} N s/m^2, T = 300K, ρ_f = 1113.2 kg/m^3, t_p=4.146 x 10^{-10} m.

The present model was also validated for ZnO-EG nanofluids. Table 4.24 epitomizes the thermal conductivity values for different volume fractions. This time also the model completely agreed with the experimental data. The results are plotted as shown in the figure 4.16. The other model predations followed the same pattern as that observed for previous nanofluids. For ZnO-Water/EG nanofluids Prasher et al. [16], Timofeeva et al. [44], Hamilton & Crosser [32] and Jeffrey [46] models performed significantly well but not the predictions were not as close as that obtained from the current model

Table 4. 23 Volume fraction and mean diameter of cluster for ZnO (60 nm) – EG nanofluids

Nanocluster	Simple Cubic	Body centered	Face Centered	Spherical
ϕ_c	0.4875	0.6056	0.6891	0.3793
γ_p (nm)	150.9418	150.9418	162.0856	182.4877

Table 4. 24 Comparison of Effective Thermal Conductivity values for ZnO (60 nm) – EG

nanofluids

| Volume fraction	K_exp (W/m-k)	K_exp_sc (W/m-K)	K_exp_bc (W/m-K)	K_exp_fc (W/m-K)	K_exp_sp (W/m-K)	Hamilton & Crosser (W/m-k)
0.01	0.2601	0.26345	0.26313	0.26342	0.26281	0.2594
0.02	0.2699	0.27127	0.27081	0.27115	0.27077	0.267
0.03	0.279	0.27942	0.27872	0.27913	0.27917	0.2747
Volume fraction	Prasher (W/m-k)	Timofeeva (W/m-k)	Murshed (W/m-k)	Jeffrey (W/m-k)	Kumar (W/m-k)	
0.01	0.2693	0.2594	0.2667	0.2595	0.2547	
0.02	0.2752	0.2667	0.2816	0.2672	0.2575	
0.03	0.2813	0.2741	0.2969	0.2751	0.2604	
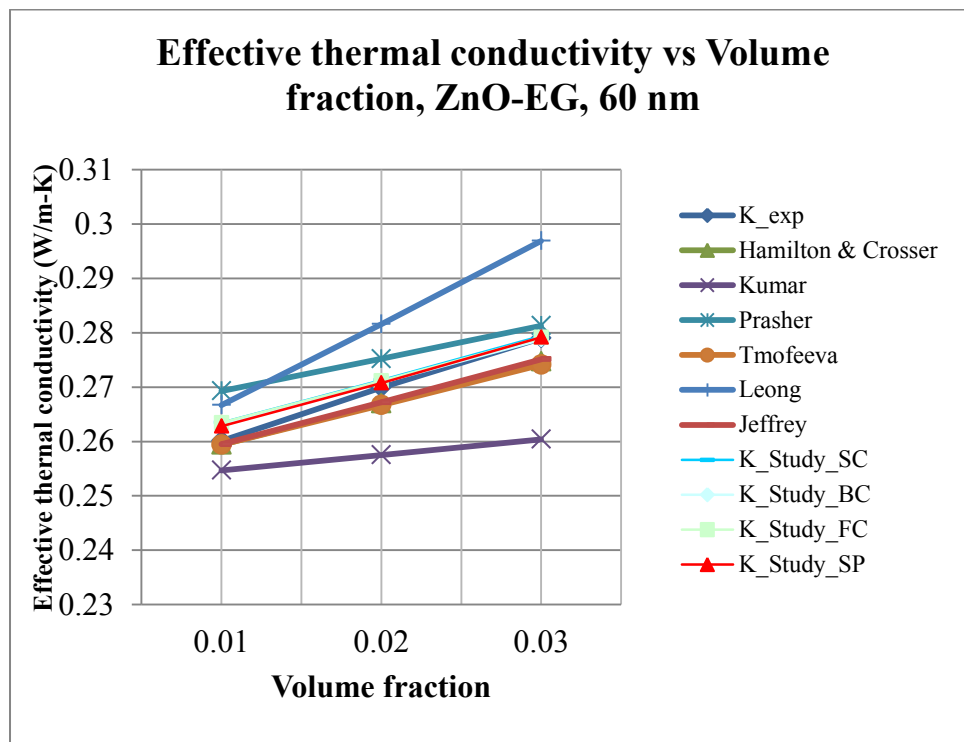
Figure 4. 16 Plot for the comparison of "K_eff " values for different models

ZnO (60 nm) – EG nanofluids

Cu-Water 100 nm

The experimental data was collected from Xuan et al. [31]. The nanofluids parameters used for the model predictions are as follow:k_p = 401 W/m-k, k_f = 0.613 W/m-k, C_p = 4170 J/kg k, μ_f = 8.55× 10^{-4} N s/m^2 , v_f= 8.55× 10^{-7} N s/m^2, T = 300K, ρ_f = 997 kg/m^3, t_p=2.844 x 10^{-10} m.

The thermal conductivity values are calculated sign the various models and tabulated in Table 4.26. It is seen in Figure 4.17 that the developed model does not model the 100nm Cu-Water nanofluids system. The reason may be due to the larger diameter of the nanoparticles. Till date there is no procedure for accurate calculation of the nanolayer thickness and the previous investigators arbitrarily chose the nanolayer thickness without proof. As stated by Tillman [51] the nanolayer thickness is dependent on the diameter of the nanoparticles. From the figure 4.13 it is visible that the present model does not match with experimental data except the Leong et al. [45] model but it overestimated the experimental data.

Table 4. 25 Volume fraction and mean diameter of cluster for Cu (100 nm) – Water nanofluids

Nanocluster	Simple Cubic	Body centered	Face Centered	Spherical
ϕ_c	0.4875	0.6056	0.6891	0.3793
γ_p (nm)	249.5517	249.5517	267.9757	301.7065

Table 4. 26 Comparison of Effective Thermal Conductivity values for Cu (100 nm) – Water

nanofluids

| Volume fraction	K_exp (W/m-k)	K_exp_sc (W/m-K)	K_exp_bc (W/m-K)	K_exp_fc (W/m-K)	K_exp_sp (W/m-K)	Hamilton &Crosser (W/m-k)
0.01	0.6559	0.63526	0.63490	0.63519	0.63474	0.6315
0.02	0.711	0.65468	0.65399	0.65438	0.65450	0.6504
0.03	0.7539	0.67490	0.67361	0.67420	0.67533	0.6696
0.04	0.8091	0.69597	0.69381	0.69468	0.69730	0.6893
Volume fraction	Prasher (W/m-k)	Timofeeva (W/m-k)	Murshed (W/m-k)	Jeffrey (W/m-k)	Kumar (W/m-k)	
0.01	0.6435	0.6313	0.6664	0.6316	0.6286	
0.02	0.6581	0.6496	0.7219	0.6508	0.6444	
0.03	0.6729	0.6679	0.7795	0.6705	0.6606	
0.04	0.688	0.6862	0.8395	0.6909	0.6772	
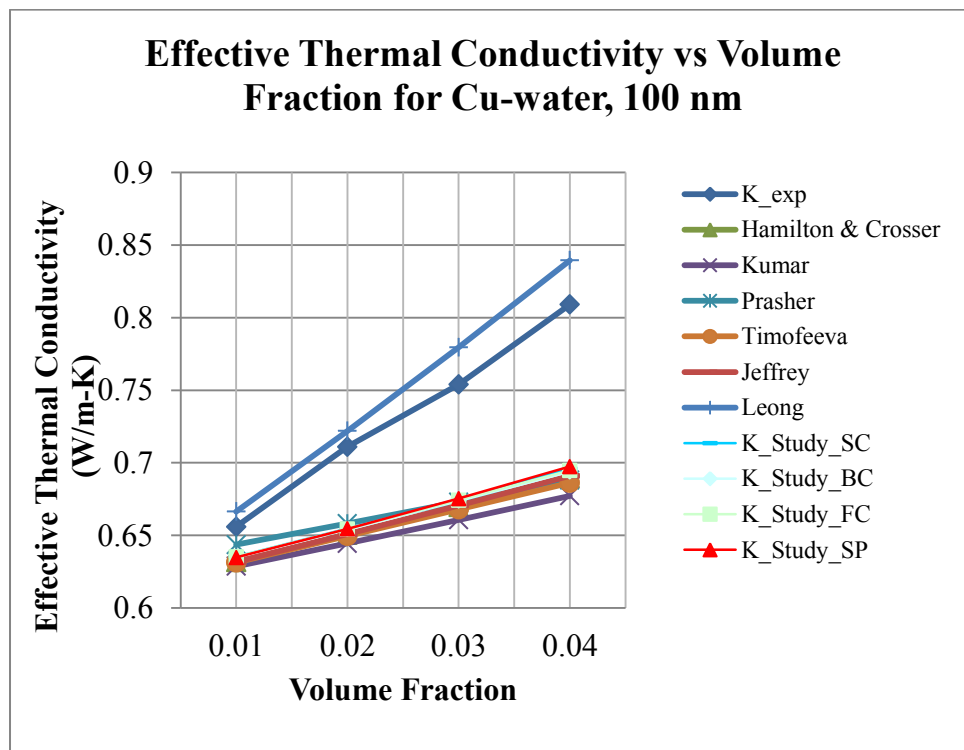
Figure 4. 17 Plot for the comparison of "K_eff " values for different models

Cu (100 nm) – Water nanofluids

Al-Water 20 nm

The experimental data was collected from Xuan et al. [31]. The model parameters are:

k_p = 237 W/m-k, k_f = 0.613 W/m-k, C_p = 4170 J/kg k, μ_f = 8.55× 10^{-4} N s/m^2 ,

v_f = 8.55× 10^{-7} N s/m^2, T = 300K, ρ_f = 997 kg/m^3, t_p=2.844 x 10^{-10} m.

The developed model was also validated for Al-Water nanofluids. The results are

calculated and tabulated in Table 4.28 also It is seen in Figure 4.18 that the present model is in

excellent agreement with the experimental data. The other models repeated the same trends in

over prediction and underestimation as observed earlier. An interesting phenomenon was

observed from Kumar et al. [39] model. Up to this point the results predicted by the model

developed by Kumar was always under predicting the experimental data. However, in this

system it overestimated not only experimental data but also all other models. The study could

not figure any conclusions from this eccentric behavior of the Kumar et al. [39] model.

Table 4. 27 Volume fraction and mean diameter of cluster for Al (20 nm) – Water

nanofluids

Nanocluster	Simple Cubic	Body centered	Face Centered	Spherical
ϕ_c	0.4875	0.6056	0.6891	0.3793
γ_p (nm)	51.0395	51.0395	54.8077	61.7065

Table 4. 28 Comparison of Effective Thermal Conductivity values for Al (20 nm) – Water

nanofluids

| Volume fraction	K_exp (W/m-k)	K_exp_sc (W/m-K)	K_exp_bc (W/m-K)	K_exp_fc (W/m-K)	K_exp_sp (W/m-K)	Hamilton &Crosser (W/m-k)
0.01	0.6345	0.64919	0.64787	0.64911	0.64604	0.6314
0.02	0.659	0.66863	0.66694	0.66831	0.66512	0.6502
0.03	0.6878	0.68892	0.68660	0.68818	0.68478	0.6694
0.04	0.7049	0.71014	0.70687	0.70876	0.70505	0.689
Volume fraction	Prasher (W/m-k)	Timofeeva (W/m-k)	Murshed (W/m-k)	Jeffrey (W/m-k)	Kumar (W/m-k)	
0.01	0.6538	0.6312	0.6529	0.6315	0.659	
0.02	0.6587	0.6495	0.6941	0.6506	0.7059	
0.03	0.6637	0.6677	0.7369	0.6703	0.7537	
0.04	0.6686	0.686	0.7811	0.6906	0.8026	
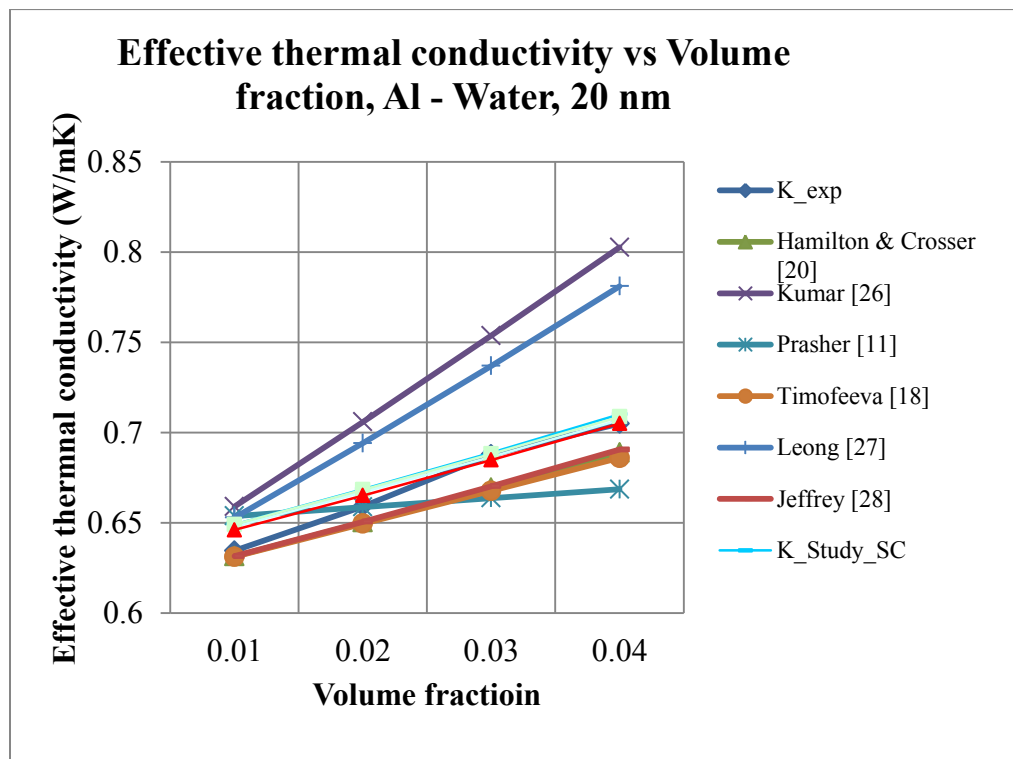
Figure 4. 18 Plot for the comparison of "K_eff " values for different model

Al (20 nm) – Water nanofluids

Fe-EG 10nm

The experimental data was taken from Hong and Yang [50]. For the experiment, Hong and Yang [50] used transient hot wire method for calculating thermal conductivity of nanofluids. The experiment procedure is the same as that of Eastman et al. [48] except that the wire used was Teflon-coated pure platinum wire. The model parameters used are: $k_p = 80.4$ W/m-k, $k_f = 0.253$ W/m-k, $C_p = 2145$ J/kg k, $\mu_f = 0.0157$ N s/m^2, $\nu_f = 1.57 \times 10^{-5}$ N s/m^2, T = 300K, $\rho_f = 1113.2$ kg/m^3, $t_p = 2.844 \times 10^{-10}$ m.

The model predictions are shown in figure 4.19. At the first glance the model does not seem to model the nanofluids system well. However a closer scrutiny showed some interesting information. This time the Prasher et al. [16] model and Kumar et al. [39] model prediction were is close agreement to the experimental data, when compared to the developed model. In all the cases discussed thus far in the thesis, the model by Leong et al. [45] overestimated the thermal conductivities but in this case it underestimated the experimental data. So this hypothesized that a very low volume fraction may be responsible for the disagreement of the results. In addition, the thermal conductivity values of nanofluids are measured after sonicating the nanofluids for 70 mins. After sonicating, the thermal conductivity was increased to 6.5% for the volume fractions given below [50]. This directly indicates that the solids dispersion was not efficient in the beginning and a good dispersion may yield better thermal conductivites –closer to the predicted values.

Table 4. 29 Volume fraction and mean diameter of cluster for Fe (10 nm) – Water nanofluids

Nanocluster	Simple Cubic	Body centered	Face Centered	Spherical
ϕ_c	0.4875	0.6056	0.6891	0.3793
γ_p (nm)	26.2255	26.2255	28.1617	31.7065

Table 4. 30 Comparison of Effective Thermal Conductivity values for Fe (10 nm) – Water

nanofluids

Volume fraction	K_exp (W/m-K)	K_exp_sc (W/m-K)	K_exp_bc (W/m-K)	K_exp_fc (W/m-K)	K_exp_sp (W/m-K)	Hamilton & Crosser (W/m-K)
0.002	0.2693	0.27479	0.27377	0.27476	0.27241	0.2545
0.003	0.2758	0.28284	0.28166	0.28270	0.28062	0.2552
0.004	0.2779	0.29129	0.28981	0.29095	0.28936	0.256
0.0055	0.2802	0.30014	0.29824	0.29952	0.29867	0.2571
Volume Fraction	**Prasher (W/m-K)**	**Timofeeva (W/m-K)**	**Leong (W/m-K)**	**Jeffrey (W/m-K)**	**Kumar (W/m-K)**	
0.002	0.2811	0.2515	0.2529	0.2545	0.262	
0.003	0.2812	0.2522	0.2543	0.2553	0.2666	
0.004	0.2814	0.253	0.2558	0.256	0.2711	
0.0055	0.2815	0.2541	0.258	0.2572	0.2779	
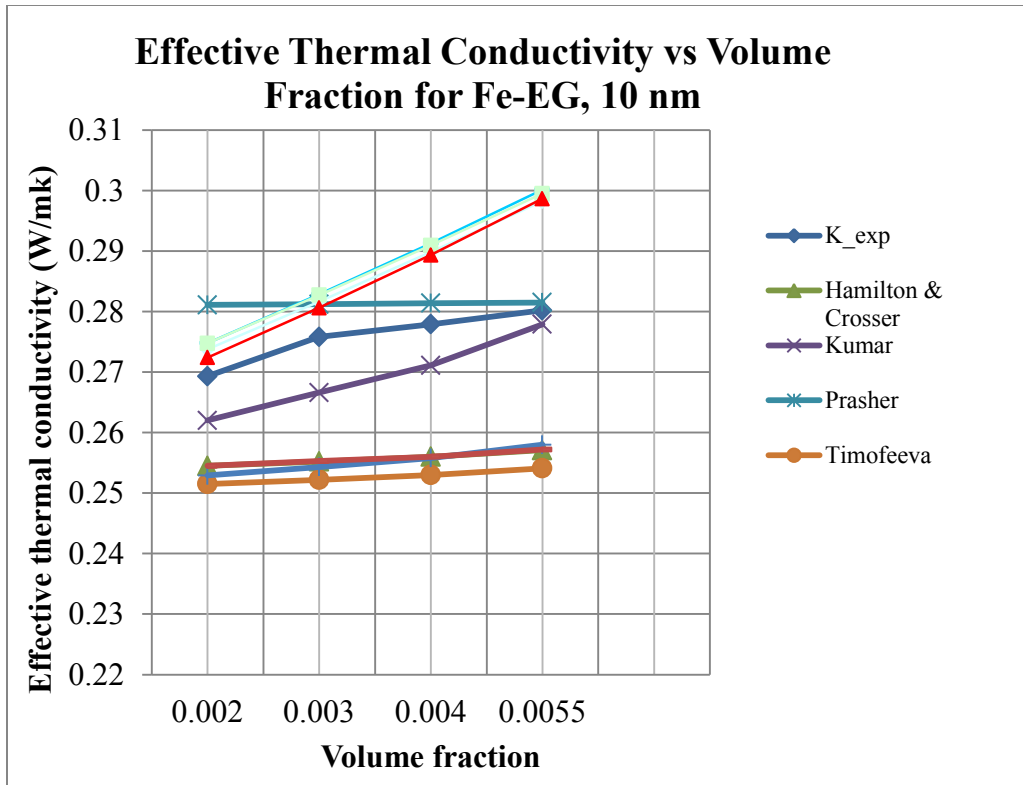
Figure 4. 19 Plot for the comparison of "K_eff " values for different models
Fe-EG 10 nm

The above mentioned experimental thermal conductivities at all volume fractions are decreased by about 6.5 % and tabulated in Table 4.15. The reason for the decrease is that the values were measured after sonicating the nanofluid for 70 min. Now the calculated values represent the natural thermal conductivity of the nanofluids. The new results were plotted in Figure 4.6. As seen from Figure the present model has shown a decent behavior by getting closer to experimental data. Previously predictions by Prasher et al. [16] model were a better, match to experimental data but now it overestimated the experimental data. Also looking closely, as the volume fraction of nanoparticles increased, no enhancement of thermal conductivity values was predicted by the Prasher et al. [16] model. This is in contrast to theory

because the thermal conductivity should increase when concentration of nanoparticles are increased. So far Kumar et al. [39] model did not explain the unusual behavior of nanofluids. But as seen from Figure 4.2 it is the only model that successfully agreed to the experimental data. This shows that Kumar et al. [39] model is not consistent but may have some characteristic that is worth investigating to improve the current model.

Conclusion

From the discussions above and all the graphs, the study concluded that the developed model is more accurate than the other models. The model was validated for a wide range of available nanofluid combinations. Previous studies by many researchers did not include the results as depicted in the present study. The value of the constant $C = 0.7*Pr$ is used for all Water and Ethylene Glycol based nanofluids. The thermal conductivity of the nanofluids increased with increase in volume fraction of the nanoparticles. The model is in good agreement with experimental data for almost all the nanofluids except for Cu –water and Fe – EG. The reasons for the discrepancy were explained in their respective sections (4.13 and 4.15). The assumptions and estimation of possible critical factors for explaining the thermal conductivity of nanofluids is justified.

The predictions from four cluster models are in good agreement with the experimental values. The spherical cluster is the one which has the least deviation from the experimental values. Hence we assume that the analyzed nanofluids form a spherical cluster and the Brownian motion and the nanolayer formed around the cluster, the volume fraction of the cluster and the nanofluid trapped in the clusters helps to increase the thermal conductivity in nanofluids.

CHAPTER 5

PARAMETRIC STUDY OF THE PROPERTIES OF NANOFLUIDS

The study has developed a mathematical model for thermal conductivity of nanofluids. This chapter deals with issues that would help us understand the properties which affect the thermal conductivity of nanofluids. The effect of volume fraction and nanoclustering effect on thermal conductivity were seen in chapter 4, where the thermal conductivity increases linearly with increase in the volume fraction of the nanoparticles. Three other factors such as nanolayer thickness, diameter of the nanoparticles and effect of Brownian motion are also considered for study. The results are determined by varying one factor while keeping others constant.

A.   Effect of Nanolayer thickness on the overall thermal conductivity of nanofluids:

The nanolayer thickness was considered as a critical parameter for thermal conductivity enhancement. The nanolayer thickness values for water and Ethylene Glycol was calculated. The nanolayer thickness for water as a base fluid was found to be 0.2884 nm. The values of the nanolayer thickness were varied from 0.01 nm to 1 nm in case of water used as a base fluid. In case of Ethylene Glycol, the nanolayer thickness was found to be 0.414 nm. The thickness was varied from 0.2 to 1 nm to carry out the parametric study. The volume fraction was varied from 0.01 to 0.04. Spherical clusters was considered for the thermal conductivity calculations. The values of thermal conductivity were calculated for various nanofluids and the graphs are plotted and are shown below.

CuO – Water / EG

Table 5. 1 Variation of effective thermal conductivity with nanolayer thickness

 CuO (18 nm) - Water nanofluids

Nanolayer Thickness (nm)	Volume Fraction			
	0.01	0.02	0.03	0.04
0.01	0.6485	0.66656	0.68555	0.70553
0.05	0.64842	0.6665	0.68552	0.70556
0.1	0.64833	0.66643	0.6855	0.7056
0.2	0.64815	0.6663	0.68545	0.70568
0.2884	0.648	0.66619	0.68542	0.70576
0.3	0.64797	0.66617	0.68541	0.70578
0.4	0.6478	0.66605	0.68538	0.70589
0.6	0.64746	0.66582	0.68534	0.70614
0.8	0.64715	0.66562	0.68534	0.70645
1	0.64685	0.66543	0.68537	0.70681
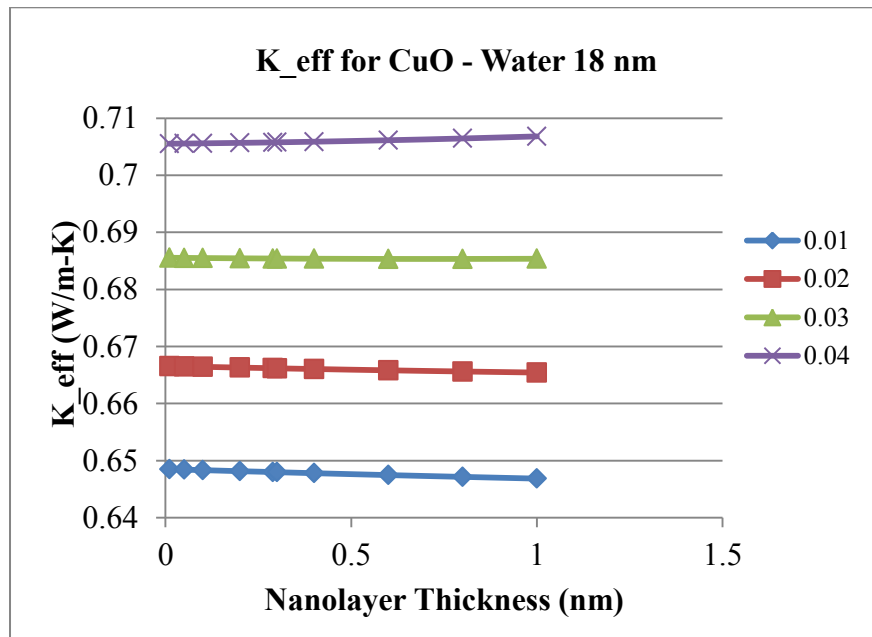
Figure 5. 1 Effective thermal conductivity versus the nanolayer thickness for CuO (18 nm) -

Water nanofluids

Table 5. 2 Variation of effective thermal conductivity with nanolayer thickness   CuO

(23.6 nm) - Water nanofluids

Nanolayer thickness (nm)	Volume fraction			
	0.01	0.02	0.03	0.04
0.01	0.6442	0.6622	0.6812	0.7012
0.05	0.6441	0.6622	0.6812	0.7012
0.1	0.6441	0.6622	0.6812	0.7013
0.2	0.6440	0.6621	0.6812	0.7014
0.2884	0.6440	0.6621	0.6812	0.7014
0.3	0.6439	0.6620	0.6812	0.7015
0.4	0.6438	0.6620	0.6812	0.7016
0.6	0.6436	0.6618	0.6812	0.7018
0.8	0.6434	0.6617	0.6813	0.7021
1	0.6432	0.6616	0.6813	0.7024

Figure 5. 2 Effective thermal conductivity versus the nanolayer thickness for   CuO

(23.6 nm) - Water nanofluids

CuO – EG 30.8 nm

Table 5. 3. Variation of effective thermal conductivity with nanolayer thickness CuO (30.8 nm)

– EG nanofluids

Nanolayer	Volume Fraction			
thickness(nm)	0.01	0.02	0.03	0.04
0.2	0.2659	0.2739	0.2823	0.2912
0.3	0.2659	0.2739	0.2823	0.2913
0.4	0.2659	0.2739	0.2823	0.2913
0.414	0.2658	0.2739	0.2823	0.2913
0.6	0.2658	0.2738	0.2823	0.2914
0.8	0.2657	0.2738	0.2823	0.2914
1	0.2656	0.2737	0.2823	0.2915
2	0.2653	0.2736	0.2825	0.2921
3	0.2651	0.2735	0.2827	0.2928
4	0.2649	0.2735	0.2831	0.2938
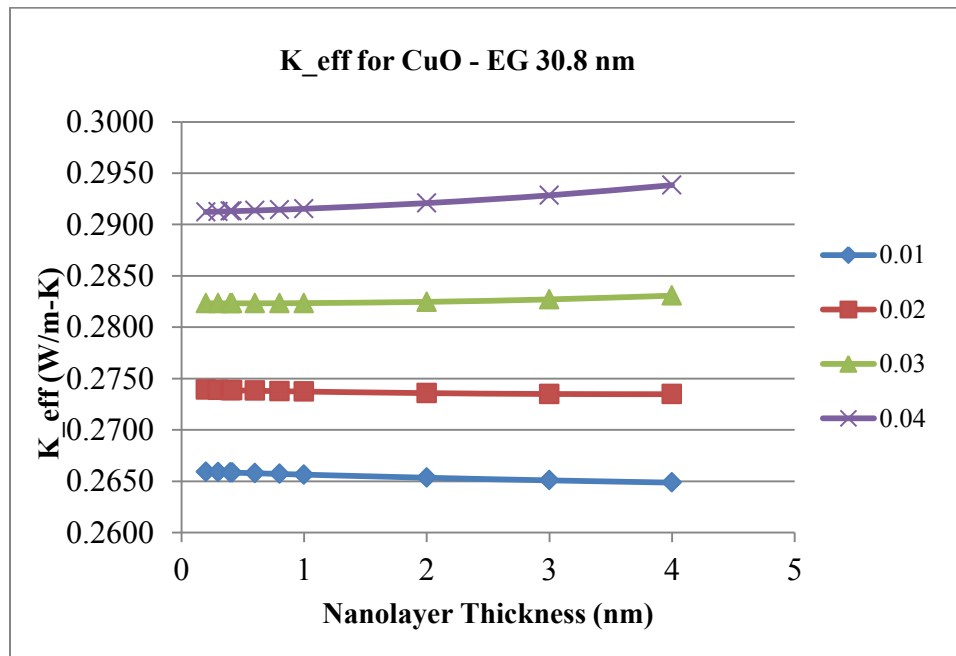
Figure 5. 3 Effective thermal conductivity versus the nanolayer thickness for

CuO (30.8 nm) – EG nanofluids

The values are calculated and tabulated in table 5.1, 5.2, 5.3 and plotted in figures 5.1, 5.2 and 5.3. As seen from the figures, the effective thermal conductivity decreased with increase in the nanolayer thickness except for higher volume fractions. The results suggest that nanolayer formation is a crucial factor for the abnormal thermal conductivity of the nanofluids.

Al_2O_3– Water / EG

Table 5. 4 Variation of effective thermal conductivity with nanolayer thickness Al_2O_3 (60.4 nm) - Water nanofluids

Nanolayer	Volume Fraction			
thickness (nm)	0.0100	0.0200	0.0300	0.0400
0.01	0.6360	0.6550	0.6749	0.6959
0.05	0.6360	0.6550	0.6749	0.6960
0.1	0.6360	0.6550	0.6749	0.6960
0.2	0.6360	0.6550	0.6750	0.6961
0.288	0.6360	0.6550	0.6750	0.6961
0.3	0.6360	0.6550	0.6750	0.6961
0.4	0.6359	0.6550	0.6750	0.6962
0.6	0.6359	0.6550	0.6751	0.6963
0.8	0.6359	0.6550	0.6752	0.6965
1	0.6359	0.6550	0.6752	0.6966

Figure 5. 4 Effective thermal conductivity versus nanolayer thickness for Al_2O_3 (60.4 nm) -

Water nanofluids

Table 5. 5 Variation of effective thermal conductivity with nanolayer thickness Al_2O_3 (26

nm) – EG nanofluids

Nanolayer thickness (nm)	Volume Fraction			
	0.01	0.02	0.03	0.04
0.2	0.2671	0.2751	0.2836	0.2926
0.3	0.2671	0.2751	0.2836	0.2926
0.4	0.2670	0.2751	0.2836	0.2926
0.414	0.2670	0.2751	0.2836	0.2926
0.6	0.2669	0.2750	0.2836	0.2927
0.8	0.2668	0.2749	0.2836	0.2928
1	0.2667	0.2749	0.2836	0.2929
2	0.2663	0.2747	0.2837	0.2936
3	0.2660	0.2745	0.2840	0.2945
4	0.2657	0.2745	0.2845	0.2959
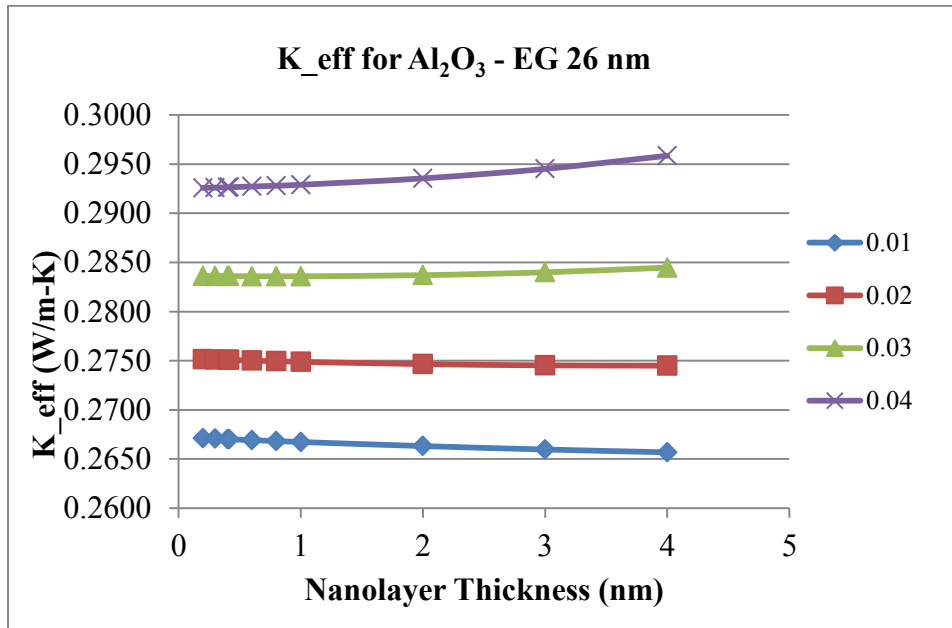
Figure 5. 5 Effective thermal conductivity versus nanolayer thickness for Al_2O_3 (26 nm) – EG nanofluids

Similar results are obtained as that of the above nanofluid. Figures 5.4 and 5.5 depict that at constant volume fraction the thermal conductivity decreases with the increase in nanolayer thickness. So the study came to conclusion that nanolayer is an important contributing factor for overall thermal conductivity of the nanofluids.

TiO$_2$- Water / EG:

Table 5. 6 Variation of effective thermal conductivity with nanolayer thickness   TiO$_2$ (10

nm) – Water nanofluids

Nanolayer thickness (nm)	Volume Fraction			
	0.0100	0.0200	0.0300	0.0400
0.01	0.6516	0.6674	0.6840	0.7014
0.05	0.6514	0.6672	0.6839	0.7014
0.1	0.6511	0.6670	0.6837	0.7013
0.2	0.6506	0.6665	0.6834	0.7012
0.288	0.6501	0.6662	0.6831	0.7012
0.3	0.6501	0.6661	0.6831	0.7011
0.4	0.6496	0.6657	0.6829	0.7011
0.6	0.6487	0.6650	0.6825	0.7013
0.8	0.6478	0.6643	0.6822	0.7016
1	0.6470	0.6637	0.6820	0.7021
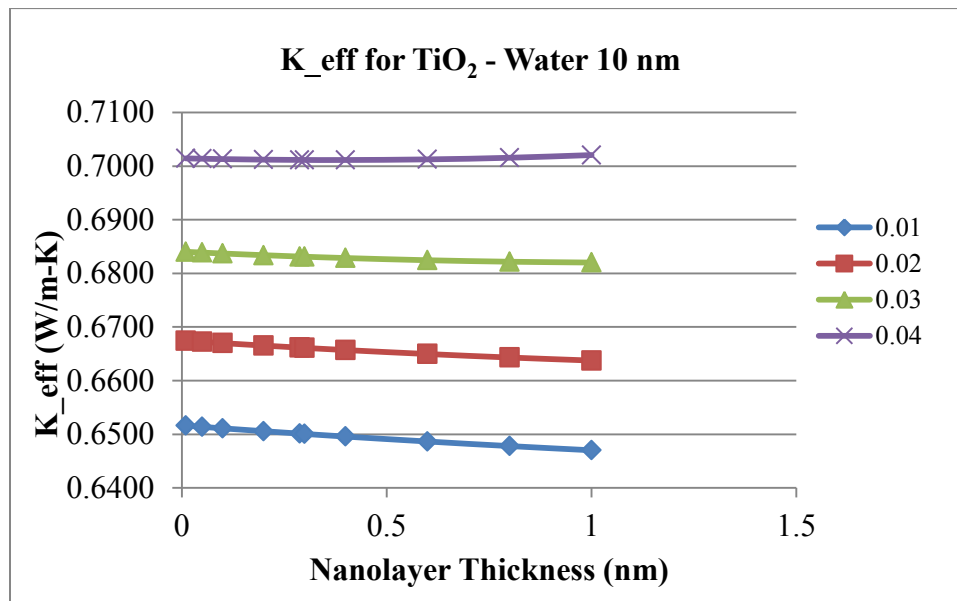
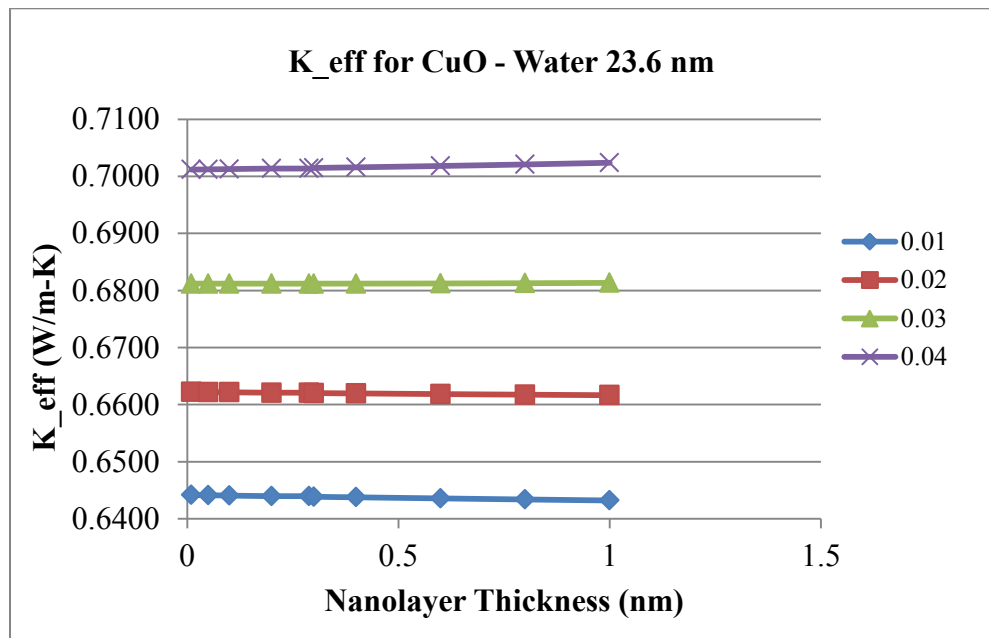
Figure 5. 6 Effective thermal conductivity versus the nanolayer thickness for

TiO$_2$ (10 nm) - Water nanofluids

Table 5. 7 Variation of effective thermal conductivity with nanolayer thickness   TiO$_2$ (34

nm) – Water nanofluids

Nanolayer thickness (nm)	Volume Fraction			
	0.0100	0.0200	0.0300	0.0400
0.01	0.6308	0.6466	0.6632	0.6806
0.05	0.6308	0.6466	0.6632	0.6806
0.1	0.6307	0.6466	0.6632	0.6806
0.2	0.6307	0.6466	0.6632	0.6807
0.288	0.6307	0.6465	0.6632	0.6808
0.3	0.6307	0.6465	0.6632	0.6808
0.4	0.6306	0.6465	0.6632	0.6809
0.6	0.6305	0.6465	0.6633	0.6811
0.8	0.6305	0.6464	0.6633	0.6812
1	0.6304	0.6464	0.6634	0.6814
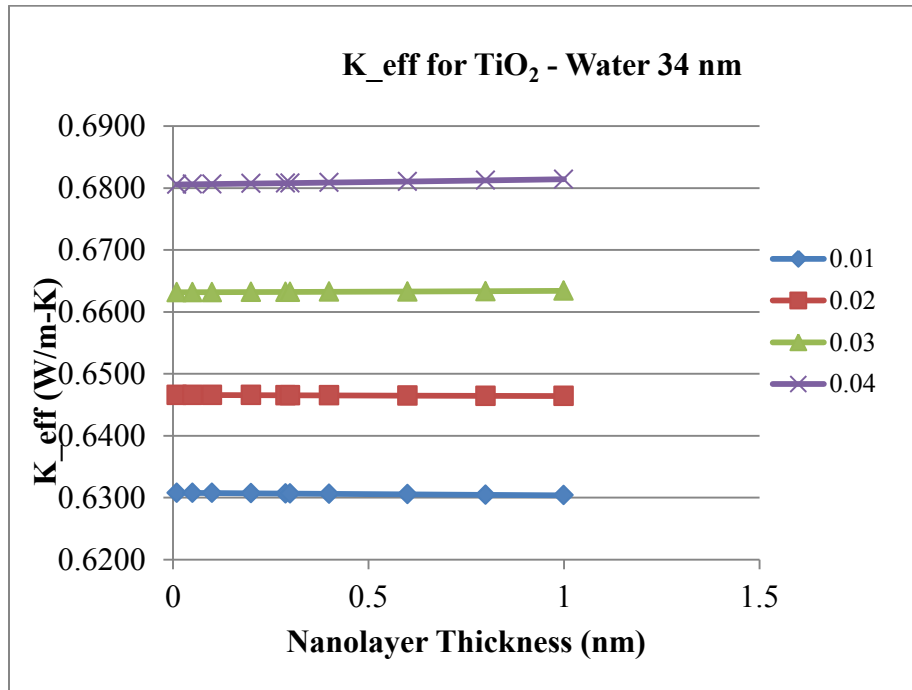
Figure 5. 7 Effective thermal conductivity versus nanolayer thickness for

TiO$_2$ (34 nm) - Water nanofluids

Table 5. 8 Variation of effective thermal conductivity with nanolayer thickness   TiO$_2$ (27 nm) – Water nanofluids

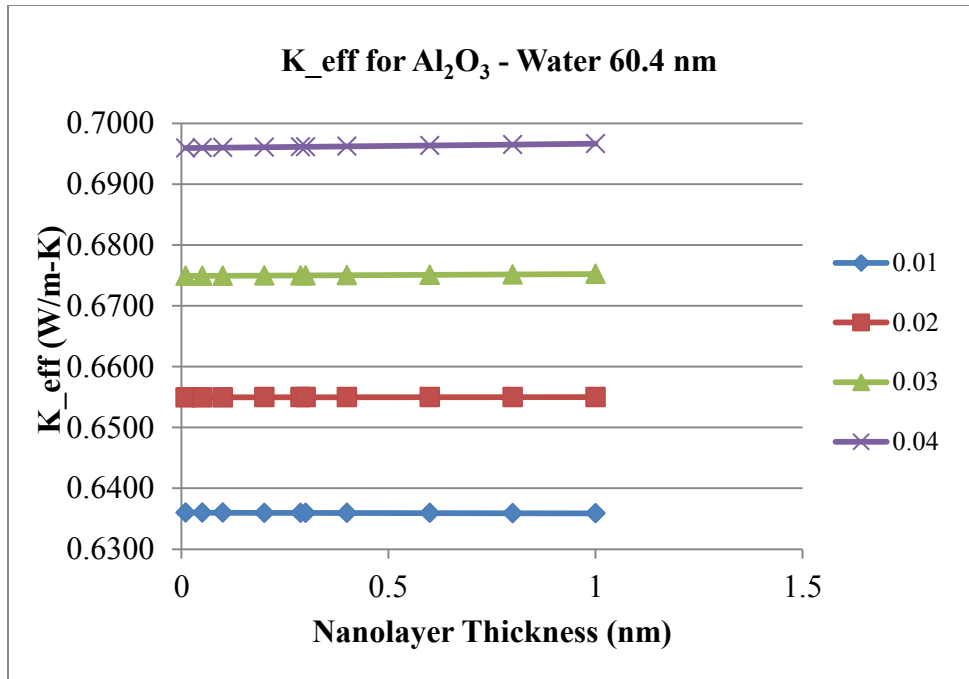| Nanolayer thickness (nm)	Volume Fraction			
	0.0100	0.0200	0.0300	0.0400
0.01	0.6393	0.6552	0.6719	0.6895
0.05	0.6392	0.6552	0.6719	0.6895
0.1	0.6392	0.6552	0.6719	0.6895
0.2	0.6391	0.6551	0.6719	0.6896
0.288	0.6391	0.6551	0.6719	0.6897
0.3	0.6391	0.6551	0.6719	0.6897
0.4	0.6390	0.6550	0.6719	0.6898
0.6	0.6389	0.6550	0.6720	0.6900
0.8	0.6387	0.6549	0.6720	0.6902
1	0.6386	0.6548	0.6721	0.6904
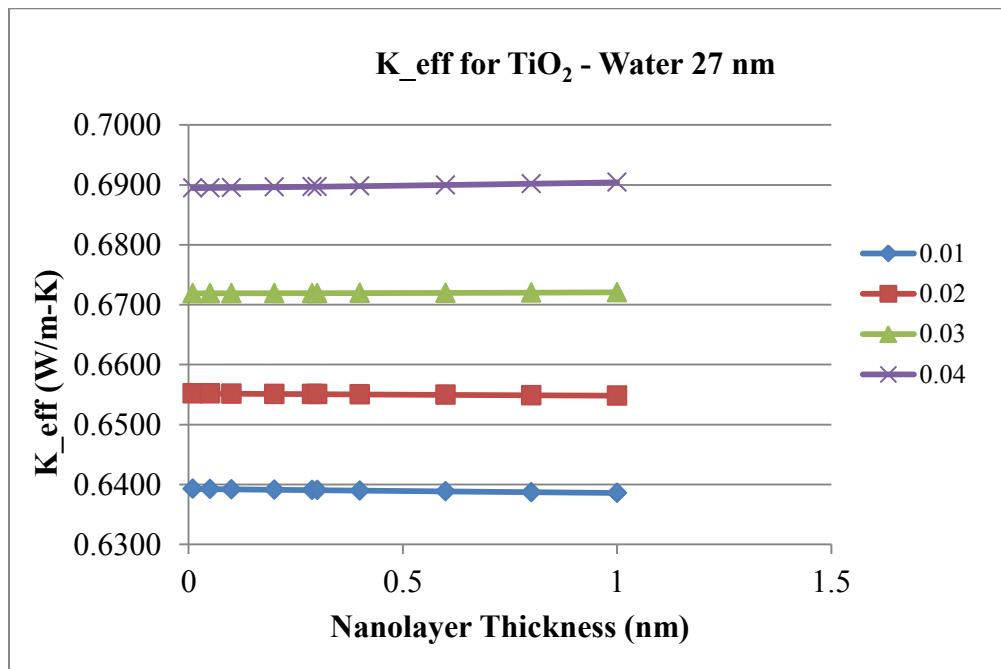
Figure 5. 8 Effective thermal conductivity versus the nanolayer thickness for   TiO$_2$ (27 nm) - Water nanolfuids

Table 5. 9 Variation of effective thermal conductivity with nanolayer thickness   TiO$_2$ (34 nm) – EG nanofluids

Nanolayer	Volume Fraction			
thickness (nm)	0.01	0.02	0.03	0.04
0.2	0.2648	0.2723	0.2802	0.2884
0.3	0.2648	0.2723	0.2802	0.2885
0.4	0.2648	0.2723	0.2802	0.2885
0.414	0.2648	0.2723	0.2802	0.2885
0.6	0.2647	0.2722	0.2802	0.2886
0.8	0.2647	0.2722	0.2802	0.2886
1	0.2646	0.2722	0.2802	0.2887
2	0.2644	0.2720	0.2803	0.2891
3	0.2641	0.2720	0.2805	0.2897
4	0.2640	0.2719	0.2807	0.2905
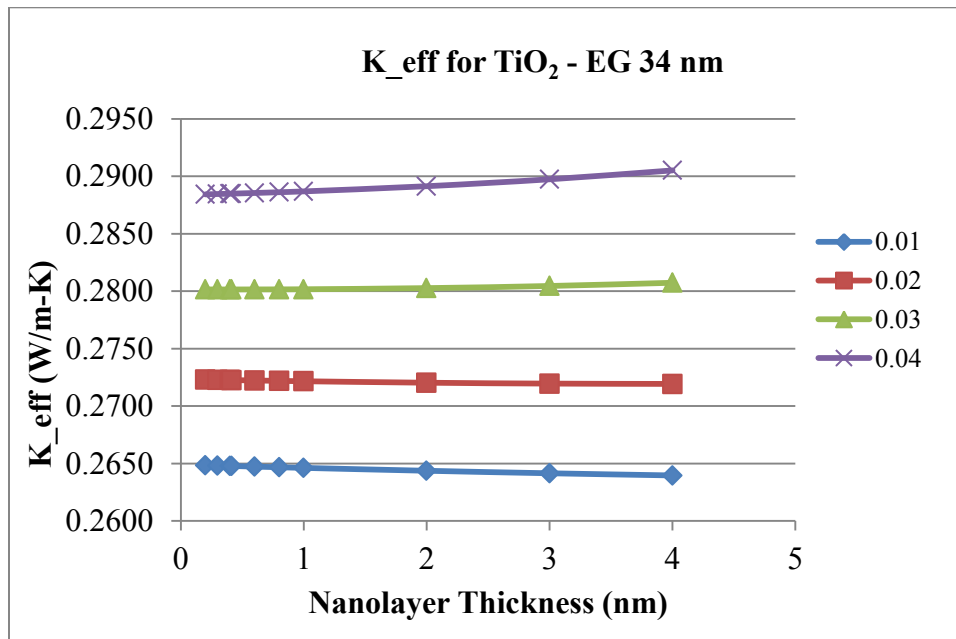
Figure 5. 9 Effective thermal conductivity versus the nanolayer thickness for TiO$_2$ (34 nm) - EG nanofluids

The results followed the same trend as that of the previous nanofluids discussed above. Again as seen from figures 5.6, 5.7, 5.8 and 5.9 the thermal conductivity of nanofluids decreased with increase in the nanolayer thickness. This clearly shows the strong dependency of nanolayer thickness on thermal conductivity of nanofluids.

ZnO – Water/EG:

Table 5. 10 Variation of effective thermal conductivity with nanolayer thickness   ZnO (10 nm) – Water nanofluids

| Nanolayer	Volume Fraction			
thickness (nm)	0.01	0.02	0.03	0.04
0.01	0.6541	0.6725	0.6919	0.7123
0.05	0.6538	0.6723	0.6917	0.7122
0.1	0.6536	0.6721	0.6916	0.7122
0.2	0.6530	0.6716	0.6913	0.7122
0.288	0.6526	0.6713	0.6911	0.7122
0.3	0.6525	0.6712	0.6911	0.7122
0.4	0.6520	0.6708	0.6909	0.7123
0.6	0.6511	0.6701	0.6906	0.7126
0.8	0.6503	0.6695	0.6904	0.7131
1	0.6495	0.6690	0.6903	0.7138
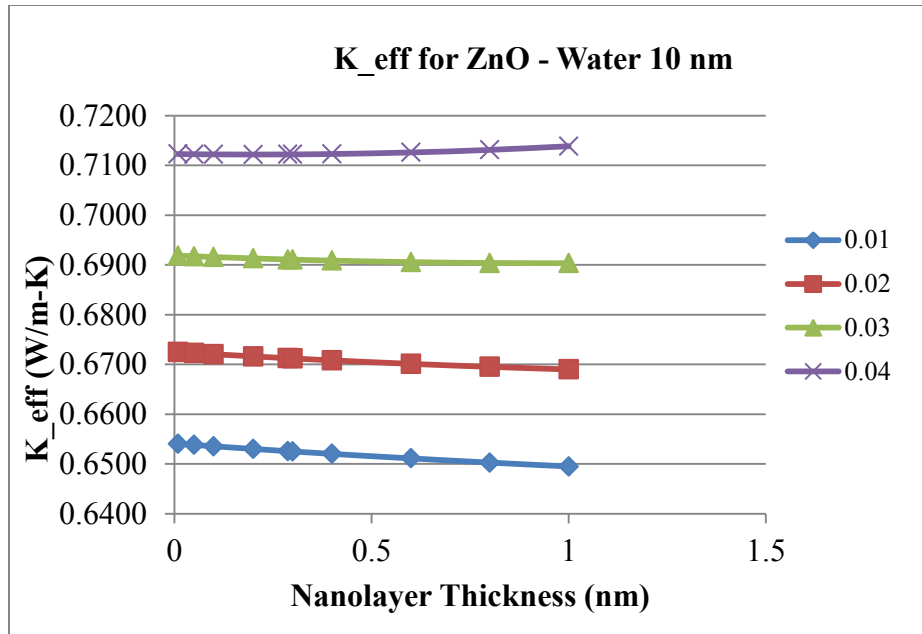
Figure 5. 10 Effective thermal conductivity versus nanolayer thickness for

ZnO (10 nm) - Water nanofluids

Table 5. 11 Variation of effective thermal conductivity with nanolayer thickness   ZnO (30

nm) – Water nanolfuids

| Nanolayer	Volume Fraction			
thickness (nm)	0.01	0.02	0.03	0.04
0.01	0.6344	0.6528	0.6722	0.6926
0.05	0.6344	0.6528	0.6722	0.6926
0.1	0.6343	0.6528	0.6722	0.6927
0.2	0.6343	0.6528	0.6722	0.6928
0.288	0.6342	0.6527	0.6722	0.6929
0.3	0.6342	0.6527	0.6722	0.6929
0.4	0.6342	0.6527	0.6723	0.6930
0.6	0.6341	0.6527	0.6723	0.6932
0.8	0.6340	0.6526	0.6724	0.6935
1	0.6339	0.6526	0.6725	0.6937
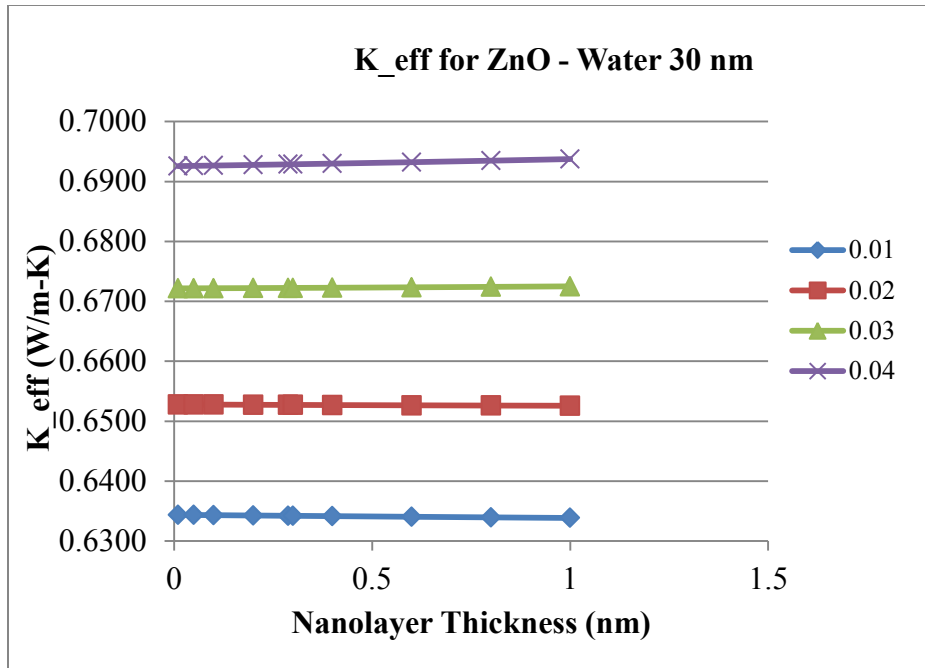
Figure 5. 11 Effective thermal conductivity versus the nanolayer thickness for

ZnO (30 nm) - Water nanofluids

Table 5. 12 Variation of effective thermal conductivity with nanolayer thickness   ZnO (60

nm) – EG nanofluids

| Nanolayer	Volume Fraction			
thickness (nm)	0.01	0.02	0.03	0.04
0.2	0.2628	0.2708	0.2792	0.2880
0.3	0.2628	0.2708	0.2792	0.2880
0.4	0.2628	0.2708	0.2792	0.2880
0.414	0.2628	0.2708	0.2792	0.2880
0.6	0.2628	0.2708	0.2792	0.2881
0.8	0.2628	0.2708	0.2792	0.2881
1	0.2628	0.2708	0.2792	0.2882
2	0.2627	0.2707	0.2793	0.2885
3	0.2626	0.2708	0.2795	0.2889
4	0.2625	0.2708	0.2796	0.2892
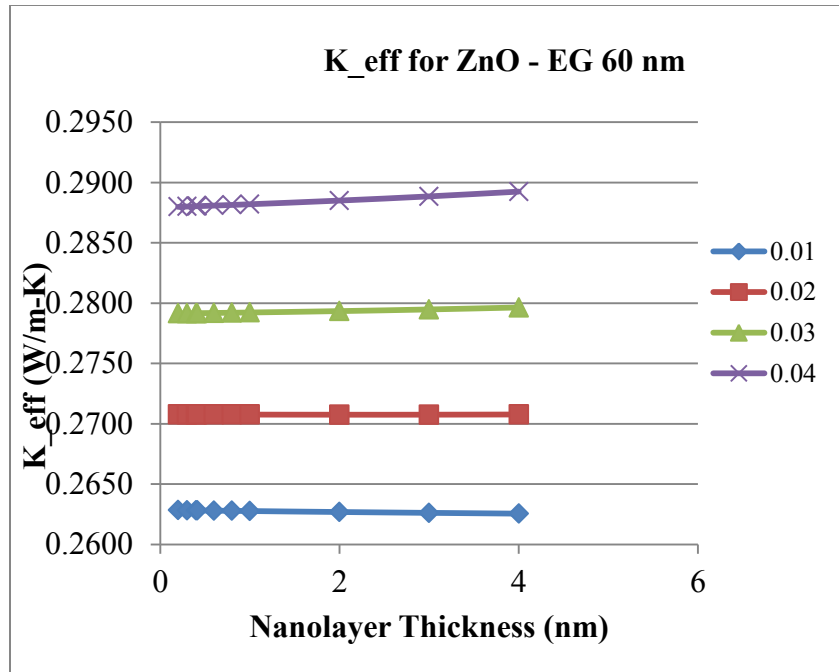
Figure 5. 12 Effective thermal conductivity versus the nanolayer thickness for

ZnO (60 nm) - EG nanofluids

The results are similar for ZnO-Water/EG nanofluids also. From the table 5.10, 5.11,
5.12 and figures 5.10, 5.11 and 5.12 the study came to conclusion that nanolayer thickness is a
significant factor for unusual thermal conductivity of nanofluids.

Cu-Water/Al-Water/Fe-EG:

Table 5. 13 Variation of effective thermal conductivity with nanolayer thickness   Al (20

nm) – Water nanofluids

| Nanolayer	Volume Fraction			
thickness (nm)	0.01	0.02	0.03	0.04
0.01	0.6464	0.6654	0.6850	0.7051
0.05	0.6464	0.6654	0.6849	0.7051
0.1	0.6463	0.6653	0.6849	0.7051
0.2	0.6462	0.6652	0.6848	0.7050
0.288	0.6460	0.6651	0.6848	0.7050
0.3	0.6460	0.6651	0.6848	0.7050
0.4	0.6459	0.6650	0.6847	0.7051
0.6	0.6456	0.6648	0.6846	0.7051
0.8	0.6454	0.6646	0.6845	0.7051
1	0.6452	0.6644	0.6844	0.7052
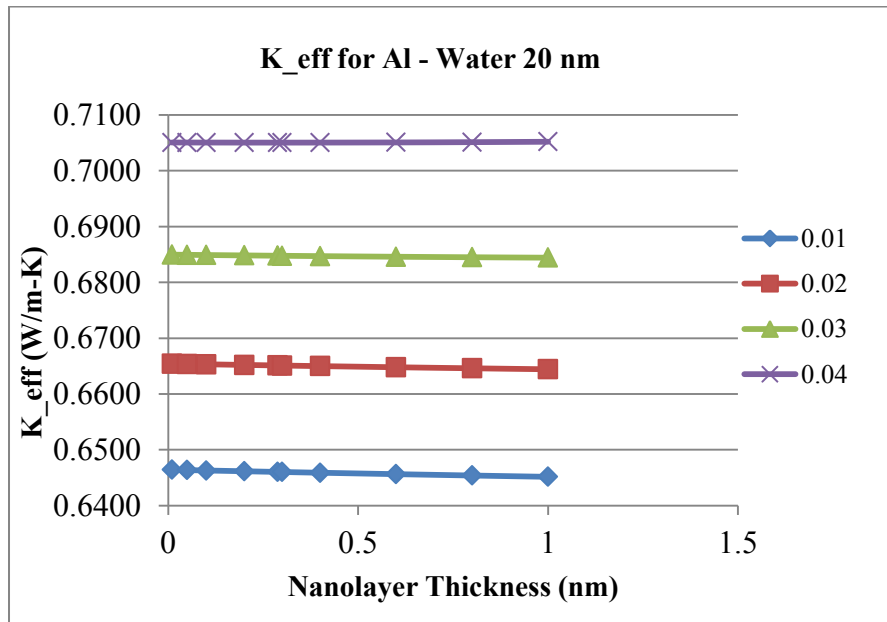
Figure 5. 13 Effective thermal conductivity versus the nanolayer thickness for

Al (20 nm) – Water nanofluids

Table 5. 14 Variation of effective thermal conductivity with nanolayer thickness   Cu (100

nm) – Water nanofluids

| Nanolayer	Volume Fraction			
thickness (nm)	0.01	0.02	0.03	0.04
0.01	0.6348	0.6545	0.6753	0.6972
0.05	0.6348	0.6545	0.6753	0.6972
0.1	0.6347	0.6545	0.6753	0.6972
0.2	0.6347	0.6545	0.6753	0.6973
0.288	0.6347	0.6545	0.6753	0.6973
0.3	0.6347	0.6545	0.6753	0.6973
0.4	0.6347	0.6545	0.6754	0.6974
0.6	0.6347	0.6545	0.6754	0.6975
0.8	0.6347	0.6545	0.6754	0.6976
1	0.6347	0.6545	0.6755	0.6977
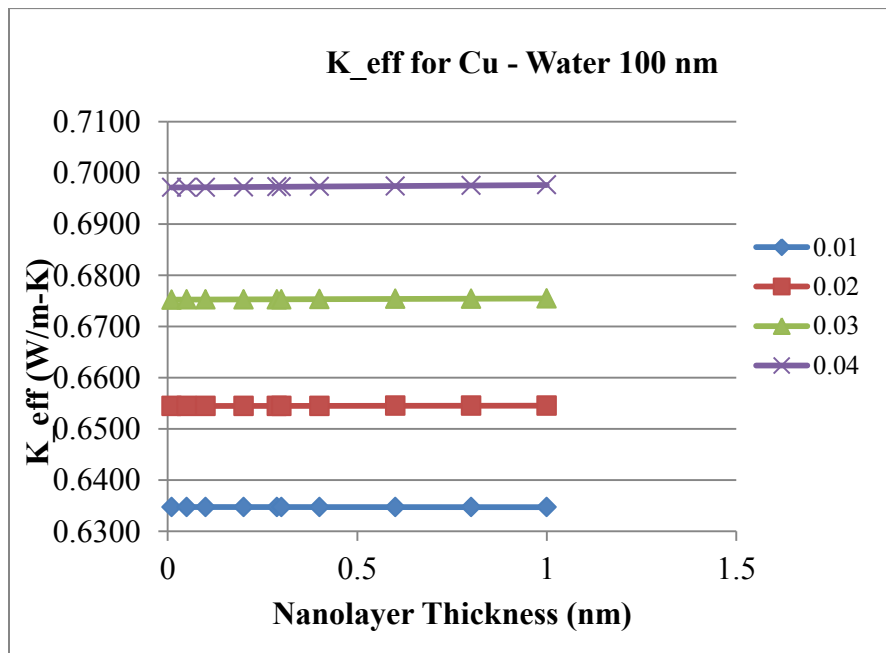
Figure 5. 14 Effective thermal conductivity versus the nanolayer thickness for

Cu (100 nm) – Water nanofluids

Table 5. 15 Variation of effective thermal conductivity with nanolayer thickness   Fe (10

nm) – EG nanofluids

| Nanolayer Thickness (nm)	Volume Fraction			
	0.01	0.02	0.03	0.04
0.2	0.2726	0.2808	0.2894	0.2986
0.3	0.2724	0.2806	0.2893	0.2987
0.4	0.2722	0.2804	0.2893	0.2987
0.414	0.2721	0.2804	0.2893	0.2987
0.6	0.2718	0.2802	0.2892	0.2989
0.8	0.2714	0.2799	0.2891	0.2991
1	0.2711	0.2797	0.2891	0.2995
2	0.2699	0.2792	0.2901	0.3029
3	0.2691	0.2795	0.2930	0.3110
4	0.2686	0.2809	0.2994	0.3302
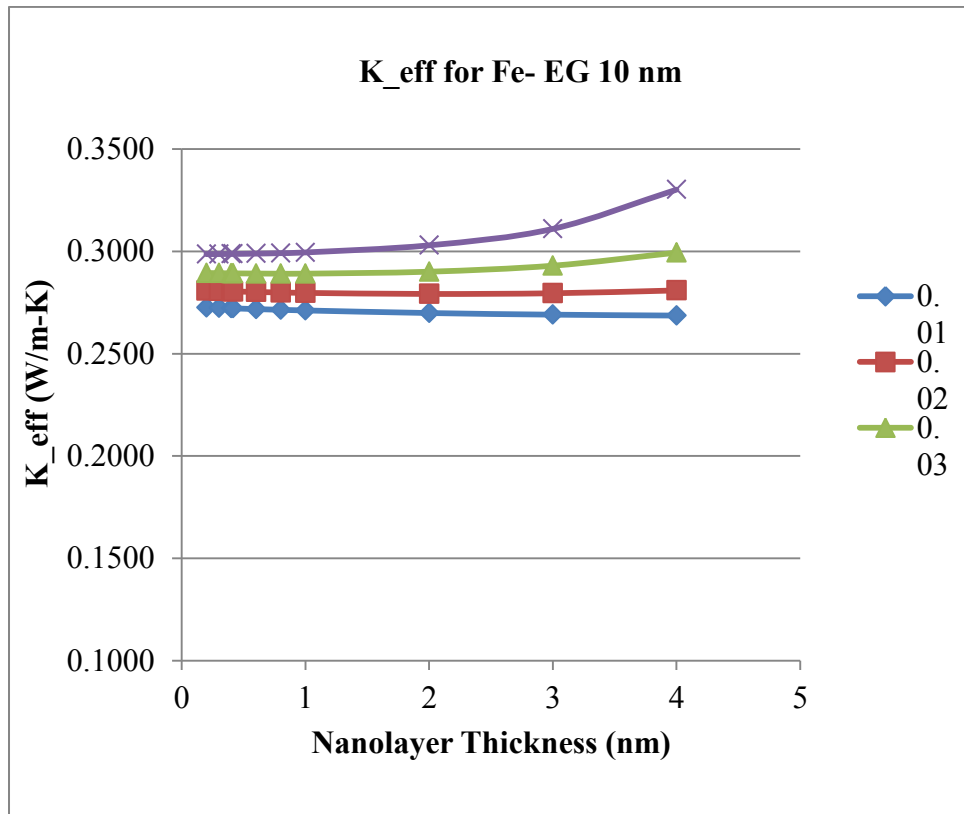
Figure 5. 15 Effective thermal conductivity versus the nanolayer thickness

Fe (10 nm) – EG nanofluids

The results are replicated above but with some deviation. As seen from table 5.13 the thermal conductivity of the nanofluid decreased with the increase in nanolayer thickness. Figure 5.14 the thermal conductivity remained almost constant for Cu-Water 100 nm nanofluid. This might be because of the large nanoparticle diameter value. Figure 5.15 Fe – EG 10 nm, the thermal conductivity increases at higher volume fractions with the increase in nanolayer thickness, may be due to the smaller size of the nanoparticle.

Tillman et al. [51] also stated that an interfacial structure formed by liquid molecular layering will play an important role. Feng et al. [40] also came to a conclusion that solid/liquid interfacial layer is the pivotal factor for thermal conductivity of the nanofluids. Leong et al. [45] proposed that nanolayer is one of the major mechanisms enhancing the thermal conductivity of the nanofluids. From the above statements made by researchers, and all the graphs discussed so far the study came to a conclusion that the nanolayer thickness is an important element in enhancing the thermal conductivity of the nanofluids

B.   Effect of particle diameter on effective thermal conductivity of nanofluids

The volume fraction and temperature were kept constant at 0.03 and 300k respectively. These numbers were taken arbitrarily. The nanolayer thickness which was earlier used for different nanofluid combinations in chapter 4 for model validation was used here too. All other parameters were kept constant while varying the particle diameter. The particle diameter has been varied from its average diameter in increments of 1 nm and decrements of 1nm for all respective nanofluids. The values for the thermal conductivities were calculated and tabulated in

the tables which are shown below. Using these values, graphs were plotted to understand the variation.

Table 5. 16 Variation of thermal conductivity with particle diameter CuO-Water

Diameter of nano particle (nm)	ϕ_C	K(W/m-k) CuO-water 18 nm	Diameter of nano particle (nm)	ϕ_C	K(W/m-k) CuO-water 23.6 nm
18	0.3711	0.7058	23.6	0.3793	0.7015
19	0.3729	0.7048	25	0.3808	0.7007
20	0.3745	0.7040	26	0.3818	0.7002
21	0.3760	0.7032	27	0.3827	0.6997
22	0.3774	0.7025	28	0.3836	0.6993
23	0.3786	0.7018	29	0.3843	0.6988
24	0.3798	0.7012	30	0.3851	0.6985
25	0.3808	0.7007	31	0.3858	0.6981
26	0.3818	0.7002	32	0.3864	0.6978
27	0.3827	0.6997	33	0.3870	0.6975

Figure 5. 16 Effective thermal conductivity versus Particle Diameter for CuO (18 nm)

Figure 5. 17 Effective thermal conductivity versus Particle diameter for

CuO (23.6 nm)-Water

Table 5. 17 variation of thermal conductivity with particle diameter CuO - EG and   Al$_2$O$_3$ -

Water

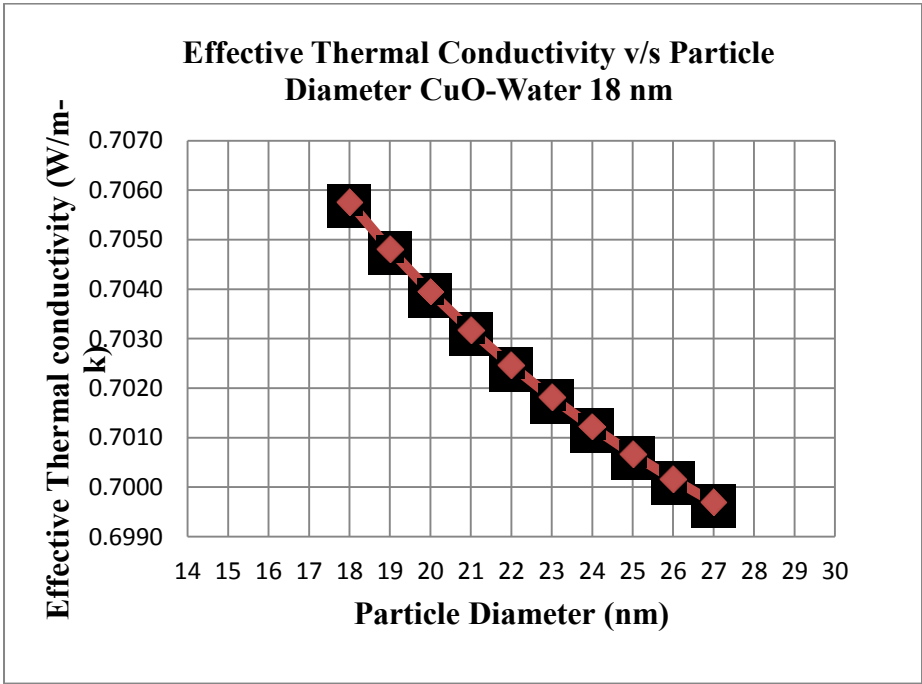| Diameter of nano particle (nm)	ϕ_C	K(W/m-k) CuO-EG 30.8nm	Diameter of nanoparticle (nm)	ϕ_C	K(W/m-k) Al$_2$O$_3$-water 60.4 nm
30.8	0.3762	0.2913	60.4	0.3961	0.6961
32	0.3773	0.2911	62	0.3964	0.6960
33	0.3782	0.2909	63	0.3966	0.6959
34	0.3790	0.2907	64	0.3967	0.6958
35	0.3798	0.2905	65	0.3969	0.6958
36	0.3805	0.2904	66	0.3971	0.6957
37	0.3812	0.2902	67	0.3972	0.6956
38	0.3819	0.2901	68	0.3974	0.6956
39	0.3825	0.2899	69	0.3975	0.6955
40	0.3831	0.2898	70	0.3976	0.6954

Figure 5. 18 Effective thermal conductivity versus Particle diameter for CuO (30.8 nm)
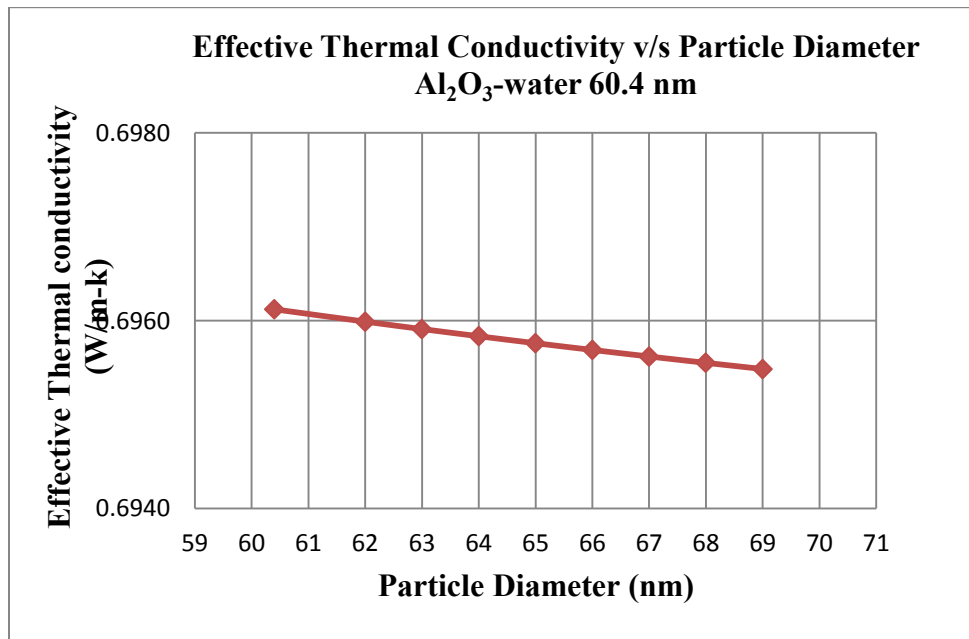
Figure 5. 19 Effective thermal conductivity versus Particle diameter for Al$_2$O$_3$ (60.4 nm)

As seen from the table 5.16 the diameter of the CuO-Water 18 nm has been varied from 18 nm to 27 nm with the increments of 1nm and for CuO-Water 23.6 nm the diameter has been varied from 25 nm to 33 nm with an increment of 1nm. The increase in diameter increases the cluster size. Spherical cluster formation has been assumed for this study. The values of thermal conductivity were calculated and tabulated in table 5.16. It can be observed from the table 5.16 and figures 5.16 and 5.17 that at constant volume fraction, the thermal conductivity of the nanofluid decreases as the particle diameter increases.

Also the diameter of CuO-EG 35 nm has been varied from 30 nm to 40 nm with an increment of 1nm and for the Al2O3-Water 60.4 nm the particle diameter has been varied from 60 nm to 70 nm. The results were tabulated in table 5.17 and graphs were plotted. Similar results were obtained as the above mentioned nanofluids. So the thermal conductivity of the nanofluid decreases with the increase in the diameter of the nanoparticle.

Table 5. 18 Variation of thermal conductivity with particle diameter Al_2O_3-EG and TiO_2 – Water

Diameter of nano particle (nm)	ϕ_C	K(W/m-k) Al2O3-EG 26 nm	Diameter of nano particle (nm)	ϕ_C	K(W/m-k) TiO2-Water 10 nm
26	0.3708	0.2926	10	0.3451	0.7012
27	0.3721	0.2924	11	0.3502	0.6986
28	0.3733	0.2921	12	0.3546	0.6965
29	0.3744	0.2919	13	0.3583	0.6946
30	0.3754	0.2916	14	0.3615	0.6931
31	0.3764	0.2914	15	0.3644	0.6917
32	0.3773	0.2912	16	0.3669	0.6905
33	0.3782	0.2910	17	0.3691	0.6894
34	0.3790	0.2909	18	0.3711	0.6885
35	0.3798	0.2907	19	0.3729	0.6876
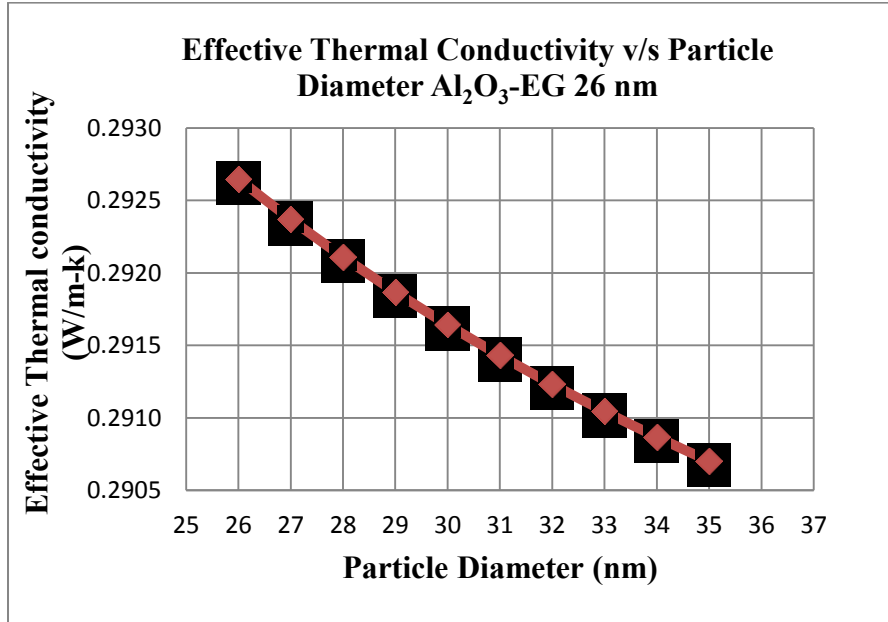
Figure 5. 20 Effective thermal conductivity versus Particle diameter for
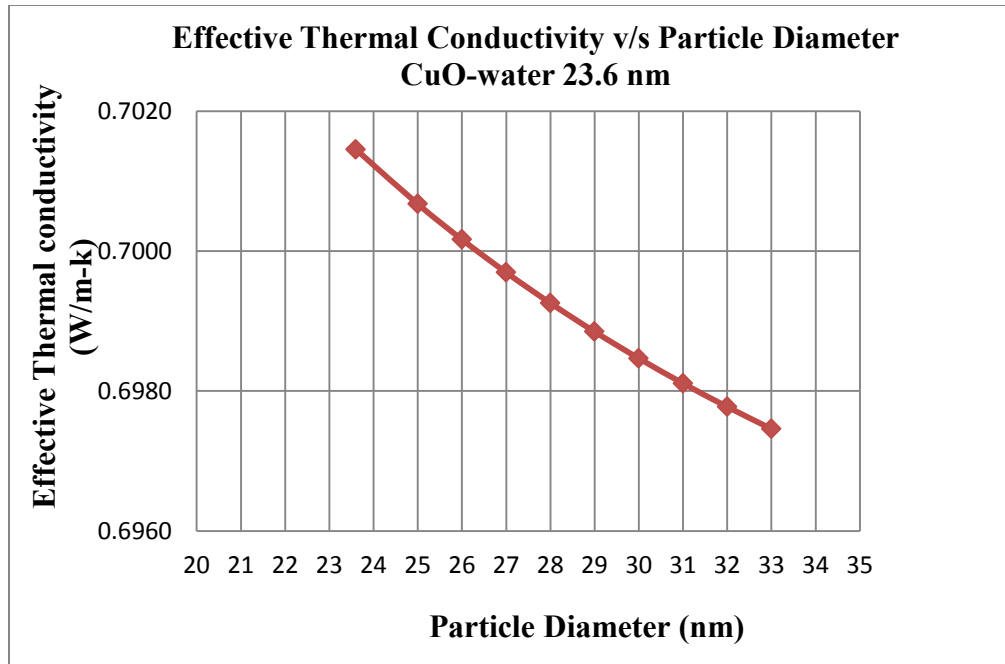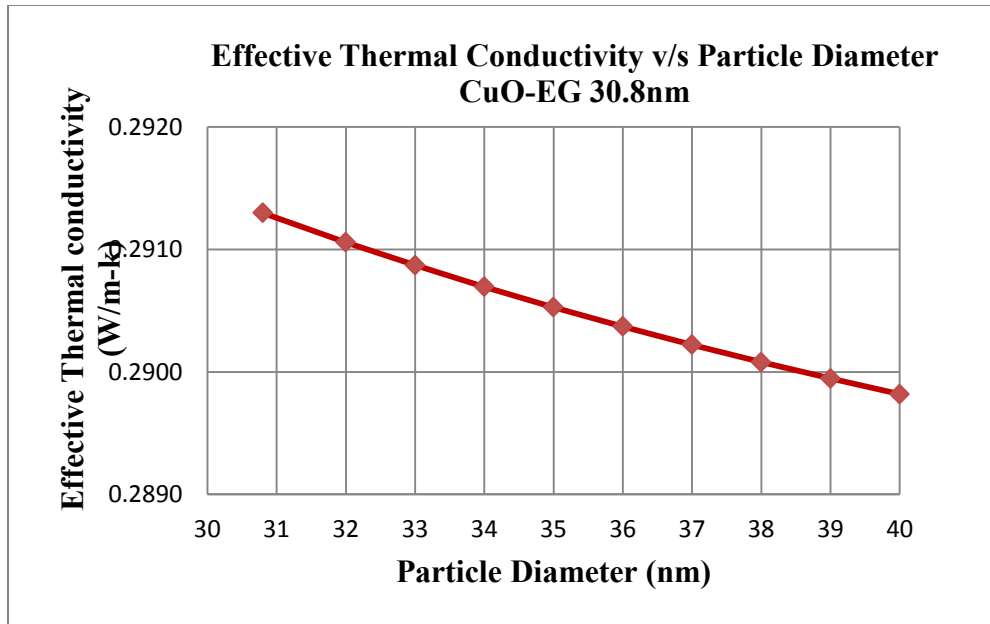
Al_2O_3 (26 nm)

Figure 5. 21 Effective thermal conductivity versus Particle diameter for

TiO$_2$ – Water 10 nm

Table 5. 19 Variation of thermal conductivity with particle diameter TiO$_2$ – Water 34 nm and

TiO$_2$ – Water 27 nm

Diameter of nanoparticle (nm)	ϕ_C	K(W/m-k) TiO2-Water 34 nm	Diameter of nanoparticle (nm)	ϕ_C	K(W/m-k) TiO2-Water 27 nm
34	0.3876	0.6808	27	0.3827	0.6897
35	0.3882	0.6805	28	0.3836	0.6893
36	0.3887	0.6803	29	0.3843	0.6889
37	0.3892	0.6801	30	0.3851	0.6886
38	0.3896	0.6799	31	0.3858	0.6882
39	0.3901	0.6797	32	0.3864	0.6879
40	0.3905	0.6795	33	0.3870	0.6877
41	0.3909	0.6793	34	0.3909	0.6859
42	0.3913	0.6791	35	0.3913	0.6857
43	0.3917	0.6789	36	0.3917	0.6855
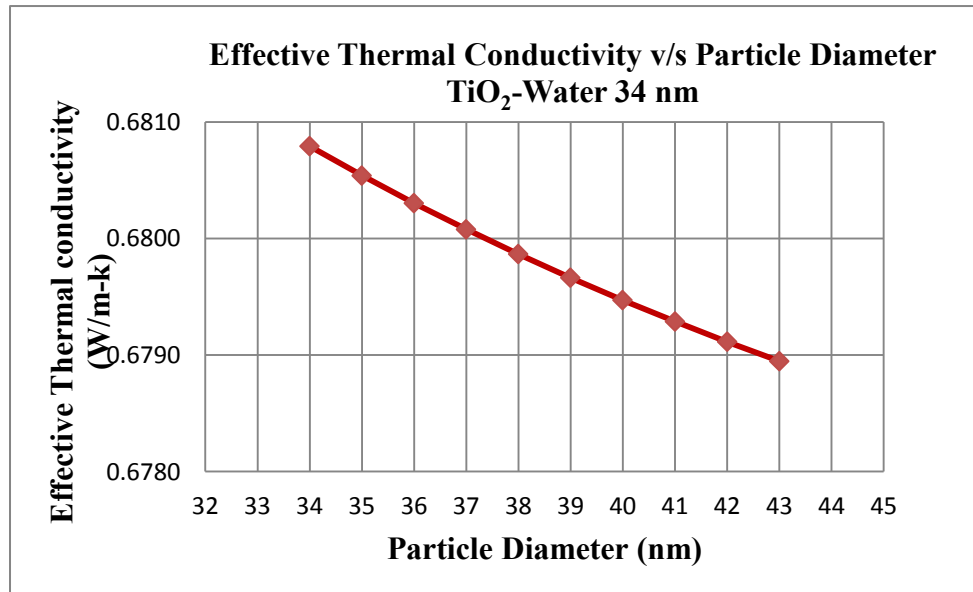
Figure 5. 22 Effective thermal conductivity versus Particle diameter for
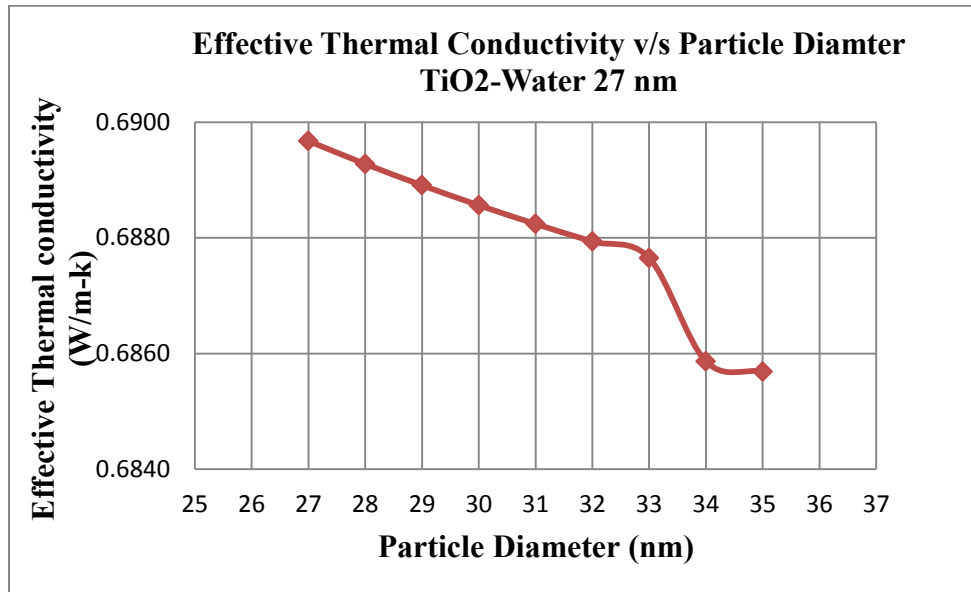
TiO$_2$ – Water

Figure 5. 23 Effective thermal conductivity versus Particle diameter for TiO_2 – Water

Table 5.18 summarizes the dependency of thermal conductivity on particle diameter for

Al2O3– EG 26 nm. The diameter has been varied from 26 nm to 35 nm for

As seen from figures 5.20 and 5.21 the thermal conductivity decreased with increase in

the particle diameter.

Table 5.19 provides information on TiO2 – Water combination. The results were

repetitive as shown in the graphs above that the thermal conductivity decreases with

nanoparticle size.

Table 5. 20 Variation of thermal conductivity with particle diameter TiO_2 – EG 34 nm and ZnO

– Water 10 nm

| Diameter of nanoparticle (nm)	ϕ_C	K(W/m-k) TiO2-EG 34 nm	Diameter of nanoparticle (nm)	ϕ_C	K(W/m-k) ZnO-Water 10 nm
34	0.3790	0.2885	10	0.3451	0.7122
35	0.3798	0.2883	11	0.3502	0.7096
36	0.3805	0.2882	12	0.3546	0.7075
37	0.3812	0.2880	13	0.3583	0.7056
38	0.3819	0.2879	14	0.3615	0.7041
39	0.3825	0.2877	15	0.3644	0.7027
40	0.3831	0.2876	16	0.3669	0.7015
41	0.3837	0.2875	17	0.3691	0.7004
42	0.3842	0.2874	18	0.3711	0.6994
43	0.3847	0.2873	19	0.3729	0.6986
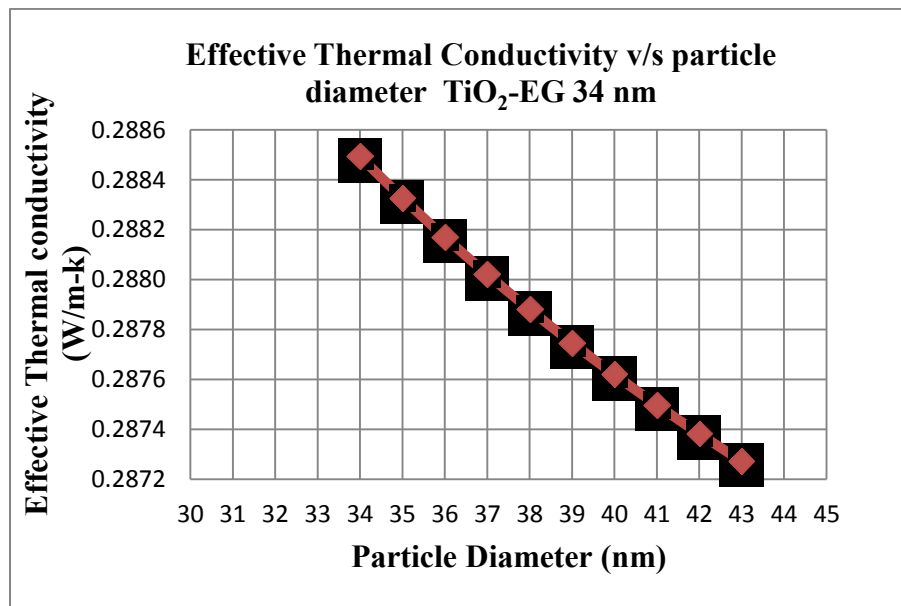
Figure 5. 24 Effective thermal conductivity versus Particle diameter for
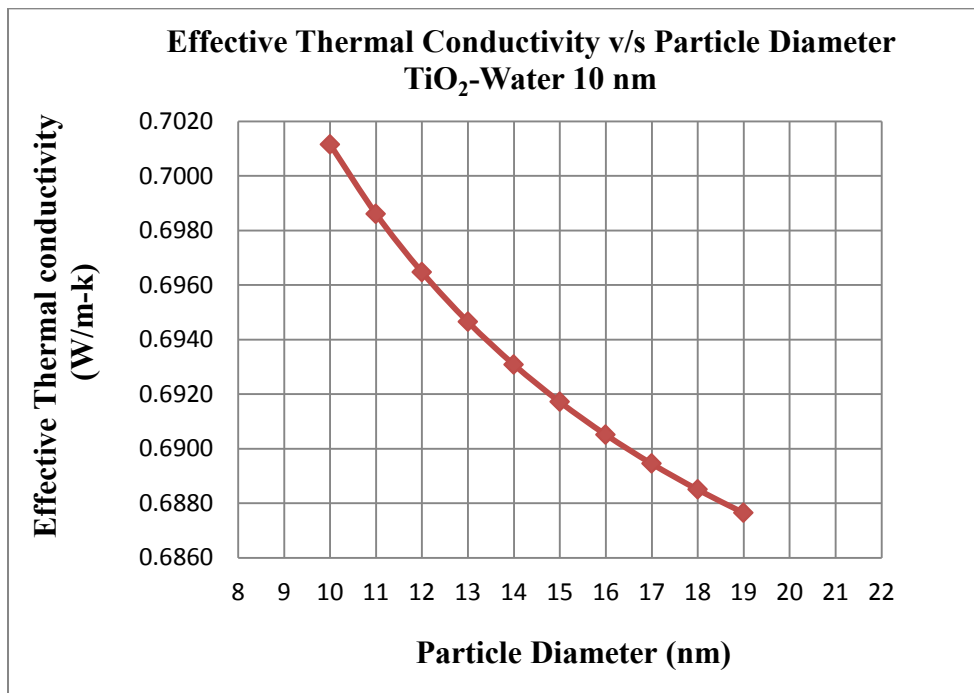
TiO_2 - EG 34 nm
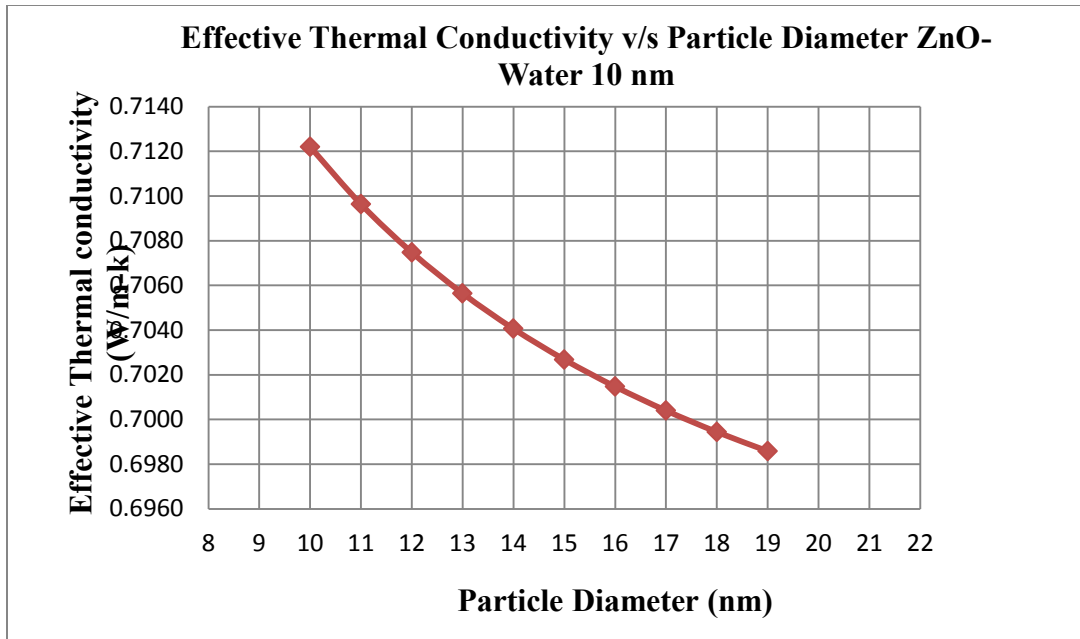
Figure 5. 25 Effective thermal conductivity versus Particle diameter for

ZnO - Water 10 nm

Table 5. 21 Variation of thermal conductivity with particle diameter ZnO – Water and ZnO –

EG

| Diameter of nanoparticle (nm)	ϕ_C	K(W/m-k) ZnO- Water 30 nm	Diameter of nanoparticle (nm)	ϕ_C	K(W/m-k) ZnO- EG 60 nm
30	0.3851	0.6929	60	0.3910	0.2880
31	0.3858	0.6925	61	0.3912	0.2880
32	0.3864	0.6922	62	0.3915	0.2879
33	0.3870	0.6919	63	0.3917	0.2879
34	0.3876	0.6917	64	0.3920	0.2878
35	0.3882	0.6914	65	0.3922	0.2878
36	0.3887	0.6912	66	0.3924	0.2877
37	0.3892	0.6910	67	0.3926	0.2877
38	0.3896	0.6907	68	0.3929	0.2876
39	0.3901	0.6905	69	0.3931	0.2876
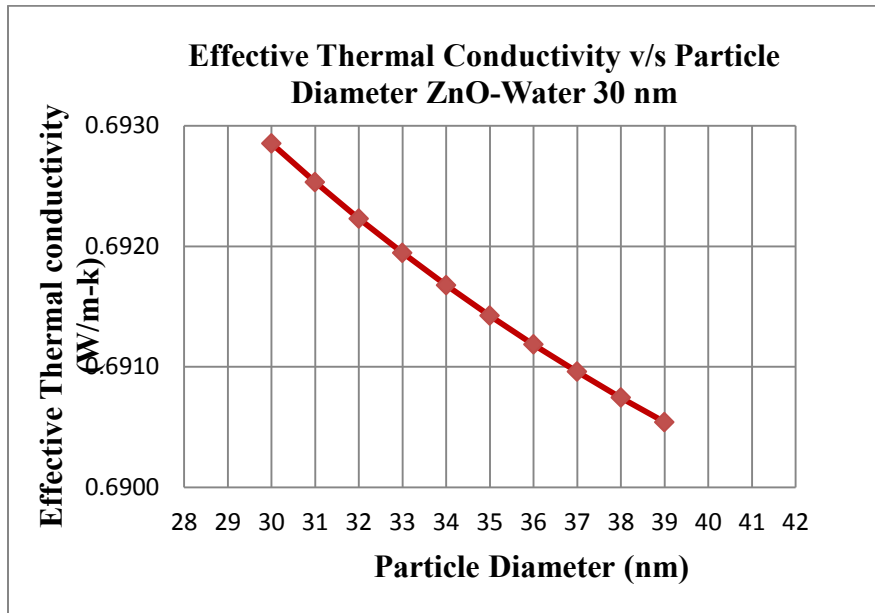
Figure 5. 26 Effective thermal conductivity versus Particle diameter for
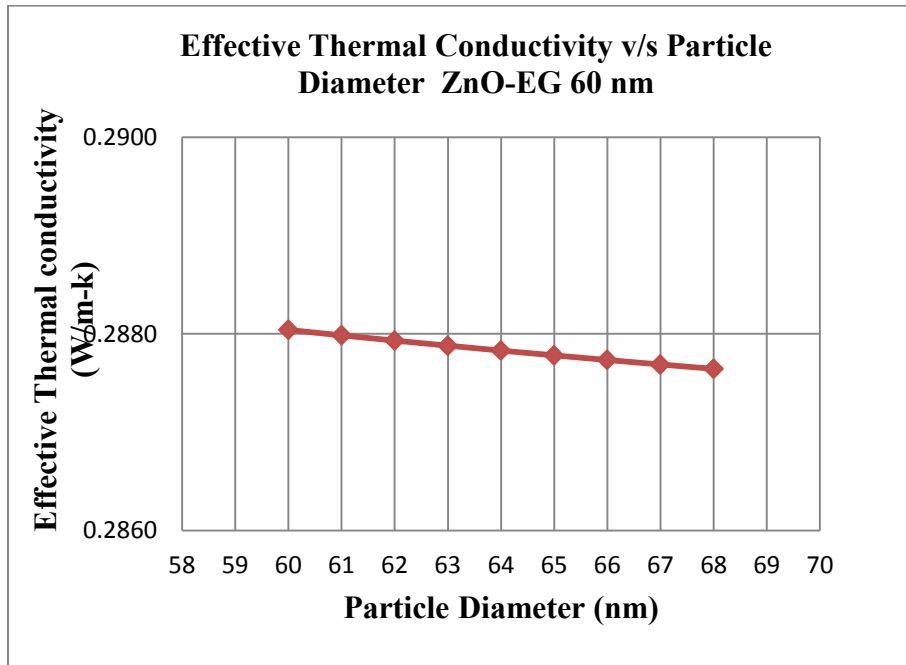
ZnO – Water

Figure 5. 27 Effective thermal conductivity v/s Particle diameters for ZnO – Water

As seen from tables 5.20 and 5.21 the thermal conductivity still maintained its decreasing nature for increasing particle diameter. The range of diameter variation of nanoparticle for different nanofluid combination is mentioned below.For all the above nanofluid combinations it can be seen that the thermal conductivity decreased with the increase in the nanoparticle diameter.

Table 5. 22 Variation of thermal conductivity with particle diameter Cu – Water 100 nm and Al – Water 20 nm

| Diameter of nanoparticle (nm)	ϕ_C	K(W/m-k) Cu- Water 100 nm	Diameter of nanoparticle (nm)	ϕ_C	K(W/m-k) Al- Water 20 nm
100	0.4005	0.6973	20	0.3745	0.7092
102	0.4007	0.6972	21	0.3760	0.7085
104	0.4008	0.6972	22	0.3774	0.7079
106	0.4009	0.6972	23	0.3786	0.7073
108	0.4009	0.6971	24	0.3798	0.7067
110	0.4010	0.6971	25	0.3808	0.7062
112	0.4010	0.6971	26	0.3818	0.7057
114	0.4012	0.6970	27	0.3827	0.7053
116	0.4013	0.6970	28	0.3836	0.7049
118	0.4014	0.6969	29	0.3843	0.7045
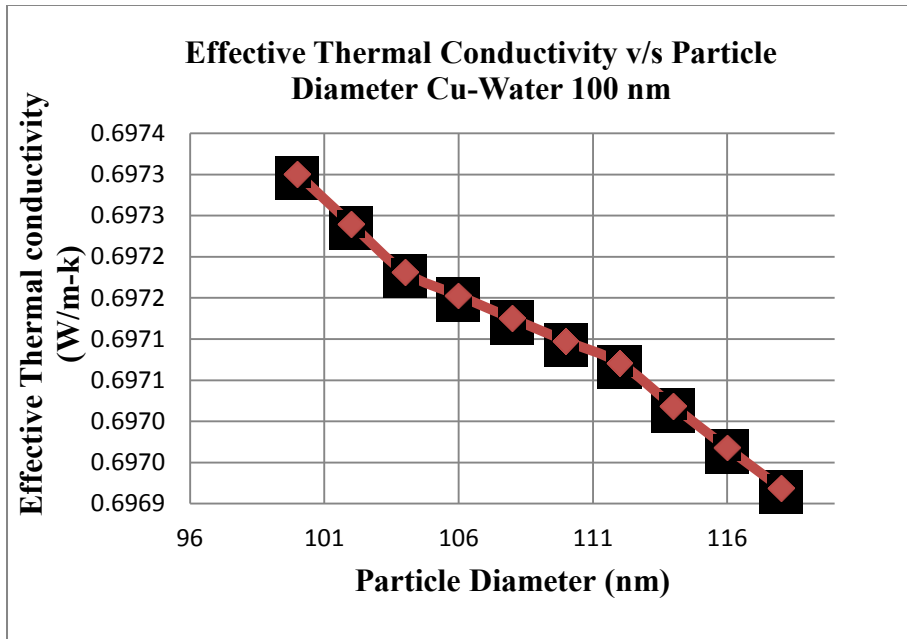
Figure 5. 28 Effective thermal conductivity versus Particle diameter for

Cu-Water 100 nm
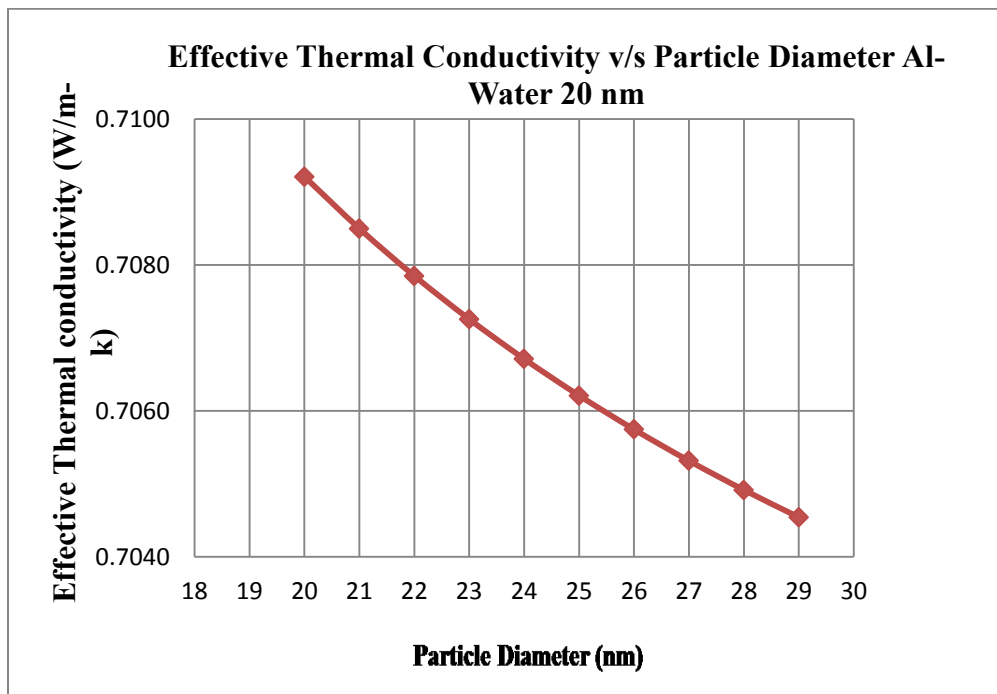
Figure 5. 29 Effective thermal conductivity versus Particle diameter for Al-Water 20 nm

From the above values and all the graphs discussed, the study came to a conclusion that at constant volume fraction and temperature the thermal conductivity decreases with increase in diameter of the nanoparticle. The conclusion is supported by many researchers. Kim et al. [49] from experiments stated that thermal conductivity is inversely proportional to the mean diameter of the suspended particles. Jang et al. [38] and Jang and choi [35] showed that as the nanoparticle diameter is reduced, the thermal conductivity of nanofluids increases. Feng et al. [17] examined the influence of particle diameter on the effective thermal conductivity of CuO-Water nanofluid and found that the thermal conductivity decreased with the increase in particle diameter. Prasher et al. [16] performed a controlled experimental investigation to observe the impact of decreasing the particle size on thermal conductivity and came out with a similar conclusion as the present study and other researchers concluded. Kang et al. [52] from his experiments showed that the enhancement of thermal conductivity decreases with the increase of particle size.

C. Effect of Brownian motion on thermal conductivity of nanofluids

As a part of the validation for the mathematical model developed, Brownian motion effect in the thermal conductivity of nanofluids were analyzed. The mathematical model was solved without taking the Keff due to the moving particles. The final equation which was used to find out the Keff was

$$\frac{K_s}{K_f} = \frac{[K_s + 2\,K_f - 2\,\varphi'\,(K_s - K_f)]}{[K_s + 2\,K_f + \varphi'\,(K_s - K_f)]}$$

The results were plotted against the Experimental and Hamilton-Crosser model for different volume fractions [32]. Spherical Cluster pattern was used to solve the model.

Hamilton-Crosser model does not address the issue of Brownian motion, and the obtained

values follows Hamilton-Crosser model values thereby indicating that the assumptions made for

the Keff of the stationary particles are true.

The experimental data was collected from Kim et al. [49]. Solving the model using

spherical clusters and ignoring the effect of Brownian motion we get the following results. The

values are compared with the experimental data [49] and Hamilton-Crosser model [32]

The two evaluation of the effect of Brownian motion in thermal conductivity indicated

that the Brownian motion plays a role in enhancement of thermal conductivity marginally.

Further evaluation on various combinations of nanofluids will provide a baseline decision on

the role of Brownian motion in the enhancement of thermal conductivity.

Table 5. 23 Variation of thermal conductivity without Brownian motion for

 CuO (18 nm) - Water nanofluids

Volume Fraction	K_exp (W/m-K)	K_cluster (W/m-K)	Hamilton &Crosser (W/m-K)	K_total (W/m-K)
0.01	0.6 355	0.6 302	0.6297	0.6480
0.02	0.6 562	0.6 484	0.6468	0.6662
0.03	0.6 772	0.6 677	0.6643	0.6854
0.04	0.6 985	0.6 880	0.6820	0.7058

Figure 5. 30 Thermal conductivity without Brownian motion for CuO (18 nm) - Water

nanofluids

Table 5. 24 Variation of thermal conductivity without Brownian motion for

CuO (23.6 nm) - Water nanofluids

Volume Fraction	K_exp (W/m-K)	K_cluster (W/m-K)	Hamilton& Crosser (W/m-K)	K_total (W/m-K)
0.01	0.6359	0.63024	0.6297	0.6439
0.02	0.6577	0.64840	0.6468	0.6620
0.03	0.6743	0.66756	0.6643	0.6812
0.04	0.6972	0.68782	0.682	0.7015

Figure 5. 31 Thermal conductivity without Brownian motion for CuO (23.6 nm) - Water

nanofluids

Table 5. 25 Variation of thermal conductivity without Brownian motion for

CuO (30.8 nm) - EG nanofluids

Volume Fraction	K_exp (W/m-K)	K_cluster (W/m-K)	Hamilton&Crosser (W/m-K)	K_total (W/m-K)
0.01	0.26210	0.25959	0.25940	0.26585
0.02	0.27970	0.26760	0.26700	0.27386
0.03	0.28730	0.27607	0.27480	0.28233
0.04	0.29740	0.28504	0.28270	0.29130

Figure 5. 32 Thermal conductivity without Brownian motion for

CuO (30.8 nm) - EG nanofluids

Table 5. 26 Variation of thermal conductivity without Brownian motion for Alumina (60.4 nm)

- Water nanofluids

Volum Fraction	K_exp (W/m-K)	K_cluster (W/m-K)	Hamilton& Crosser (W/m-K)	K_total (W/m-K)
0.01	0.6375	0.6311	0.6307	0.6360
0.02	0.6589	0.6501	0.6489	0.6550
0.03	0.6804	0.6701	0.6669	0.6750
0.04	0.6988	0.6912	0.6862	0.6961

Figure 5. 33 Thermal conductivity without Brownian motion for Alumina (60.4 nm) - Water

nanofluids

Table 5. 27 Variation of thermal conductivity without Brownian motion for

Alumina (26 nm) - EG nanofluids

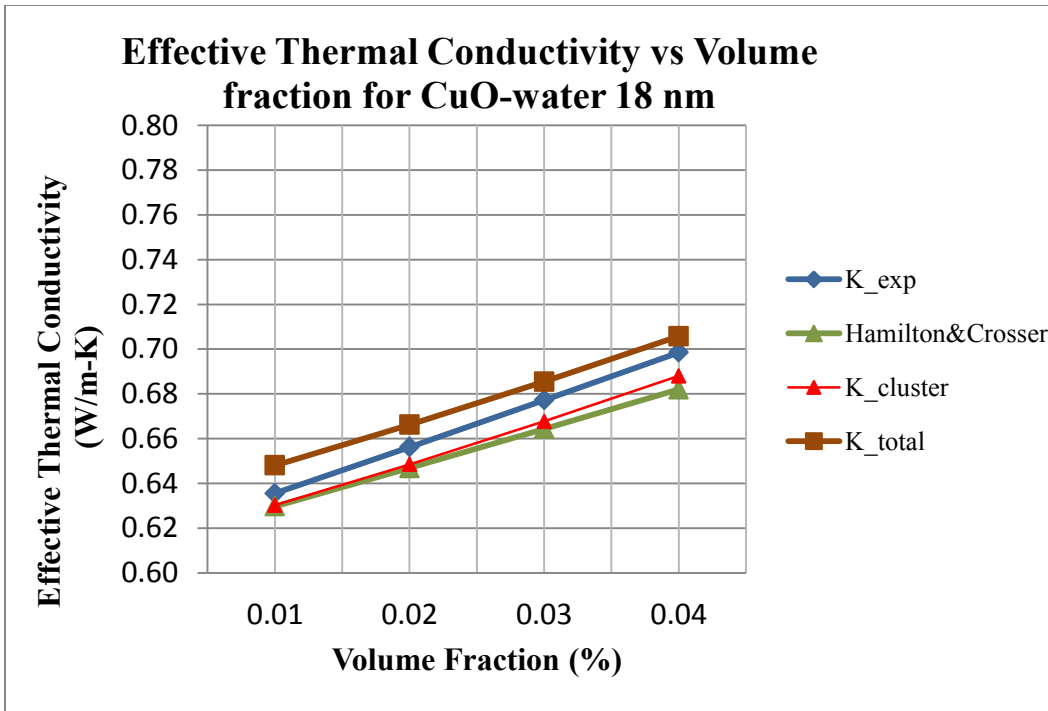| VolumeFraction	K_exp (W/m-K)	K_cluster (W/m-K)	Hamilton& Crosser (W/m-K)	K_total (W/m-K)
0.01	0.2625	0.2596	0.2595	0.2670
0.02	0.272	0.2677	0.2682	0.2751
0.03	0.2834	0.2762	0.276	0.2836
0.04	0.2909	0.2853	0.284	0.2926

Figure 5. 34 Thermal conductivity without Brownian motion for Alumina (26 nm) - EG

nanofluids

Table 5. 28 Variation of thermal conductivity without Brownian motion for

TiO$_2$ (10 nm) - Water nanofluids

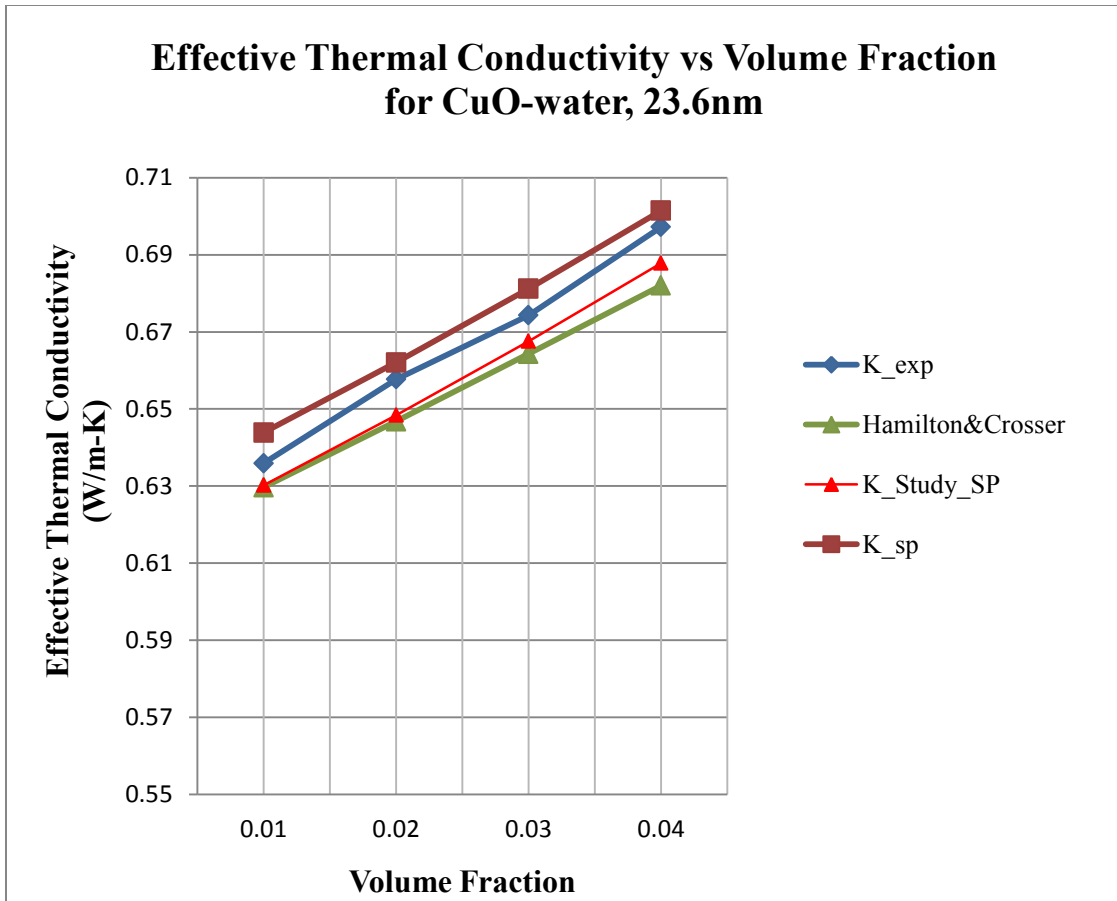| VolumeFraction	K_exp (W/m-K)	K_cluster (W/m-K)	Hamilton&Crosser (W/m-K)	K_total (W/m-K)
0.01	0.627	0.6222	0.6218	0.6501
0.02	0.6537	0.6382	0.6369	0.6662
0.03	0.6761	0.6552	0.6523	0.6831

Figure 5. 35 Thermal conductivity without Brownian motion for TiO$_2$ (10 nm) - Water

nanofluids

Table 5. 29 Variation of thermal conductivity without Brownian motion for TiO_2 (34 nm) - Water nanofluids

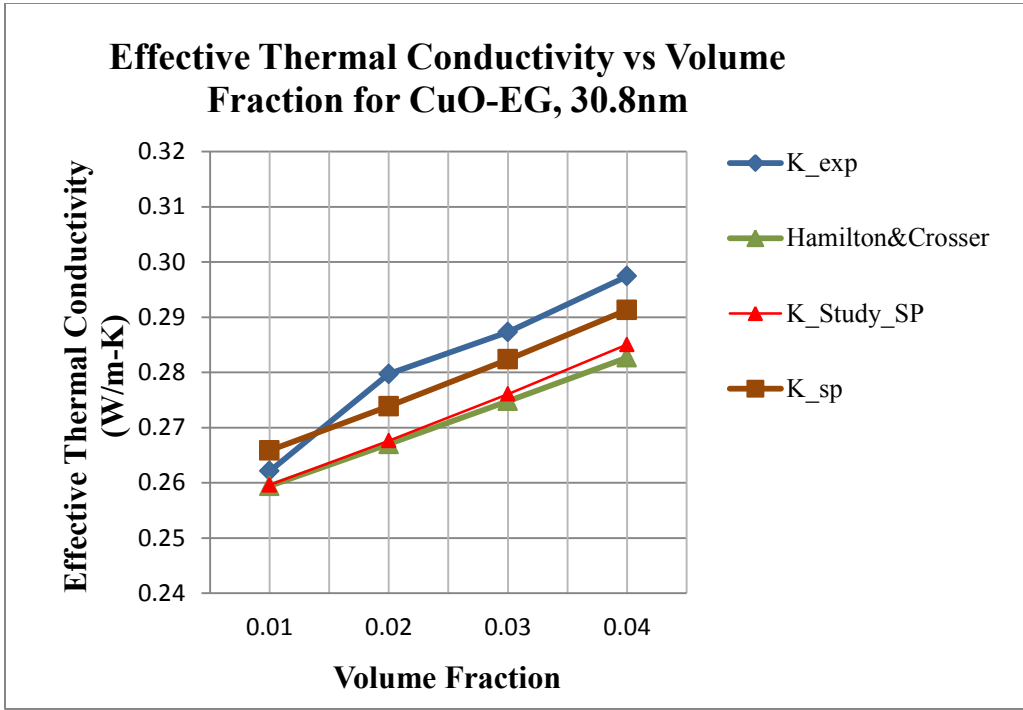| VolumeFraction	K_exp (W/m-K)	K_cluster (W/m-K)	Hamilton&Crosser (W/m-K)	K_total (W/m-K)
0.01	0.6239	0.6221	0.6218	0.6307
0.02	0.6452	0.6380	0.6369	0.6465
0.03	0.6598	0.6547	0.6523	0.6632

Figure 5. 36 Thermal conductivity without Brownian motion for TiO_2 (34 nm) - Water nanofluids

Table 5. 30 Variation of thermal conductivity without Brownian motion for TiO_2 (34 nm) – EG

nanofluids

VolumeFraction	K_exp (W/m-K)	K_cluster (W/m-K)	Hamilton&Crosser (W/m-K)	K_total (W/m-K)
0.01	0.261	0.2591	0.2589	0.2648
0.02	0.2719	0.2666	0.267	0.2723
0.03	0.2829	0.2745	0.2733	0.2802

Figure 5. 37 Thermal conductivity without Brownian motion for TiO_2 (34 nm) –

EG nanofluids

Table 5. 31 Variation of thermal conductivity without Brownian motion for ZnO (10 nm) -

Water nanofluids

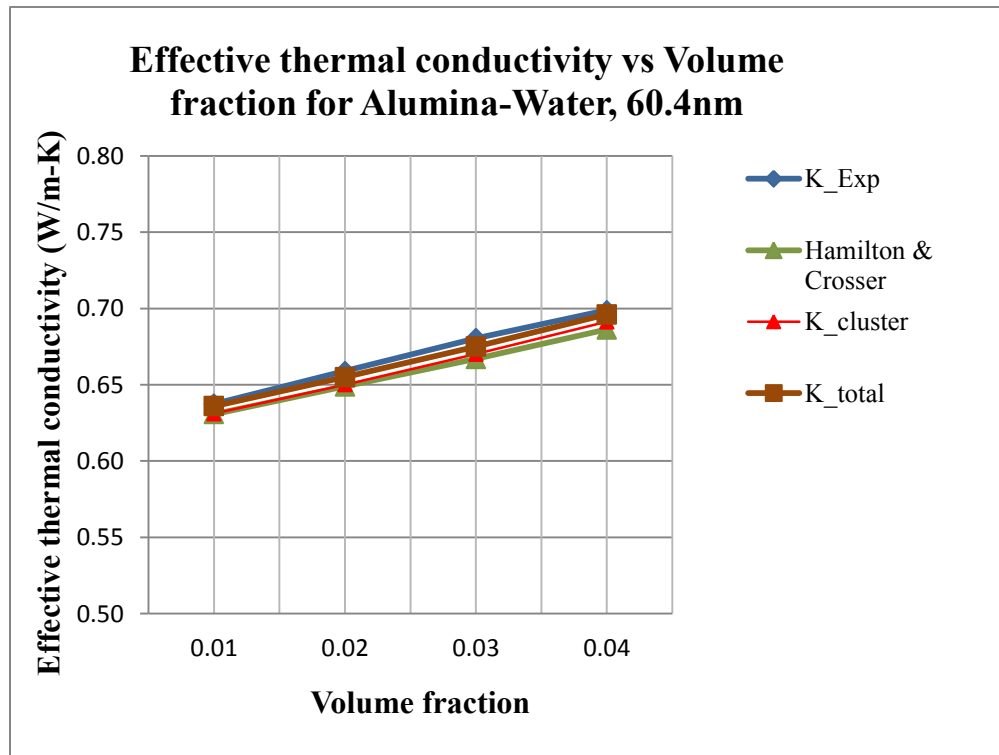| VolumeFraction	K_exp (W/m-K)	K_cluster (W/m-K)	Hamilton&Crosser (W/m-K)	K_total (W/m-K)
0.01	0.6367	0.6246	0.6242	0.6526
0.02	0.6652	0.6433	0.6419	0.6713
0.03	0.6931	0.6631	0.6579	0.6911
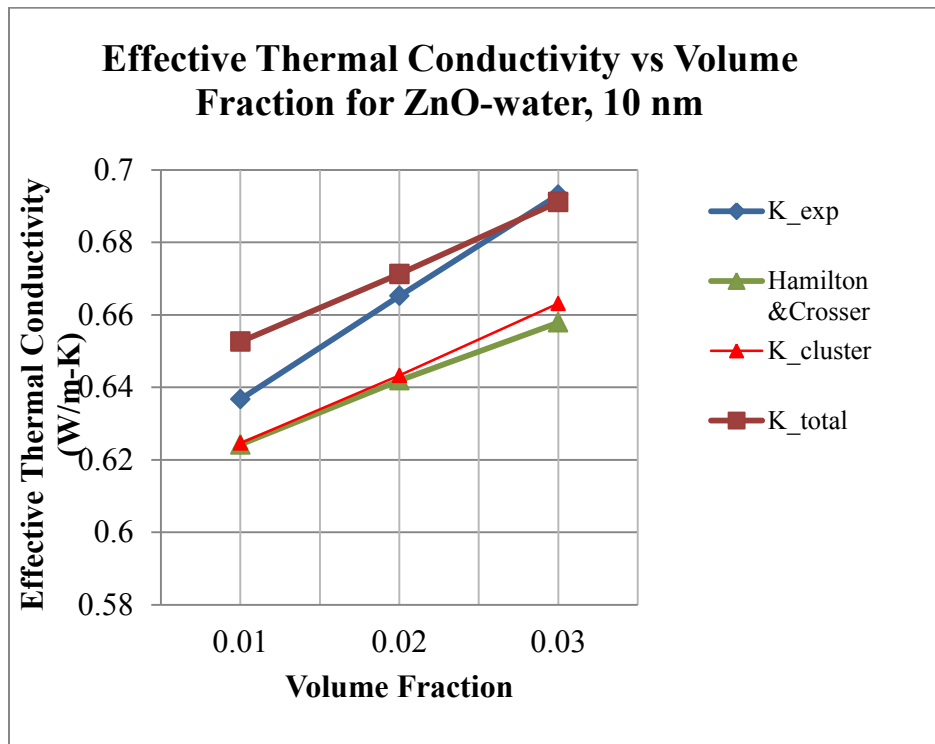
Figure 5. 38 Thermal conductivity without Brownian motion for ZnO (10 nm) –

Water nanofluids

Table 5. 32 Variation of thermal conductivity without Brownian motion for ZnO (30 nm) -

Water nanofluids

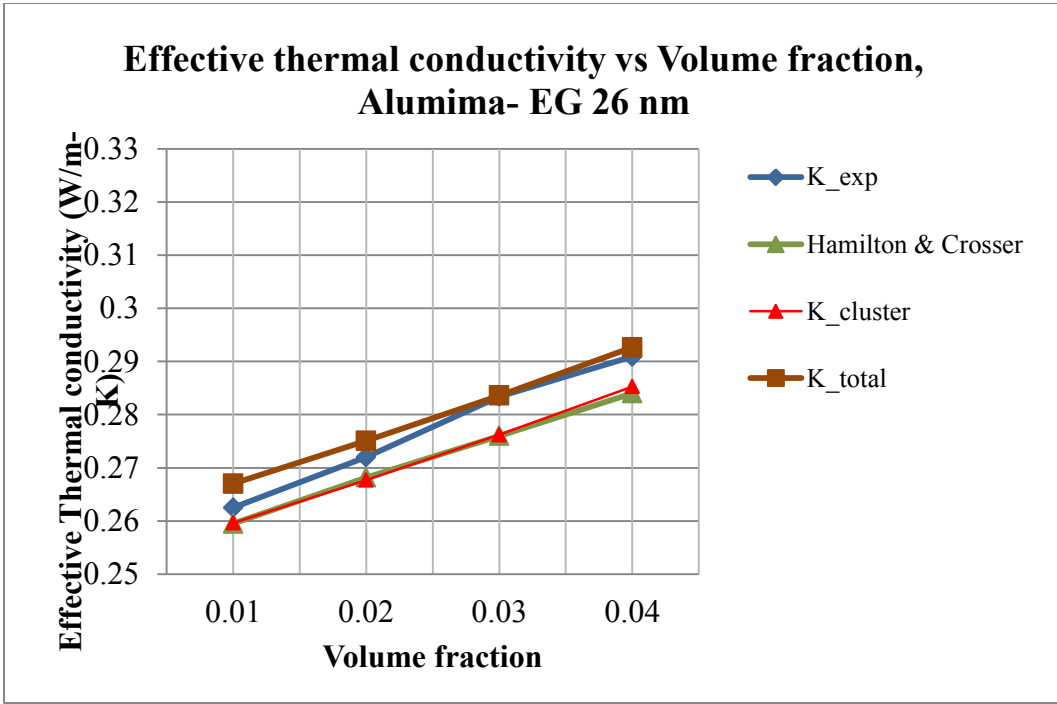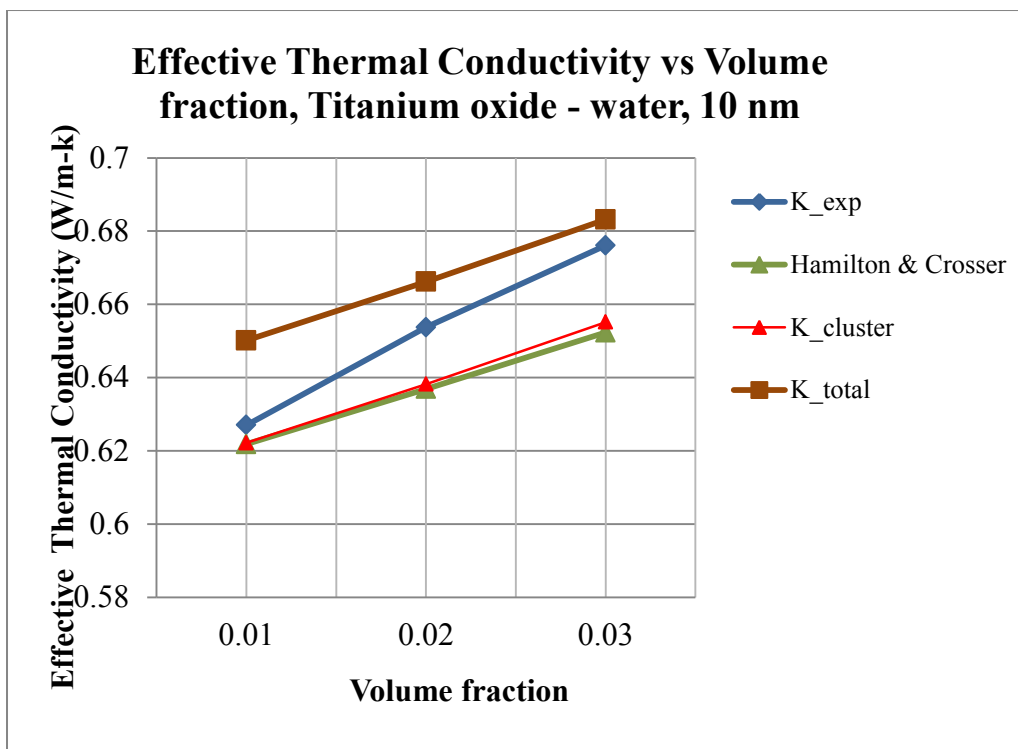| Volume Fraction	K_exp (W/m-K)	K_cluster (W/m-K)	Hamilton& Crosser (W/m-K)	K_total (W/m-K)
0.01	0.627	0.6246	0.6242	0.6342
0.02	0.65	0.6431	0.6419	0.6527
0.03	0.6768	0.6626	0.6598	0.6722
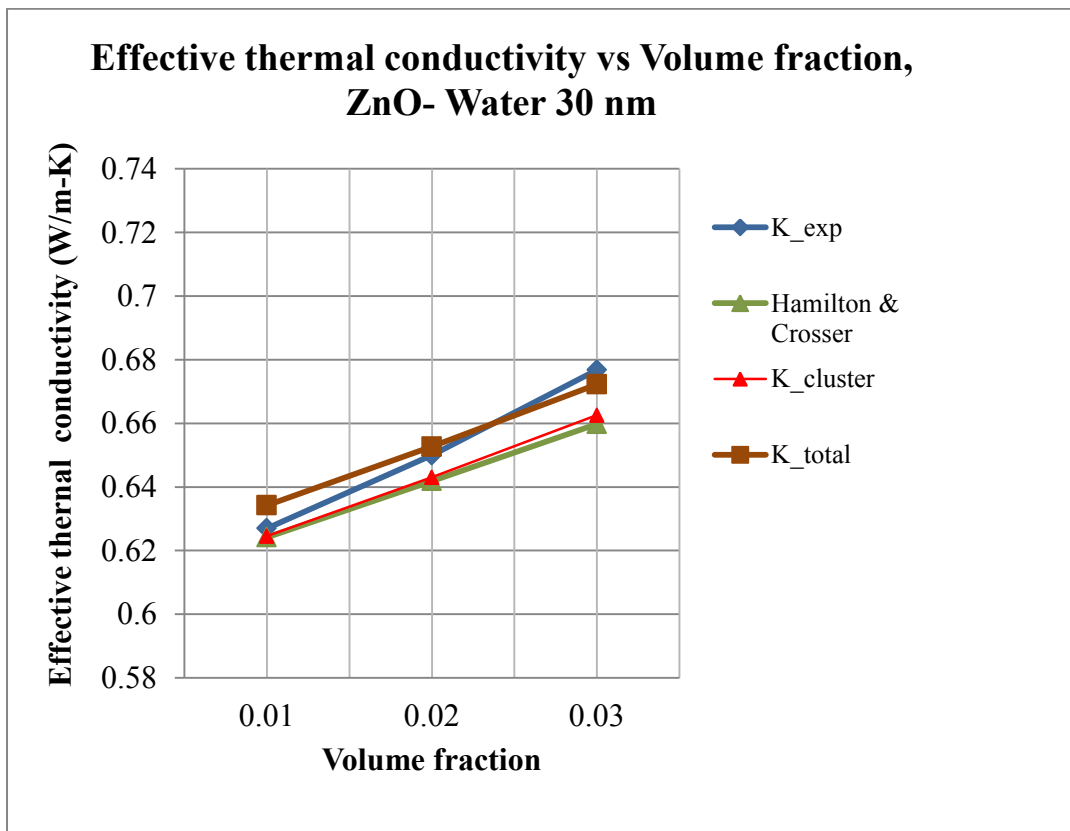
Figure 5. 39 Thermal conductivity without Brownian motion for ZnO (30 nm) - Water

nanofluids

Table 5. 33 Variation of thermal conductivity without Brownian motion for ZnO (60 nm) – EG

nanofluids

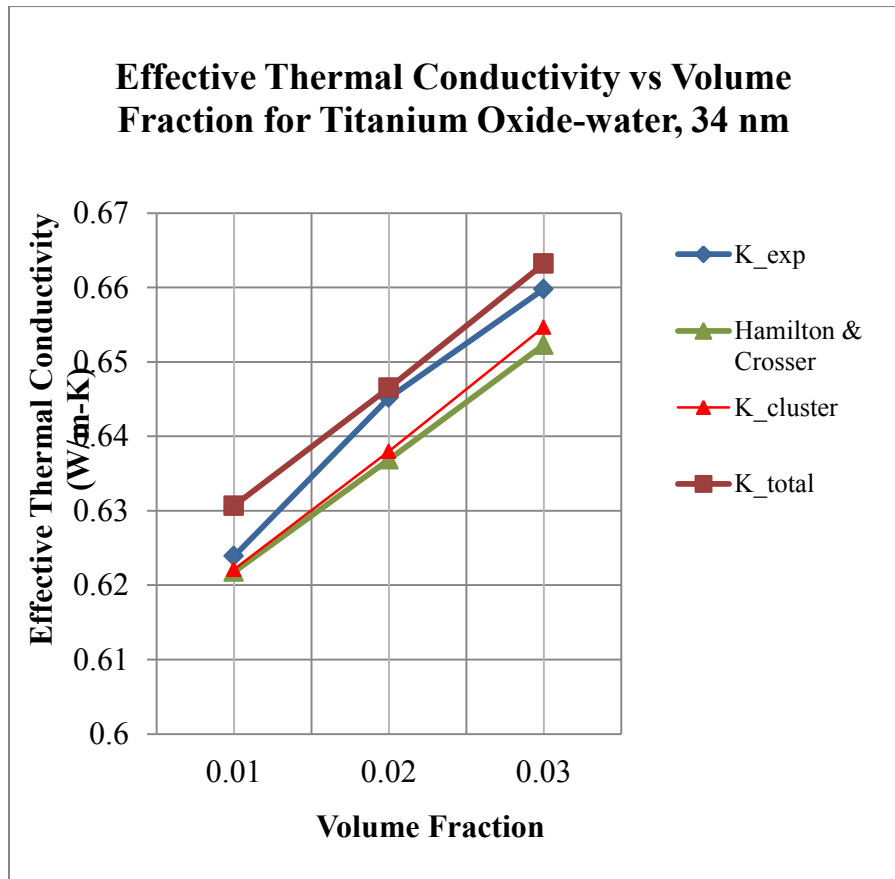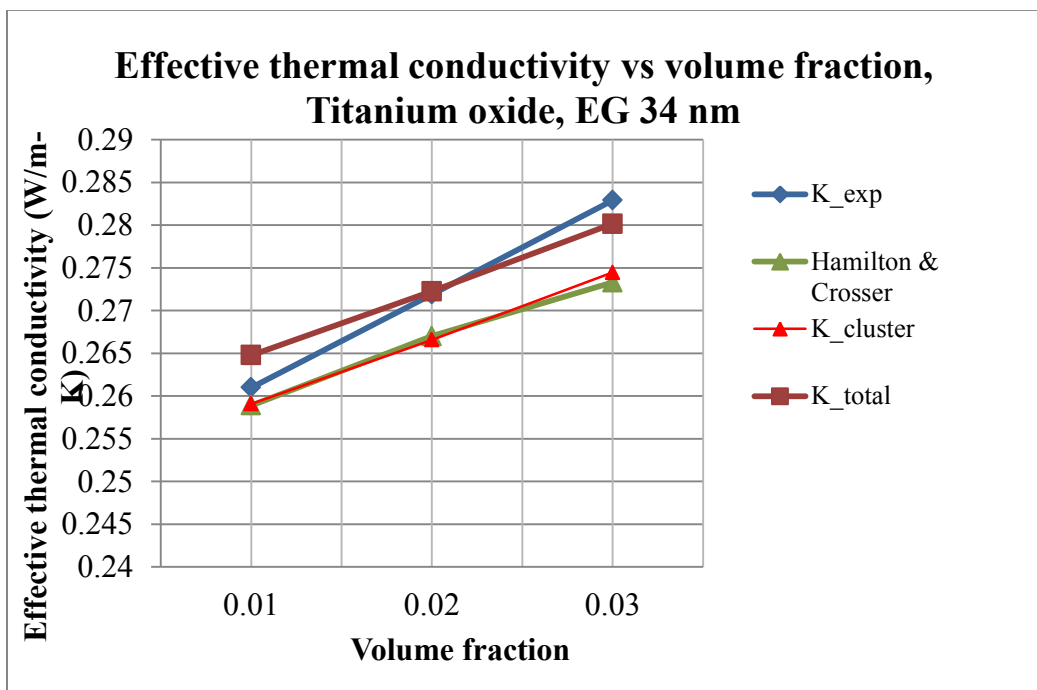| Volume Fraction	K_exp (W/m-K)	K_cluster (W/m-K)	Hamilton&Crosser (W/m-K)	K_total (W/m-K)
0.01	0.2601	0.2596	0.2594	0.2628
0.02	0.2699	0.2675	0.267	0.2708
0.03	0.279	0.2759	0.2747	0.2792
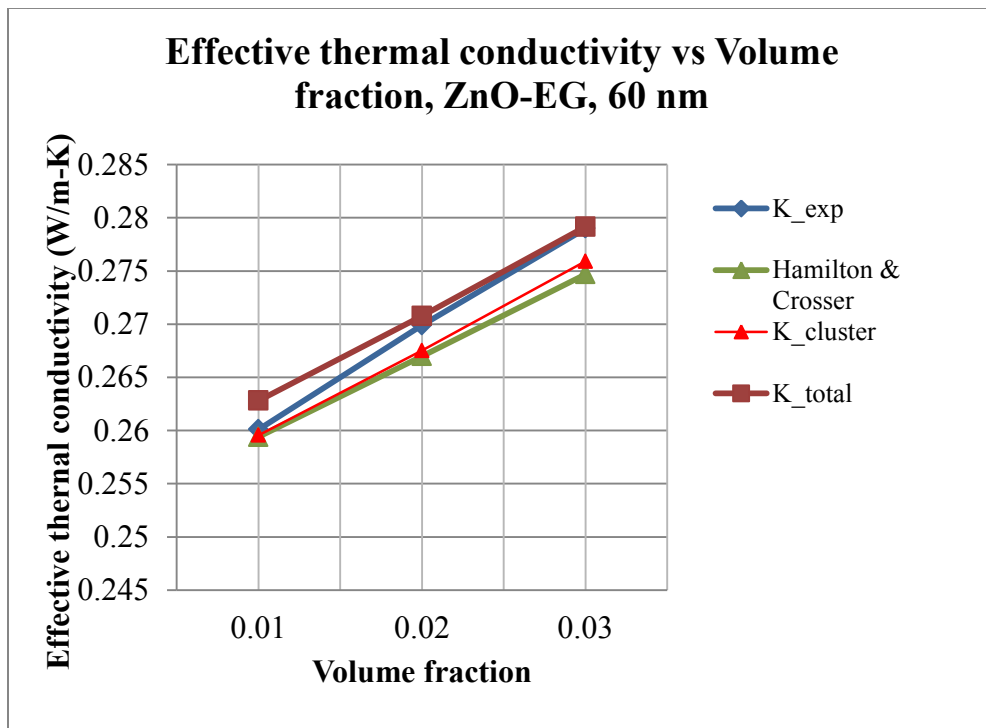
Figure 5. 40 Thermal conductivity without Brownian motion for ZnO (60 nm) – EG nanofluids

Table 5. 34 Variation of thermal conductivity without Brownian motion for Al (20 nm) - Water

nanofluids

Volume Fraction	K_exp (W/m-K)	K_cluster (W/m-K)	Hamilton&Crosser (W/m-K)	K_total (W/m-K)
0.01	0.6344	0.6315	0.6314	0.6460
0.02	0.6589	0.6506	0.6502	0.6651
0.03	0.6877	0.6703	0.6694	0.6848
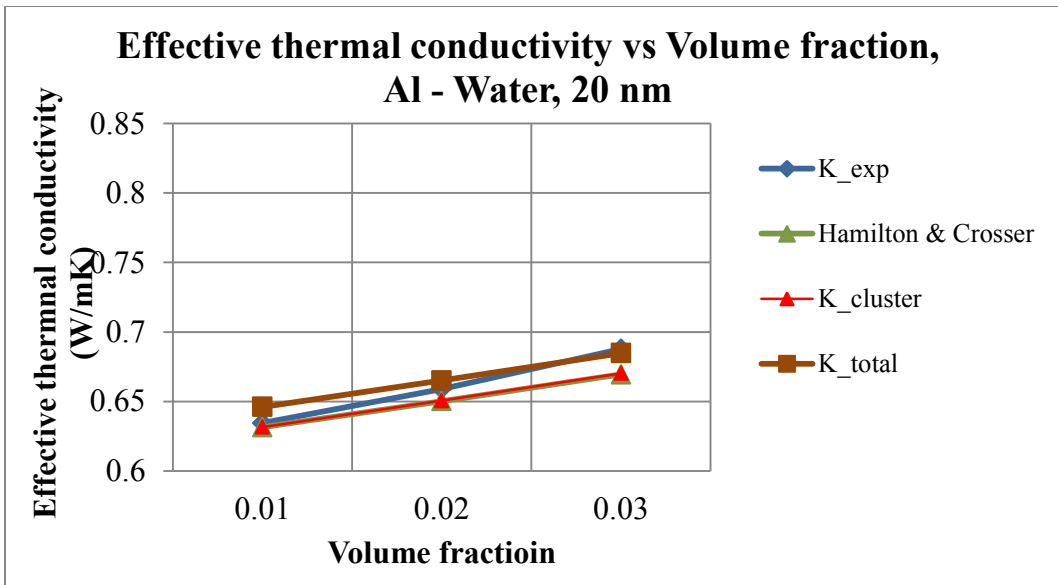
Figure 5. 41 Thermal conductivity without Brownian motion for Al (20 nm) - Water nanofluids

The mathematical models were solved without the Brownian motion and the graphs were plotted against experimental data's published and Hamilton-Crosser equation for various combinations of nanofluids and the total thermal conductivity values. The above graphs lie on par with the Hamilton-Crosser equation values, which validates that the mathematical model. The graphs also shows that the thermal conductivity values lie below the experimental values, which indicate that the Brownian motion contributes to the thermal conductivity enhancements

in nanofluids. It was found that the contribution of Brownian Motion was around 5% in lower nanoparticle size (10 nm) and gradually decreased as the nanoparticle size increases. This also validates the mathematical data developed. The size increase of the nanoparticle may have less Brownian Motion thereby having a low impact in larger nanoparticles.

D.   Effect of Cluster Stacking

The final parametric study that was done to study the effect of thermal conductivity by stacking the nanoclusters. The clusters were assumed to stack together and the effective lengths of the clusters were assumed to range from 0.33 to 2. The mathematical model was solved for volume fractions 0.01 to 0.04. The values were plot as shown below for various nanofluid combinations.

Table 5. 35 Effect of Cluster Stacking CuO (18 nm) – Water nanofluids

Mean	Volume Fraction			
$\gamma_c/\gamma_{unit\ cell}$	0.01	0.02	0.03	0.04
0.33	0.6840	0.7022	0.7215	0.7418
0.5	0.6657	0.6839	0.7032	0.7235
1	0.6480	0.6662	0.6854	0.7058
1.2599	0.6443	0.6625	0.6818	0.7021
1.4423	0.6426	0.6607	0.6800	0.7003
1.5874	0.6414	0.6596	0.6788	0.6992
1.71	0.6406	0.6588	0.6780	0.6984
1.8171	0.6400	0.6582	0.6774	0.6978
1.9129	0.6395	0.6577	0.6769	0.6973
2	0.6391	0.6573	0.6765	0.6969

Figure 5. 42 Effect of Cluster Stacking on thermal conductivity for CuO(18 nm) –Water

nanofluids

Table 5. 36 Effect of Cluster Stacking CuO (23.6 nm) – Water nanofluids

Number of	Volume Fraction			
$\gamma_c/\gamma_{unit\ cell}$	0.01	0.02	0.03	0.04
0.33	0.6840	0.7022	0.7215	0.7418
0.5	0.6657	0.6839	0.7032	0.7235
1	0.6480	0.6662	0.6854	0.7058
1.2599	0.6443	0.6625	0.6818	0.7021
1.4423	0.6426	0.6607	0.6800	0.7003
1.5874	0.6414	0.6596	0.6788	0.6992
1.71	0.6406	0.6588	0.6780	0.6984
1.8171	0.6400	0.6582	0.6774	0.6978
1.9129	0.6395	0.6577	0.6769	0.6973
2	0.6391	0.6573	0.6765	0.6969

Figure 5. 43 Effect of Cluster Stacking on thermal conductivity for CuO (23.6 nm)–

Water nanofluids

Table 5. 37 Effect of Cluster Stacking CuO (30.8 nm) – EG nanofluids

Number of	Volume Fraction			
$\gamma_c/\gamma_{unit\ cell}$	0.01	0.02	0.03	0.04
0.33	0.2786	0.2866	0.2950	0.3040
0.5	0.2721	0.2801	0.2886	0.2976
1	0.2658	0.2739	0.2823	0.2913
1.2599	0.2646	0.2726	0.2810	0.2900
1.4423	0.2639	0.2719	0.2804	0.2894
1.5874	0.2635	0.2715	0.2800	0.2890
1.71	0.2632	0.2713	0.2797	0.2887
1.8171	0.2630	0.2710	0.2795	0.2885
1.9129	0.2629	0.2709	0.2793	0.2883
2	0.2627	0.2707	0.2792	0.2882

112
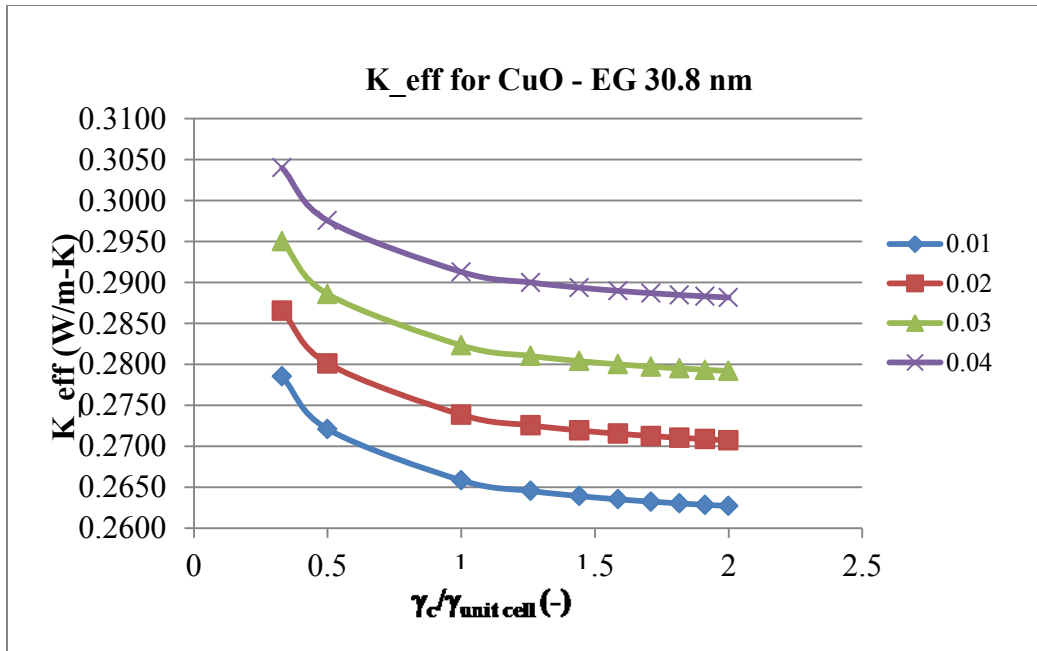
Figure 5. 44 Effect of Cluster Stacking on thermal conductivity

CuO (30.8 nm) – EG nanofluids

Table 5. 38 Effect of Cluster Stacking Al_2O_3 (60.4 nm) – Water

nanofluids

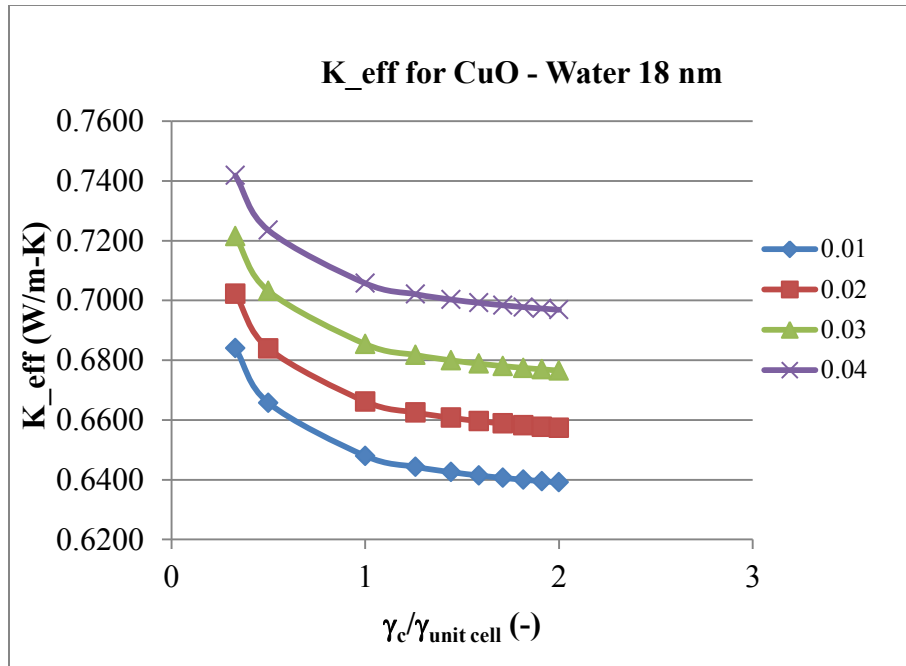| Number of	Volume Fraction			
$\gamma_c/\gamma_{unit\ cell}$	0.01	0.02	0.03	0.04
0.33	0.6459	0.6649	0.6849	0.7061
0.5	0.6409	0.6599	0.6799	0.7010
1	0.6360	0.6550	0.6750	0.6961
1.2599	0.6350	0.6540	0.6740	0.6951
1.4423	0.6345	0.6535	0.6735	0.6946
1.5874	0.6341	0.6532	0.6732	0.6943
1.71	0.6339	0.6529	0.6730	0.6941
1.8171	0.6338	0.6528	0.6728	0.6939
1.9129	0.6336	0.6526	0.6727	0.6938
2	0.6335	0.6525	0.6725	0.6937

Figure 5. 45 Effect of Cluster Stacking on thermal conductivity Al$_2$O$_3$ (60.4 nm) – Water nanofluids

Table 5. 39 Effect of Cluster Stacking Al$_2$O$_3$ (26 nm) – EG nanofluids

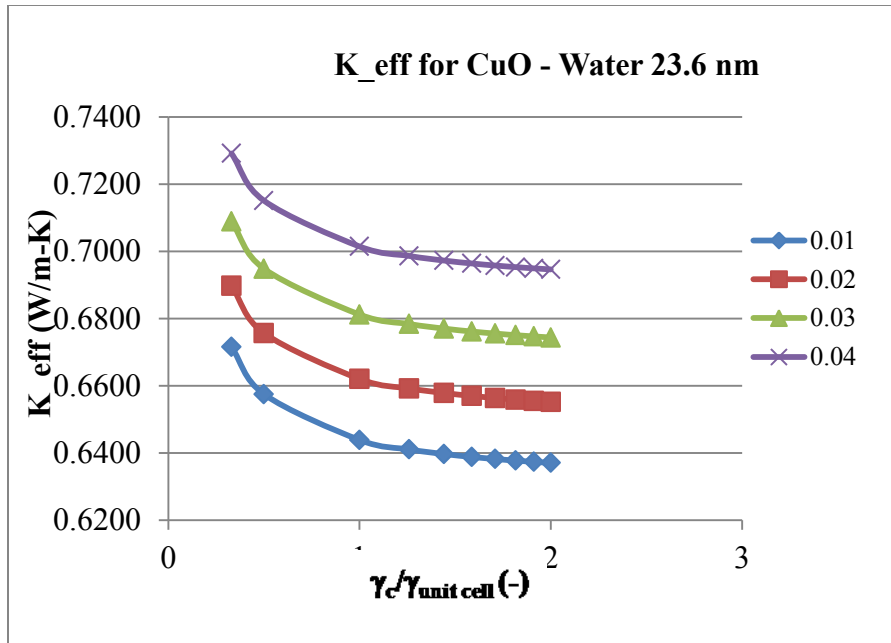| Number of	Volume Fraction			
$\gamma_c/\gamma_{unit\ cell}$	0.01	0.02	0.03	0.04
0.33	0.2820	0.2900	0.2986	0.3076
0.5	0.2744	0.2824	0.2910	0.3000
1	0.2670	0.2751	0.2836	0.2926
1.2599	0.2655	0.2735	0.2821	0.2911
1.4423	0.2647	0.2728	0.2813	0.2904
1.5874	0.2643	0.2723	0.2809	0.2899
1.71	0.2639	0.2720	0.2805	0.2896
1.8171	0.2637	0.2718	0.2803	0.2893
1.9129	0.2635	0.2716	0.2801	0.2891
2	0.2633	0.2714	0.2799	0.2890

114

Figure 5. 46 Effect of Cluster Stacking on thermal conductivity for Al_2O_3 (26 nm) – EG

nanofluids

Table 5. 40 Effect of Cluster Stacking TiO_2 (10 nm) – Water nanofluids

Number of	Volume Fraction			
$\gamma_c/\gamma_{unit\ cell}$	0.01	0.02	0.03	0.04
0.33	0.7070	0.7230	0.7400	0.7580
0.5	0.6781	0.6942	0.7111	0.7291
1	0.6501	0.6662	0.6831	0.7012
1.2599	0.6444	0.6604	0.6774	0.6954
1.4423	0.6416	0.6576	0.6746	0.6926
1.5874	0.6398	0.6558	0.6728	0.6908
1.71	0.6385	0.6546	0.6715	0.6895
1.8171	0.6376	0.6536	0.6706	0.6886
1.9129	0.6368	0.6528	0.6698	0.6878
2	0.6362	0.6522	0.6692	0.6872

Figure 5. 47 Effect of Cluster Stacking on thermal conductivity for

TiO$_2$ (10 nm) – Water nanofluids

Table 5. 41 Effect of Cluster Stacking TiO$_2$ (34 nm) – Water nanofluids

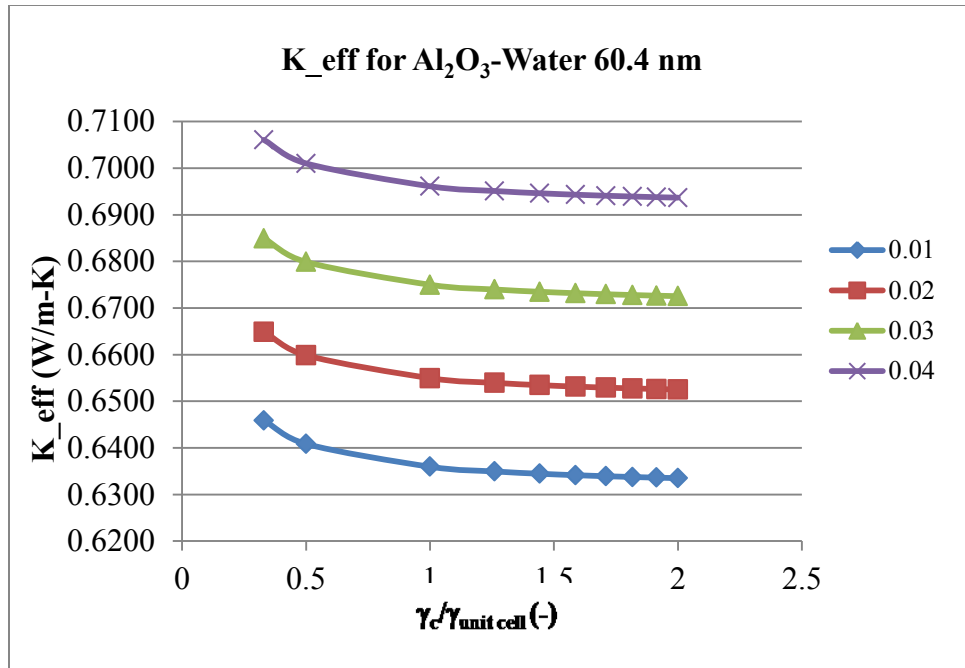| Number of	Volume Fraction			
$\gamma_c/\gamma_{\text{unit cell}}$	0.01	0.02	0.03	0.04
0.33	0.6480	0.6639	0.6806	0.6982
0.5	0.6392	0.6551	0.6718	0.6893
1	0.6307	0.6465	0.6632	0.6808
1.2599	0.6289	0.6448	0.6615	0.6790
1.4423	0.6280	0.6439	0.6606	0.6782
1.5874	0.6275	0.6434	0.6601	0.6776
1.71	0.6271	0.6430	0.6597	0.6772
1.8171	0.6268	0.6427	0.6594	0.6769
1.9129	0.6266	0.6425	0.6591	0.6767
2	0.6264	0.6423	0.6589	0.6765

Figure 5. 48 Effect of Cluster Stacking on thermal conductivity for TiO_2 (34 nm) – Water nanofluids

Table 5. 42 Effect of Cluster Stacking TiO_2 (27 nm) – Water nanofluids

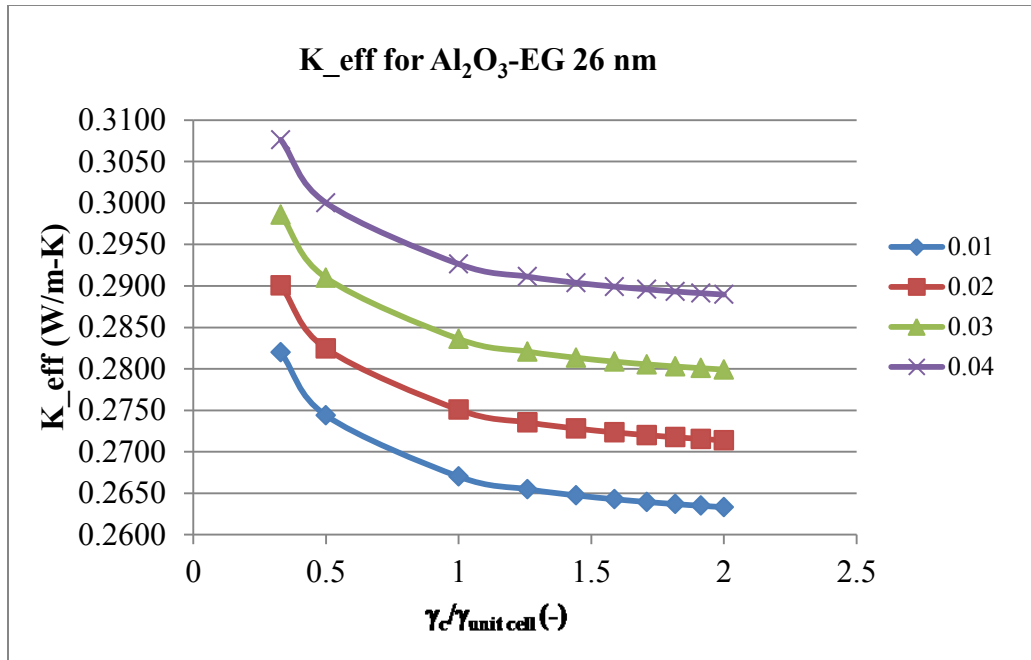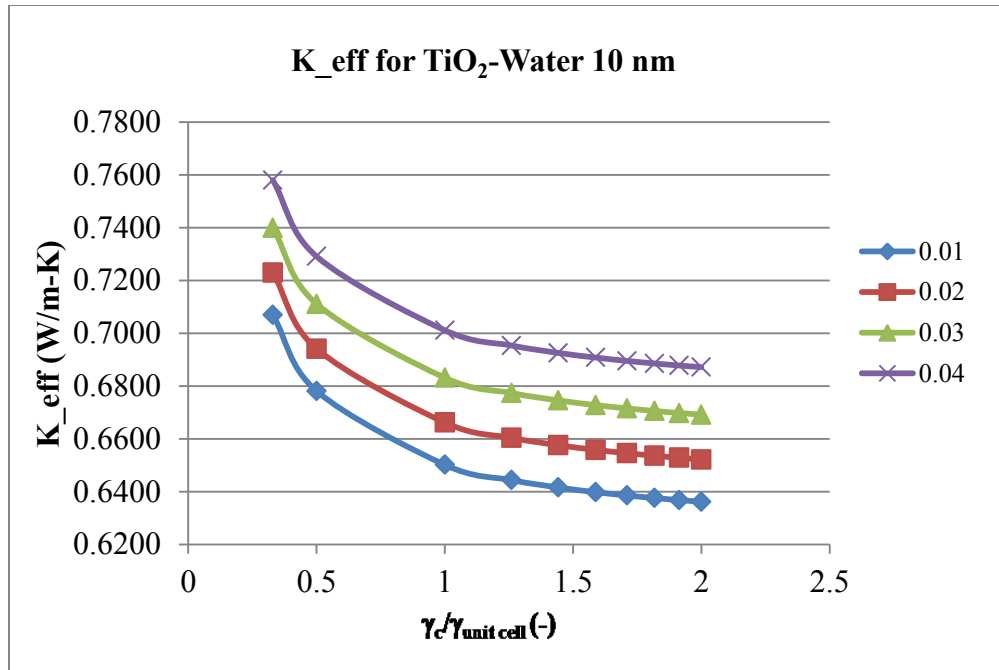| Number of	Volume Fraction			
$\gamma_c/\gamma_{unit\ cell}$	0.01	0.02	0.03	0.04
0.33	0.6611	0.6771	0.6939	0.7117
0.5	0.6499	0.6659	0.6828	0.7005
1	0.6391	0.6551	0.6719	0.6897
1.2599	0.6368	0.6528	0.6697	0.6874
1.4423	0.6357	0.6518	0.6686	0.6864
1.5874	0.6351	0.6511	0.6679	0.6857
1.71	0.6346	0.6506	0.6674	0.6852
1.8171	0.6342	0.6502	0.6671	0.6848
1.9129	0.6339	0.6499	0.6668	0.6845
2	0.6337	0.6497	0.6665	0.6843
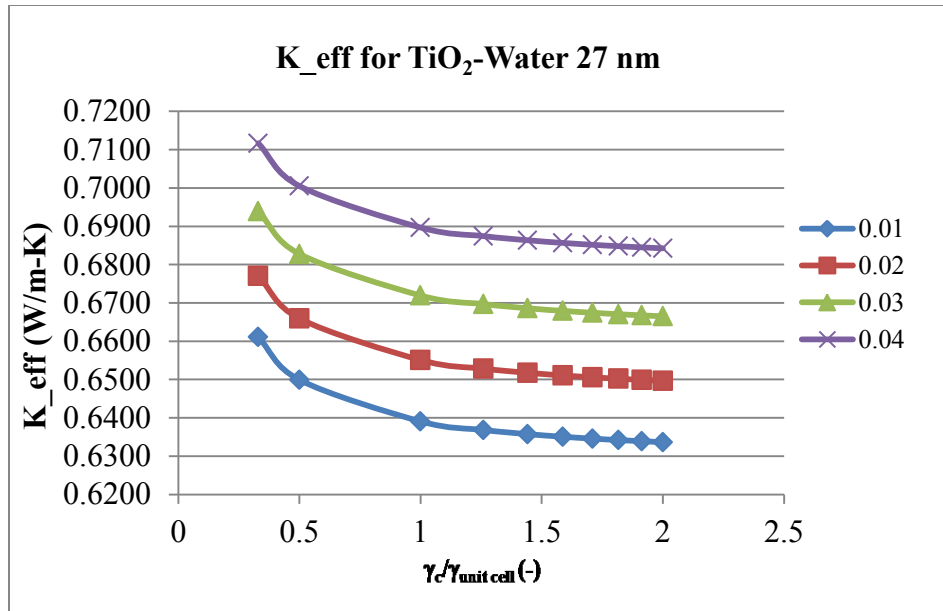
Figure 5. 49 Effect of Cluster Stacking on thermal conductivity for TiO_2 (27 nm) – Water nanofluids

Table 5. 43 Effect of Cluster Stacking TiO_2 (34 nm) – EG nanofluids

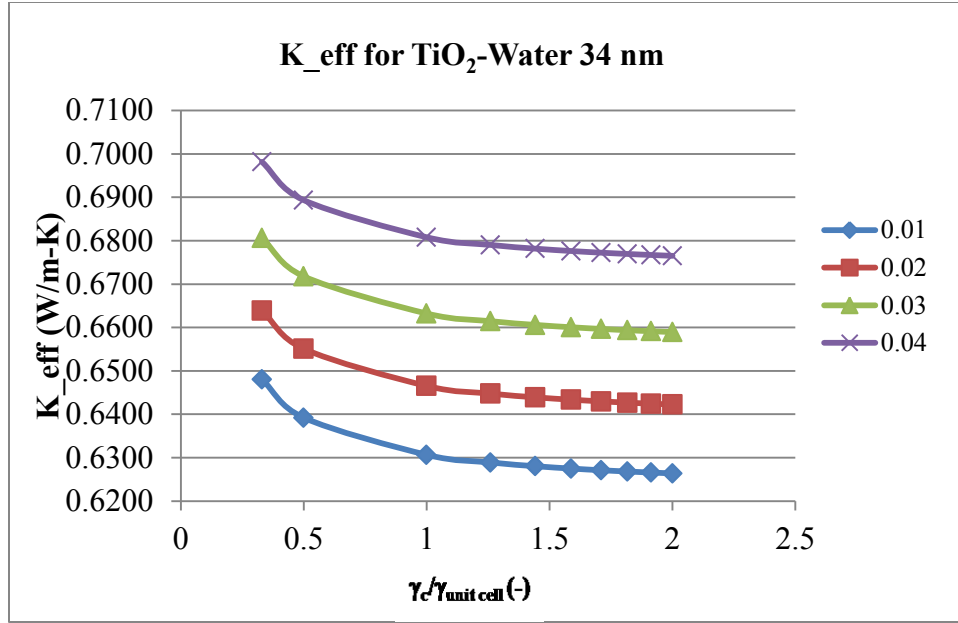| Number of	Volume Fraction			
$\gamma_c/\gamma_{unit\ cell}$	0.01	0.02	0.03	0.04
0.33	0.2763	0.2838	0.2917	0.3000
0.5	0.2705	0.2779	0.2858	0.2942
1	0.2648	0.2723	0.2802	0.2885
1.2599	0.2636	0.2711	0.2790	0.2873
1.4423	0.2630	0.2705	0.2784	0.2868
1.5874	0.2627	0.2702	0.2780	0.2864
1.71	0.2624	0.2699	0.2778	0.2861
1.8171	0.2622	0.2697	0.2776	0.2859
1.9129	0.2621	0.2695	0.2774	0.2858
2	0.2619	0.2694	0.2773	0.2857
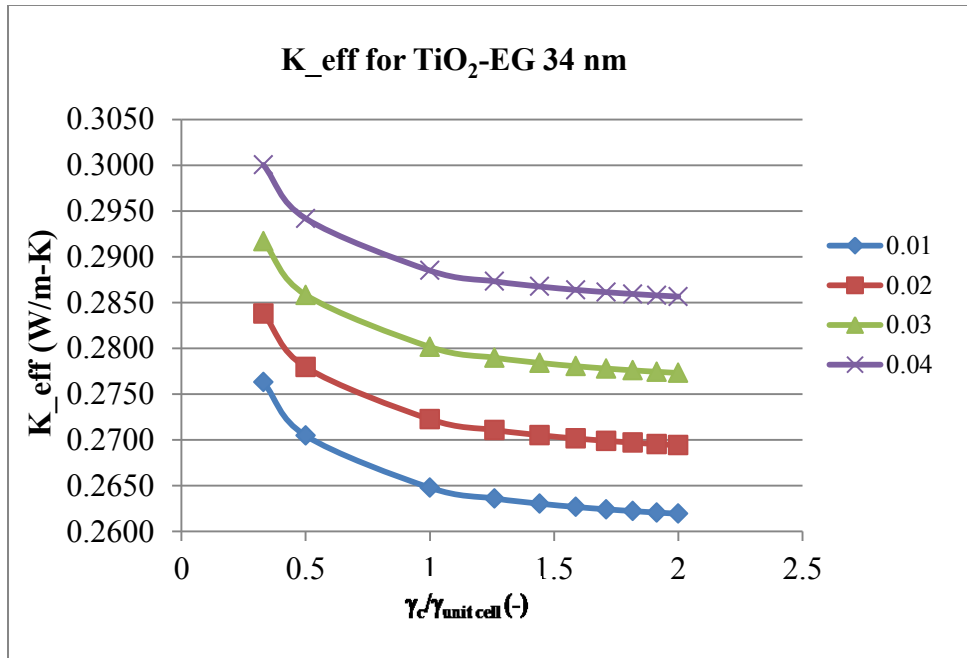
Figure 5. 50 Effect of Cluster Stacking on thermal conductivity for TiO_2 (34 nm) – EG

nanofluids

Table 5. 44 Effect of Cluster Stacking ZnO (10 nm) – Water nanofluids

Number of	Volume Fraction			
$\gamma_c/\gamma_{unit\ cell}$	0.01	0.02	0.03	0.04
0.33	0.7094	0.7281	0.7479	0.7690
0.5	0.6806	0.6993	0.7191	0.7402
1	0.6526	0.6713	0.6911	0.7122
1.2599	0.6468	0.6655	0.6853	0.7064
1.4423	0.6440	0.6627	0.6825	0.7036
1.5874	0.6422	0.6609	0.6807	0.7018
1.71	0.6410	0.6596	0.6795	0.7006
1.8171	0.6400	0.6587	0.6785	0.6996
1.9129	0.6392	0.6579	0.6777	0.6988
2	0.6386	0.6573	0.6771	0.6982

K_eff for ZnO-Water 10 nm
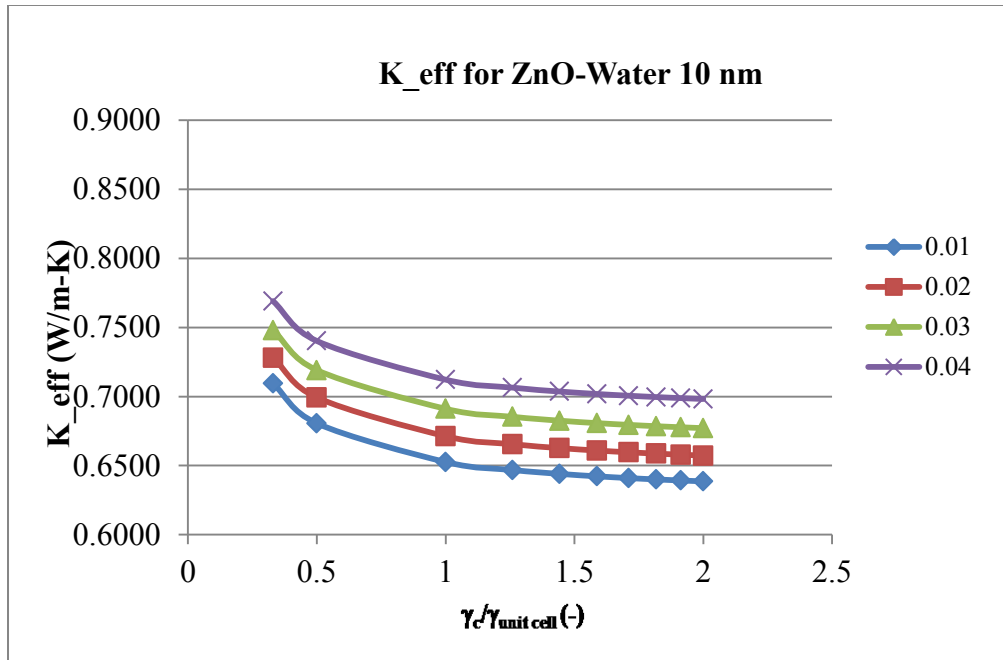
Figure 5. 51 Effect of Cluster Stacking on thermal conductivity for ZnO (10 nm) – Water

nanofluids

The above graphs indicate that the thermal conductivity decreases as the nanoclusters

begin to stack. There is a steep reduction in thermal conductivity as the nanocluster is divided in

half and then decreases linearly when the clusters join to combine. Further study can be done to

find out the reason behind the strange behavior.

E.   Discussion of results of the parametric studies

Based on the preliminary results and validation, it is found that the clustering of

nanoparticles in a nanofluid, the nanolayer thickness around the nanoparticles and the Brownian

motion play a critical role in the thermal conductivity enhancement of nanofluids. The

mathematical model developed lies on par with experimental data which confirms that the

assumptions made for the development of mathematical model are accurate and well within the

practical limitations. The contribution due to the Brownian motion due to moving nanoparticles

in nanofluids is negligible when compared to the clustering effect of nanoparticles. The effect of

nanoparticle diameter on the Brownian motion will be further analyzed using different sample sets from various research and experimental data. The influence of zeta potential and the nanolayer thickness will also be further analyzed. The factors governing the overall enhancement of thermal conductivity will be understood better by solving the mathematical model using the various assumptions. Validation of these results will provide an insight to increase the thermal conductivity of nanofluids.

CHAPTER 6

CONCLUSION

A model for effective thermal conductivity of nanofluids was developed based on the clustering of nanoparticles, nanolayer thickness, Brownian motion of the nanoparticle and volume fraction of nanoclusters. The mathematical model developed to calculate the thermal conductivity is a function of the thermal conductivities of the fluid and the nanoparticle, clustering effect, the nanolayer, volume fraction, nanoparticle diameter. The developed equation was compared to other models in the literature to understand the proximity of the results. Parametric studies were conducted to know the effect of different factors on thermal conductivity of nanofluids.

Based on the results obtained and validation, it is found that the clustering of nanoparticles in a nanofluid, the nanolayer thickness around the nanoparticles and the Brownian motion play a critical role in the thermal conductivity enhancement of nanofluids. The mathematical model developed lies on par with experimental data which confirms that the assumptions made for the development of mathematical model are accurate and well within the practical limitations. The contribution due to the Brownian motion due to moving nanoparticles in nanofluids is negligible when compared to the clustering effect of nanoparticles. The factors governing the overall enhancement of thermal conductivity is also understood better by solving the mathematical model using the various assumptions.

The conclusions drawn from this study are as follows: Kinetic theory was found to be negligible in explaining the thermal conductivity behavior of nanofluids. Clustering of the particles proved to be an important factor in enhancing the thermal conductivity of the

122

nanofluids. The model developed was found to be applicable for almost all the nanofluids. Thermal conductivity of nanofluids increases with increase in the concentration of the nanoparticles, nanolayer thickness and spherical clustering of nanofluids. The thermal conductivity of nanofluids decreases with increase in the diameter of the nanoparticles.

Overall, the model predictions were found to be in good agreement with experimental data. The study can be further scrutinized by varying some of the parameters such as nanocluster structure formation, such as a nanoparticle chain, the effect on thermal conductivity when the nanoparticle combine to form various shapes based on the surface charge in the nanoparticle and the base fluid. The mathematical model solved for nanolayer thickness resulted in decreased thermal conductivity for low volume fraction 0.01 and remained almost steady for volume fractions 0.02 and 0.03 and increased at 0.04 volume fraction. Exploring the limiting factors based on this result can be a topic for future studies. So this advanced technology of suspending nanoparticles in base fluids might provide answers to improved thermal management. Improved understanding of complex nanofluids will have an even broader impact.

REFERENCES

1. Wang, B. X., Sheng, W.Y., and Peng, X.F., 2009, "A novel statistical clustering model for predicting thermal conductivity of nanofluid", International Journal of Thermophysics, **30**, pp. 1992-1998.

2. Visinee, T., and Somchai, W., 2010, ''Critical review of heat transfer characteristics of Nano fluids, Renewable and Sustainable Energy Reviews, **11**, pp. 512-523.

3. Liu, M.S., Lin, M.C.C., Huang, I.T., and W, C.C., 2006, "Enhancement of thermal conductivity with CuO for Nanofluids, Chemical Engineering and Technology, **29**, pp. 72-77.

4. Kwak, K., and Kim, C., 2005, "Viscosity and thermal conductivity of copper oxide nanofluid dispersed in ethylene glycol", Korea-Australia Rheology Journal, **17**, pp. 35-40.

5. Li, Q., and Xuan, Y. M., 2002, "Convective heat transfer and flow characteristics of Cu–water nano fluid", Science in China, **45E,** pp. 408–416.

6. Guo, S. Z., Li, Y., Jiang, J. S., Xie, H. Q., 2010, "Nanofluids Containing gamma- γ-Fe_2O_3 Nanoparticles and Their Heat Transfer Enhancements", Nanoscale Res Lett, pp. 1222-1227.

7. Wang, X. Q., Mujumdar, A. S., 2007, "Heat transfer characteristics of nanofluids: a review", International Journal of Thermal Sciences, **46**, pp. 1-19.

8. Pawel, K., Jeffrey, A., and David, G. C., 2005, "Nanofluids for thermal transport", Materials today, **8**, pp. 36-44.

9. Vijay, K. K., "Model for energy transport in nanofluids"

10. Eapen, J., Li, J., and Yip, S., 2006, "Probing transport mechanisms in nanofluids by molecular dynamics simulations", Proceeding of the 18th National and 7th ISHMT–ASME Heat and Mass Transfer Conference, IIT Guwahati, India.

11. Keblinski, P., Phillpot, S. R., Choi, S. U. S., and Eastman, J. A., 2002, "Mechanisms of heat flow in suspensions of nano-sized particles (nanofluids)", International Journal of Heat and Mass Transfer, **45**, pp. 855-863.

12. Eapen, J., 2004, "Modeling Transport Mechanism in Nanofluids", Project Report. 2.57, Nano–to–Micro Transport Processes.

13. Xuan, Y., Li, Q., and Hu, W., 2003, "Aggregated Structure and Thermal Conductivity of Nanofluids", AIChE Journal, **49**, pp.1038-1043.

14. Shukla, R. K., and Dhir, V. K., 2005, "Study of the effective thermal conductivity of nanofluids", ASME International Mechanical Engineering Congress and Exposition, Florida, USA.

15. Prasher, R., Phelan, P. E., and Bhattacharya, P., 2006, "Effect of Aggregation kinetics on the Thermal conductivity of nanoscale colloidal solutions", NANO LETTERS, **6**, pp. 1529-1534.

16. Prasher, R., Bhattacharya, P., and Phelan, P. E., 2005, "Thermal Conductivity of Nanoscale Colloidal Solutions (Nanofluids)", The American Physical Society, **94**, pp. 025901-1- 025901-4.

17. Feng, Y., Yu, B., Xu P., and Zou M., 2007, "The effective thermal conductivity of nanofluids based on the nanolayer and the aggregation of nanoparticles", Journal of Physics D: Applied Physics, **40**, pp. 3164-3171.

18. XU, J., Bo-Ming, Y., and Mei-Juan, Y., 2006, "Effect of Clusters on Thermal conductivity in Nanofluids", Chinese physics letters, **23**, pp. 2819- 2822.

19. Patel, H. E., Sundararajan, T., and Das, S. K., 2006, "A cell approach model for thermal conductivity of nanofluids", Journal of Nanoparticle Research, **10**, pp. 87-97.

20. Prasher, P., Evans, W., Fish, J., Meakin, P., Phelan, P., and Keblinski, P., 2006, "Effect of Aggregation on Thermal Conduction in Colloidal Nanofluids", Applied Physics Letters, **89**, pp. 143119-1-143119-3.

21. Patel, H. E., Sundararajan, T., Pradeep, T., Dasgupta, A., Dasgupta, N., and Das, S. K., 2005, "A micro-convection model for thermal conductivity of nanofluids", Journal of Physics, **65**, pp. 863-869.

22. Murugesan, C., Sivan, S., 2010, "Limits for thermal conductivity of nanofluids" Thermal Science, **14**, pp 65-71.

23. Trisaksri, V., Wongwises, S., 2007, "Critical review of heat transfer characteristics of nanofluids", Renewable and Sustainable Energy Reviews, **11**, pp. 512-523.

24. Zhou, L. P., Wang, B. X., Peng, X. F., Du, X. Z., Yang, Y. P., 2009, " On the specific heat capacity of CuO", Advances in Mechanical Engineering, **2010**, pp 1-4.

25. Evans, W., Fish, J., and Keblinski, P., 2006, "Role of Brownian motion   hydrodynamics on nanofluid thermal conductivity", American Institute of Physics, **88**, pp. 093116-1 – 093116-3.

26. Shima, P., D., Philip, J., Raj, B., 2009, "Role of micro convention induced by brownian motion of nanoparticles in the enhanced thermal conductivity of stable nanofluids", Applied Physics Letters, **94**, 223101-1-223101-3.

27. Kathikeyan, N. R., Philip, J., Raj, B., 2008, "Effect of clustering on the thermal conductivity of nanofluids", Materials Chemistry and Physics, **109**, pp. 50-55.

28. Hong, K.S., Hong, T-.K., Yang, H-.S., 2006, "Thermal conductivity of Fe nanofluids depending on the cluster size of nanoparticles" Applied Physics Letters, **88**, pp. 031901-1-031901-3.

29. Wu, C., Cho, T.J., Xu, J., Lee, D., Yang, B., Zachariah, M.R., 2010, "Effect of nanoparticle clustering on the effective thermal conductivity of concentrated silica colloids", Physical Review E, **81**, pp. 011406-1-011406-6.

30. Lee, D., Kim, J.W., Kim, B.G., 2006, "A new parameter to control heat transport in nanofluids: Surface charge state of the particle in suspension", The Journal of Physical Chemistry B, **110**, pp. 4323-4328.

31. Xuan, Y., Li, Q., Zhang, X., and Fujii, M., 2006, "Stochastic thermal transport of nanoparticle suspensions", Journal of Applied Physics, **100**, pp. 043507-1 – 043507-6.

32. Hamilton, R.L., and Crosser, O.K., 1962, "Thermal Conductivity of heterogeneous two-component systems, I&EC Fundamentals, **1**, pp. 182-191.

33. Koo, J., and Kleinstreuer, C., 2005, "A new thermal conductivity model for nanofluids", Journal of Nanoparticle Research, **6**, pp. 577-588.

34. Kang, H. U., Kim, S. H., and Oh, J. M., 2006, "Estimation of Thermal Conductivity of Nanofluid Using Experimental Effective Particle Volume", Experimental Heat Transfer, **19**, pp. 181-191.

35. Jang, S.P., and Choi, S.U.S., 2004, "Role of Brownian motion in the enhanced thermal conductivity of nanofluids", Applied Physics letter, **84**, pp. 4316-4318.

36. Bejan, A., 2004, "Convection Heat Transfer", 3rd edition, John Wiley & sons.

37. Prasher, P., Bhattacharya, P., and Phelan, P. E., 2006, "Brownian-Motion-Based Convective-Conductive Model for the Effective Thermal Conductivity of Nanofluids", Journal of Heat Transfer, **128**, pp. 588-595.

38. Jang, S.P., and Choi, S.U.S., 2007, "Effects of various parameters on Nanofluid Thermal Conductivity", Journal of Heat Transfer, **129**, pp. 617- 623.

39. Kumar, H. D., Patel, H. E., Kumar, R. V. R., Sundararajan, T., Pradeep, T., and Das, S. K., 2004, "Model for Heat Conduction in Nanofluids", The American Physical Society, **93**, pp. 144301-1 – 144301-4.

40. Feng, Y., Yu, B., Xu, P., Zou, M., 2008, "Thermal conductivity of nanofluids and size distribution of nanoparticles by Monte Carlo simulations", Journal of Nanoparticle Research.

41. Bird, B. R., Stewart, W. E., and Lightfoot, E. N., 2007, "Transport Phenomenon", Second Edition, John Wiley & sons, Inc.

42. Wang, B. X., Zhou, L. P., and Peng, X. F., 2003, "A fractal model for predicting the effective thermal conductivity of liquid with suspension of nanoparticles", International Journal of Heat and Mass transfer, **46**, pp. 2265-2672.

43. Yu, B., Z, M., and F, Y., 2005, "Permeability of fractal porous media by Monte Carlo Simulations", International Journal of Heat and Mass transfer, **48**, pp. 2787-2794.

44. Timofeeva, E. V., Gavrilov, A. N., McCloskey, J. M., and Tolmachev, Y. V., 2007, "Thermal conductivity and particle aggregation in alumina nanofluids: Experiment and theory", The American Physical Society, **76**, pp. 061203-1-061203-16.

45. Leong, K.C., Yang, C., and Murshed, S.M.S., 2006, "A new model for thermal conductivity of nanofluids – the effect of interfacial layer", Journal of Nanoparticle Research, **8**, pp. 245-254.

128

46. Jeffrey, D.J., 1973, "Conduction through suspension of spheres", Royal Society of London Series A, Mathematical and Physical Sciences, **335**, pp. 355-367.

47. Lee, S., Choi, S.U.S., Li, S., and Eastman, J. A., 1999, "Measuring Thermal Conductivity of fluids containing oxide nanoparticles", ASME J. Heat Transfer, **121**, pp. 280-289.

48. Eastman, J.A., Choi, S.U.S., Li, S., Yu, W., and Thompson, L.J., 2001, "Anomalously increased effective thermal conductivities of ethylene glycol-based nanofluids containing copper nanoparticles", American Institute of Physics, **78**, pp. 718-720.

 49. Kim, S.H., Choi, S.R., and Kim, D., 2007, "Thermal conductivity of Metal-Oxide Nanofluids: Particle Size Dependence and Effect of Laser Irradiation", Journal of Heat Transfer, **129**, pp. 298-307.

50. Hong, T.K., and Yang, H.S., 2005, "Study of the enhanced thermal conductivity of Fe nanofluids", Journal of Applied Physics, **97**, pp. 064311-1 – 064311-4.

51. Tillman, P., and Hill, J. M., 2006, "A new model for Thermal Conductivity in Nanofluids", IEEE , pp. 673-676.

 52. Kang, H. U. k., Kim, S. H., and Oh, J. M., 2006, "Estimation of Thermal Conductivity of Nanofluid Using Experimental Effective Particle Volume", Experimental Heat Transfer, **19**, pp. 181-19.

APPENDICES

VITA

Graduate School

Southern Illinois University

Anand Natchimuthu Chinnaraj

Anand.chinnaraj@gmail.com

Bharathiyar University

Bachelor of Engineering, Mechanical Engineering, May 2004

Thesis Title: Thermal Conductivity Enhancement of Nanofluids – Mathematical Model

Major Professor: Dr. Kanchan Mondal